CATALYTIC CONVERSION OF METHANE TO METHANOL, FORMALDEHYDE AND HIGHER HYDROCARBONS

Jack H. Lunsford

Department of Chemistry
Texas A&M University
College Station, TX 77843

INTRODUCTION

By suitably choosing the catalyst and oxidant it is possible to direct the conversion of methane either to oxygenated products (HCHO and CH_3OH) or hydrocarbons (mainly C_2H_4). High selectivities to methanol and formaldehyde have been achieved only at low conversion levels and only using nitrous oxide as the oxidant (1,2). Considerably more progress, however, has been made in the oxidative coupling of methane to form ethane and ethylene (C_2 products) (3-8). The purpose of this paper is to show that both formation of oxygenates and C_2 products occur by a common intermediate, namely the $CH_3\cdot$ radical, which in one case reacts with the surface to form methoxide ions, and in the other reacts mainly in the gas phase to form ethane.

CONVERSION TO OXYGENATES

Molybdena supported on silica is moderately active and selective for the catalytic conversion of CH_4 to CH_3OH and HCHO when N_2O is used as the oxidant as indicated by the results of Table I (1). Up to ca. 2% conversion very high combined selectivities to CH_3OH and HCHO were obtained, but at 6% conversion the selectivities to the desired oxygenates were decreased considerably. With O_2 as the oxidant the results were considerably poorer.

Although this system holds little promise as a practical catalyst, it does provide insight into possible means of activating CH_4 and following the chemistry of surface intermediates. This study, for example, points to the role of thermally generated O^- ions in the activation of methane. Previous work by Bohme and Fehsenfeld (9) have shown that gas phase O^- ions are very effective in the abstraction of hydrogen atom from simple alkanes via the reaction

$$CH_4 + O^- \rightarrow CH_3\cdot + OH^- \qquad (1)$$

Likewise, methyl radicals are formed on Mo^{VI}/SiO_2 via the photochemical reactions

$$Mo^{VI}O^{2-} \xrightarrow{h\nu} Mo^{V}O^- \qquad (2)$$

$$Mo^{V}O^- + CH_4 \rightarrow Mo^{V}OH^- + CH_3\cdot \qquad (3)$$

and their EPR spectra are shown in Figure 1b (1,10). Of more importance in catalysis, O^- may be formed by the thermal reaction of Mo^V/SiO_2 with N_2O, and CH_4 reacts with these oxygen ions at temperatures as low as -196°C. The resulting $CH_3\cdot$ radicals are shown in Figure 1a.

Infrared results (Figure 2) suggest that these $CH_3\cdot$ radicals react with the molybdena surface via reductive addition to form methoxide ions. It is known from extensive work on the partial oxidation of methanol over supported and unsupported molybdena that methoxide ions are intermediates in the formation of formadlehyde. In the presence of water these molybdenum alkoxide ions react to form methanol. Thus, the partial oxidation of methane to oxygenates may be understood by the catalytic cycle depicted in Scheme I. In addition to the selective cycle one must also consider the possibility of a two-electron reaction with N_2O to form oxide ions. A molecule of CH_4 would then have to be consumed in a nonselective manner to reduce Mo^{VI} back to Mo^{V}. In principal the two-electron transfer could be minimized by dispersing the Mo as a dimer on the surface and by avoiding the reduction of this molybdenum to the IV oxidation state.

OXIDATIVE COUPLING

When methyl radicals are formed on oxides which contain no reducible metal ions, then the formation of methoxide ions is limited and the radicals have adequate lifetimes either to couple on the surface or to desorb into the gas phase. Several of the more active and selective catalysts for the oxidative dimerization of methane are listed in Table II, where it is apparent that the steady state yields of C_2 products may reach 25%. The starting materials are given in the table and under reaction conditions the working catalyst are mainly metal oxides which are extensively covered by alkali metal carbonates. These carbonates probably serve, in part, to prevent the formation of methoxide ions on oxides such as ZnO and Mg_6MnO_8.

In addition, alkali metal ions may yield specific centers which are capable of forming methyl radicals. For example, with the Li^+/MgO, and Na^+/CaO catalysts centers of the type $[Li^+O^-]$ and $[Na^+O^-]$ serve as sources of O^- ions, which activate methane as described in the previous section (3,5). There is increasing evidence that at reaction temperatures greater than 750°C, the alkali metal carbonates partially decompose to form their respective oxides and that the oxides themselves are able to activate methane. This is particularly true for Na_2O_2, which is the most stable oxide of sodium (13).

On the crystal faces of closed shell oxides, of which MgO is an example, the bonding of $CH_3\cdot$ radicals is weak (14), and therefore it is not surprising that the radicals emanate into the gas phase where coupling occurs. It has been demonstrated that over a Li^+/MgO catalyst >40% of the C_2 products may be formed by such gas phase coupling reactions (15,16). Unfortunately, in the presence of molecular oxygen other gas phase radical reactions may occur which ultimately result in the formation of CO_2. Similarly, C_2H_6 and C_2H_4 may be oxidized both heterogeneously and homogeneously which limits C_2 yields to ca. 25%.

ACKNOWLEDGMENTS

This work was supported mainly by the National Science Foundation under Grant No. CHE-8617436.

REFERENCES

1. Liu, H.-F., Liu, R.-S., Liew, K.Y., Johnson, R.E. and Lunsford, J.H., J. Am. Chem. Soc., 106, 4117 (1984).
2. Kahn, M.M. and Somorjai, G.A., J. Catal., 91 263 (1985).
3. Ito, T. and Lunsford, J.H., Nature (London), 314, 721 (1985); Ito, T., Wang, J.-X., Lin, C.H. and Lunsford, J.H. J. Am Chem. Soc. 107, 5062 (1985).
4. Matsuura, I., Utsumi, Y. Nakai, M. and Doi, T., Chem. Lett., 1981 (1986).
5. Lin, C.-H., Wang, J.-X. and Lunsford, J.H., J. Catal., in press.
6. Otsuka, K., Liu, Q., Hatano, M., Morikawa, A., Chem. Lett. 467 (1986).
7. Moriyama, T., Takasaki, N., Iwamatsu, E. and Aika, K. Chem. Lett., 1165 (1986); Iwamatsu, E., Moriyama, T., Takasaki, N. and Aika, K., J. Chem. Soc. Chem. Commun. 19 (1987).
8. Sofranko, J.A., Leonard, J.J., Jones, C.A., Gaffney, A.M. and Withers, H.P., Petroleum Div. Preprint, ACS Meeting, New Orleans, Aug. 1987, pp. 763-769.
9. Bohme, D.K. and Fehsenfeld, F.C., Can. J. Chem. 47, 2712 (1969).
10. Lipatkina, N.I., Shvets, V.A. and Kazansky, V.B. Kinet. Katal. 19, 979 (1978).
11. Cheng, W.-H., Chowdhry, U. Ferretti, A., Firment, L.E., Groff, R.P., Machiels, C.J., McCarron, E.M., Ohuchi, F., Staley, R.H. and Sleight, A.W. in "Heterogeneous Catalyst" (B.L. Shapiro, Ed.) pp. 165-181, Texas A&M Univ. Press, College Station, Texas, 1984.
12. Yang, T.J. and Lunsford, J.H., J. Catal. 103, 55 (1987).
13. Otsuka, K., Said, A.A., Jinno, K. and Komatsu, T., Chem. Lett. 77 (1987).
14. Mehandru, S.P. and Anderson, A.B., J. Am. Chem. Soc. 110, 1715 (1988).
15. Campbell, K.D., Morales, E. and Lunsford, J.H., J. Am. Chem. Soc. 109, 7900 (1987).
16. Campbell, K.D. and Lunsford, J.H., J. Phys. Chem., in press.

Table I. Conversion and Selectivity during Methane Oxidation[a,b]

T, °C	conven, %	selectivity, %			
		HCHO	CH_3OH	CO	CO_2
550	1.6	79.5	20.5		
560	1.9	80.1	19.9		
570	2.9	64.3	13.8	19.1	2.8
580	4.0	58.8	10.0	27.7	3.4
594	6.0	49.5	7.8	38.1	4.6

[a]1.0 g of Mo/Cab-O-Sil, P_{CH4} = 75 torr, P_{N2O} = 280 torr, P_{H2O} = 260 torr, F = 1.33 mL/s.

[b]Ref. 1.

Table II. Oxidative Coupling of Methane Over Promoted Metal Oxide Catalysts

Catalyst	Temp, °C	CH_4 Conv, %	C_2 Sel, %	C_2Yield %	Ref.
Li_2CO_3/MgO	720	43	45	19.4	1
Li_2CO_3/Sm_2O_3	750	38	54	20.7	6
$NaNO_3/MgO$	800	39	57	22.4	7
Li_2CO_3/ZnO	740	36	67	23.9	4
Na_2CO_3/CaO	725	33	45	14.8	5
$NaMnO_4/MgO$	925	22	70	15.4	8

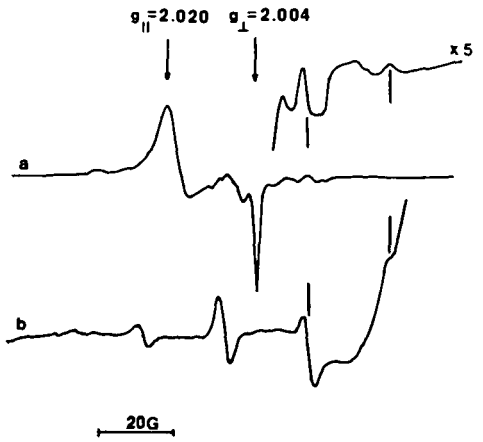

Figure 1. EPR spectra of methyl radicals: (a) after reaction of CH_4 with O^- on Mo/SiO_2; (b) after UV irradiation of oxidezed Mo/SiO_2 in the presence of CH_4. Reactions were carried out and spectra recorded with the sample at -196 °C. (Ref. 1)

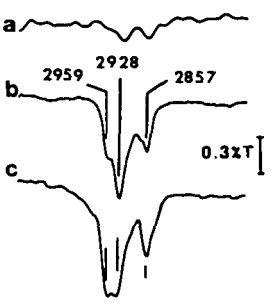

Figure 2. Infrared spectra of methoxide ions on Mo/SiO_2: (a) background after reduction of catalyst in CO, followed by adsorption of N_2O and evacuation; (b) after subsequent adsorption of CH_4 and evacuation; (c) after adsorption of CH_3OH and evacuation. (Ref. 1)

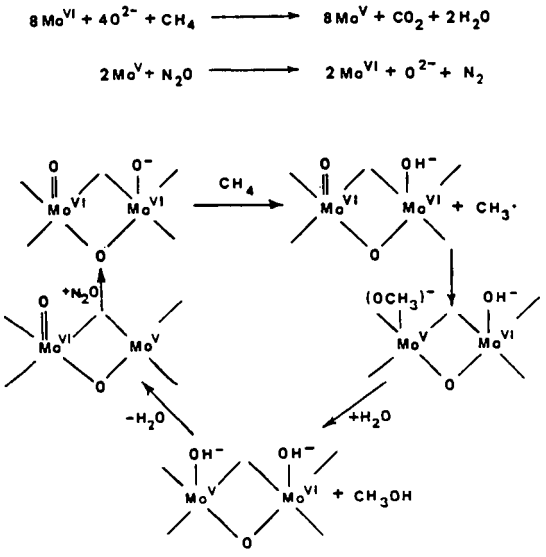
8 Mo^VI + 4 O^2- + CH4 → 8 Mo^V + CO2 + 2 H2O
2 Mo^V + N2O → 2 Mo^VI + O^2- + N2
CH4
+N2O
-H2O
+H2O
+ CH3·
+ CH3OH

SCHEME 1

THE ROLE OF ALKALI PROMOTERS IN SELECTIVE CATALYTIC COUPLING OF METHANE

Jon G. McCarty and M. A. Quinlan
SRI Int'l, 333 Ravenswood Ave., Menlo Park, CA 94025

ABSTRACT

The role of alkali promoters in increasing the hydrocarbon selectivity of catalytic methane coupling is under investigation for series of unpromoted and alkali-promoted alkaline earth and rare earth oxides. Multilayer quantities of CO_2 and fractional monolayer quantities of O_2 and H_2O evolved during temperature-programmed desorption (TPD) experiments immediately following the stationary-state oxidative dimerization of methane by Na/CaO and Li/MgO. These results suggest that a relatively passive and protective layer of molten alkali carbonate with surface hydroxide and surface oxide components is formed on the promoted CaO and MgO surfaces during partial oxidation. Isotope exchange experiments with deuterium-labeled methane in the absence of gas phase oxygen showed high rates of H-D exchange on both the unpromoted and the Na-promoted CaO catalysts, indicating that the formation of methyl radicals may not limit the rate of production of higher hydrocarbons. The presence of an adsorbed species that released methane at moderate temperature, about 550 K, was also revealed in the TPD experiments following methane dimerization. Methyl (or methoxy) and hydroxyl entities coadsorbed on the carbonate layer are suggested as the source of methane observed in these TPD experiments.

INTRODUCTION

An increase in the worldwide supply of natural gas, increasing restrictions on the flaring of remote natural gas, and the high cost of synthesis gas conversion provide great incentives to develop processes that directly and economically convert methane to readily transportable and higher value products.[1-3] Hydrocarbon formation through the selective oxidation of only the excess hydrogen in the methane molecule is thermodynamically favorable, while direct thermal conversion of methane to higher hydrocarbons is thermodynamically unfavorable and energy intensive. However, the partial oxidation of methane is difficult because of the relatively high reactivity of useful products and the very

favorable thermodynamics for deep oxidation to carbon dioxide. Successful processes for direct methane conversion into higher hydrocarbons must therefore use highly selective catalysts that strongly inhibit total oxidation, yet retain the capability of activating the stable methane molecule.

Several classes of catalysts have significant selectivity for methane activation, including alkaline earth oxides, rare earth oxides, manganese oxide, and oxides of the soft metals such as lead, cadmium, bismuth, and antimony. Alkali promoters are widely used with methane activation catalysts,[4-8] and often increase selectivity without a corresponding increase in the methane conversion rate. Thus, alkali may act more to suppress hydrocarbon oxidation than to promote methane conversion. In the present, work we have used fixed-bed reactor kinetic studies, methane H-D exchange reaction experiments, and post-reaction temperature-programmed desorption (TPD) examination to study the mechanism of methane oxidative dimerization by a variety of unpromoted and alkali-promoted alkaline earth oxide and rare earth oxide catalysts.

EXPERIMENTAL RESULTS

Catalyst Preparation

Samples of alkali-promoted alkaline earth oxide catalysts were prepared from high-purity CaO, MgO, $Ba(OH)_2$, Na_2CO_3, K_2CO_3 and Li_2CO_3 (Johnson Matthew, Puratronic®, > 99.99%). The preparation consisted of adding appropriate amounts of the alkali carbonate and alkaline earth oxide or hydroxide to a small quantity of distilled water and boiling for 1 hour. The resulting slurry was then air dried overnight at 423 K. Various mole fraction compositions were prepared where the mole fraction of alkali metal is defined as the ratio of moles of alkali metal to the sum of the moles of alkali metal and the moles of alkaline earth oxide. BET (N_2) surface area measurements were performed on these catalysts following a standard pretreatment. Complex rare earth oxide catalysts, such as $LaAlO_3$ and La_2O_3, were prepared by precipitation of nitrate salt solutions with tetramethyl ammonium hydroxide, followed by centrifugation and drying. These catalysts were calcined in air at 873 K and characterized by x-ray diffraction and BET surface area measurements prior to the kinetic studies.

Fixed-Bed Reactor Studies of Methane Activation

Isothermal reaction kinetics for methane activation by the alkali-promoted alkaline earth oxide catalyst were examined over a period of time (15 to 72 h) sufficient to establish stationary-state conditions.

catalytic rates were measured using a fixed-bed microreactor system. Approximately 50-mg samples were loaded in 4-mm-ID quartz reactors. The reaction products were analyzed by gas chromatography using a 6-ft Carbosieve® column with a flame ionization detector. The chromotographs were calibrated using a certified standard blend of reactant and product gases. The methane conversion and product selectivities were based on the number of moles of carbon reacted per unit time. C_{2+} yield is defined as the product of methane conversion and selectivity. Product distributions for the series of alkali-promoted alkaline earth oxides at 1000 K ranged from total combustion (for CaO) to 74% C_{2+} (for Li/MgO). The highest methane activation rate was observed for the Na/CaO catalyst.

The results of our kinetic studies are best understood as competition between oxidative coupling of the methane and its complete oxidation to CO_2. Both reactions show a positive reaction order with respect to CH_4; however, the coupling reaction was inhibited by increasing oxygen partial pressure. Thus, with low oxygen partial pressure, methane conversion was not altered by P_{O_2}, but the selectivity for C_2H_6 and C_2H_4 decreased with increasing P_{O_2}.

Extrapolation of our results to zero oxygen partial pressure predicts that selectivities to C_2H_6 approaching 100% are inherently possible in alkali-promoted catalyst systems. Similar results in this range of low oxygen partial pressures were reported by Ito, et al.[5] When the degree of methane conversion is high, both C_2H_4 and C_2H_6 are observed. The beneficial effect of low O_2 partial pressure on C_{2+} selectivity has long been noted, and is the basis for the redox processes involving the sequential partial oxidation of methane and regeneration of the oxide with air, as demonstrated in the work of Jones, et al.[9] and Keller and Bhasin.[10]

Temperature-Programmed Desorption Studies

The temperature-programmed desorption (TPD) technique was to identify adsorbate binding states as well as bulk phases in the alkali-enriched alkaline earth oxide catalysts. After reaction at elevated temperature, the catalyst was cooled to room temperature in the reactive gas mixture. A stream of pure helium was then passed through the reactor and the catalyst was heated to 1300 K at a rate of 1 K s^{-1}. Desorption and decomposition products were continuously monitored by on-line mass spectrometry. The principal ion masses corresponding to CH_4, H_2O, C_2H_x, CO, C_3H_x, O_2, CH_3OH, and CO_2 were continuously scanned (Figure 1 and Table 1). Variable amounts of O_2, which evolve at high temperatures (>1000 K), small amounts of H_2O, and large quantities of CO_2 indicative of bulk carbonate decomposition were observed. All catalysts unexpectedly exhibited methane desorption at low temperature (650 ± 50 K) in submonolayer quantities.

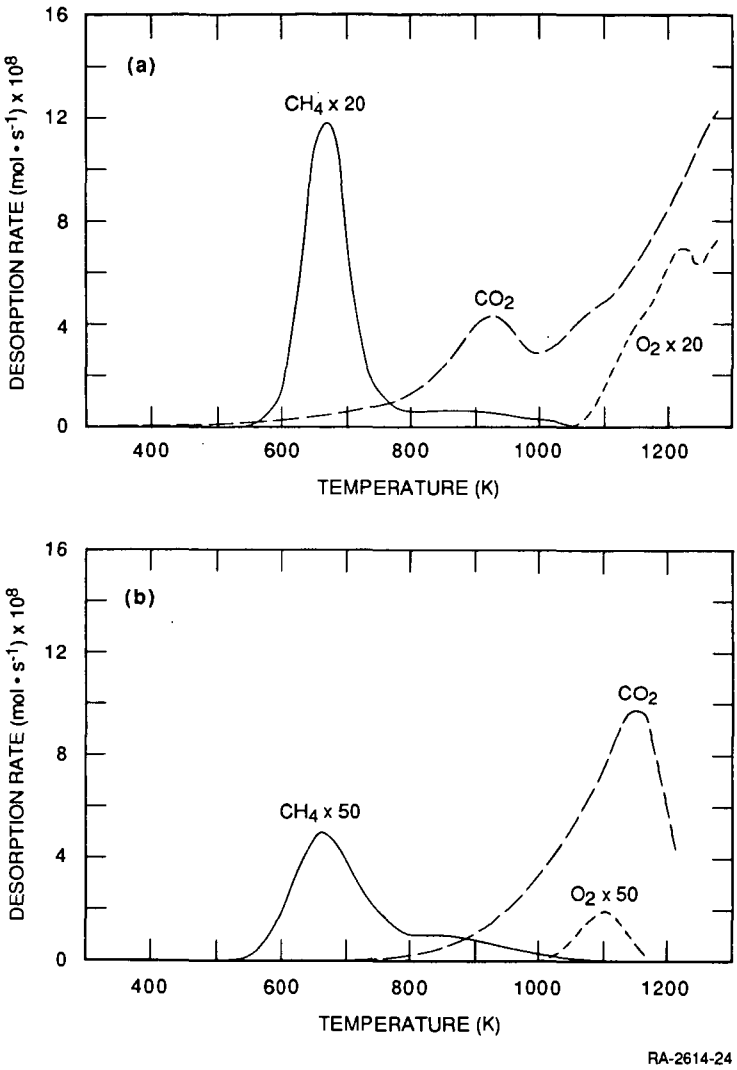

Figure 1. Temperature programmed desorption from alkali-metal-promoted alkaline earth catalysts.

(a) 30 mol % Li/MgO.
(b) 30 mol % Na/CaO.
(1 K • s^{-1} heating rate; 0.5 ml • s^{-1} He flow rate)

Table 1

TEMPERATURE-PROGRAMMED PRODUCT ANALYSIS[a]

Catalysts	Conc. of Sites (μmol g^{-1})	Amount of Desorbed Product[c] (μmol g^{-1})			
		CH_4	H_2O	O_2	CO_2
0.01 Na/CaO	96	3.5 (600)	312 (700)	1.1 (1175)	27.9 (800)
0.30 Na/CaO	46	1.7 (675)	10.5 (400+)	0.6 (1100)	583 (1150)
0.30 Li/CaO	17	0.4 (700)	0.8 (broad)	11.0 (>1100)	3.4 (>1100)
0.30 Li/MgO	40	12.9 (675)	15.8 (broad)	12.6 (1225)	683 (925, >1300)

[a]TPD conditions: 0.5 cm^3 s^{-1} He flow rate, 1 K s^{-1} heating rate, 0.04 g of catalyst.

[b]Number of surface sites estimated assuming site density of 1 x 10^{19} sites m^{-2} for the catalyst surface area following pretreatment at 973 K in air for 48 hours.

[c]Number in parenthesis refers to temperature of desorption peak maxima (K).

The quantities of evolved water vapor for 30 mol% Na/CaO and 30 mol% Li/MgO and oxygen for 30 mol% Li/CaO and 30 mol% Li/MgO approached the estimated surface cation density based on the BET surface area measurements, assuming 1.0 x 10^{19} sites m^{-2}. The CO_2 evolved for the 0.01 and 0.3 Na/CaO and 0.3 Li/MgO samples was almost equal to the quantity of carbonate expected if all alkali was converted to the carbonate during reaction. Thermodynamic calculations predict the formation of bulk carbonates under reaction conditions, despite the low CO_2 selectivity of the alkali/alkaline earth oxide catalysts. The nearly one-fourth monolayer quantities of desorbing oxygen and water vapor (the latter presumably from hydroxyl species) may arise from chemisorbed species or possibly from gas dissolved in the bulk carbonate.

Isotopic Exchange

The extent of hydrogen exchange between CD_4 and CH_4 on calcium oxide catalysts was investigated by injecting an aliquot consisting of a dilute

mixture of CD_4 and CH_4 into a stream of helium and through the catalyst bed at elevated temperatures. The degree of H-D exchange in the methane components of the effluent gas was measured by on-line mass spectrometry. Several pulses of a mixture containing 2.0 μmol CH_4 and 0.6 μmol CD_4 were injected over a temperature range from 300 to 1200 K for CaO and Na-promoted CaO catalysts and for an empty reactor containing the thermocouple assembly. Ion current for masses 15 though 20 amu corresponding to CH_3^+, CH_4^+, CDH_3^+, $CD_2H_2^+$, CD_3H^+ and CD_4^+ ions respectively, were scanned during each pulse.

Both pure CaO and sodium promoted calcium oxide showed substantial activity for hydrogen exchange with CD_4. The extent of H exchange between CH_4 and CD_4 was taken as the conversion of CD_4 since the equilibrated population of CD_4 would be very small (< 1% of the total methane) given the low D/H ratio (D/H = 0.3). At 980 K, 6% of the CD_4 was converted to $CD_{4-x}H_x$ on Na/CaO (Figure 2) while about 60% was converted on CaO. Under these conditions, stationary-state methane conversion with the Na/CaO catalyst was about 5%. Similarly exchange measurements have been reported[11] for MgO and Al_2O_3. Based on CD_4 conversion in the blank reactor, less than 15% of the observed exchange with Na/CaO was attributed to homogeneous gas phase reaction or to reactions occurring on the thermocouple assembly or reactor wall surfaces.

Apparently the hydrogen exchange reaction and the coupling reaction occur similtaneously. The temperature of the onset of hydrogen exchange (800 to 900 K) is approximately the same as the appearance of C_{2+} and CO_2 reaction products during the temperature programmed oxidative coupling of methane over 0.3 Na/CaO and the onset of H_2O and CO_2 evolution during the TPD experiments.

CONCLUSIONS

The kinetics of methane activation were examined for a series of CaO catalysts promoted by lithium, sodium, and potassium oxide/carbonate salts. The methane conversion activity and higher hydrocarbon selectivity follow the order Na > Li > K with respect to promoter. This result is in accord with the idea that cation size, and presumably intersolubility of alkali-alkaline earth cations, influences the nature and surface density of active sites.

The sodium-promoted CaO catalyst system showed high intrinsic C_2H_6 selectivity (> 80 mol% carbon basis in the limit of low conversion and low oxygen partial pressure), good activity (about twice the methane conversion rate per unit area relative to lithium-promoted magnesia under

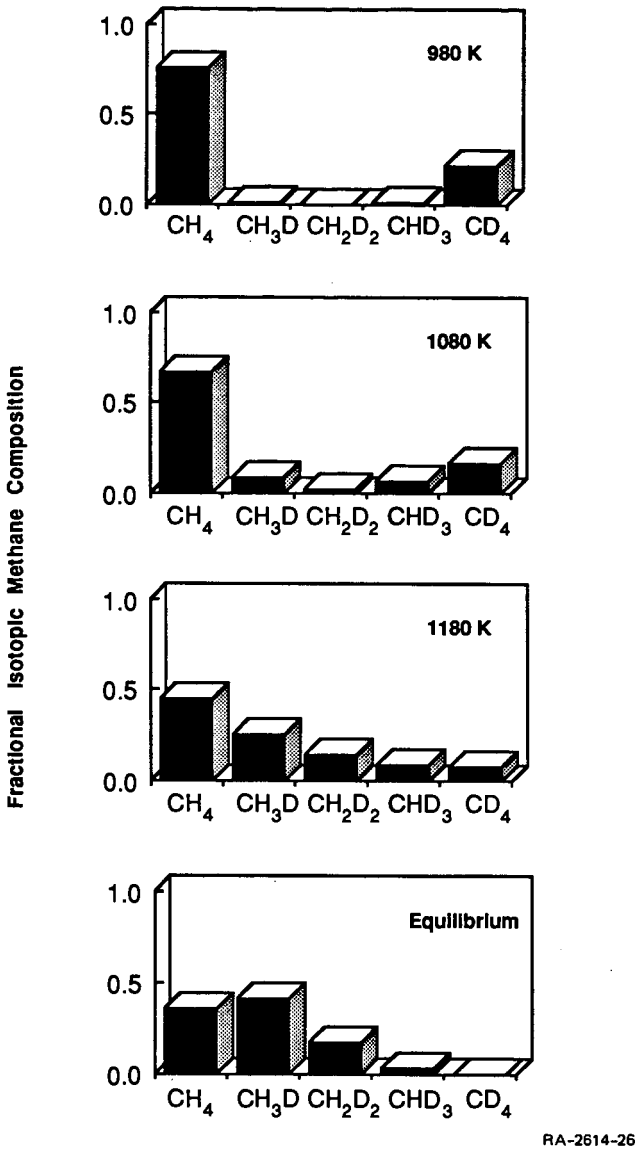

Figure 2. Isotopic concentration of methane pulses over 30 mol% Na/CaO at various temperatures. (Pulse composition: 2.1 micromoles CH_4, 0.6 micromole CD_4)

identical reaction conditions), and good stability (no observable decrease in rate and selectivity after 72 hours). Our results are in substantial agreement with published work.

Detailed reaction order experiments showed that the rate of methane conversion was linear with methane partial pressure as expected and independent of oxygen partial pressures, whereas the C_2 selectivity varied as the square root of methane partial pressure and the inverse square root of oxygen partial pressure. This result shows that operation at moderate pressure (especially with fixed low oxygen partial pressure) with Na/CaO and presumbaly other alkali-promoted alkaline earth oxide catalyst would increase the hydrocarbon yield. Other kinetic studies showed the weak dependence of C_2 selectivity of CO_2 partial pressure and the strong correlation between ethene/ethane product ratio and methane conversion.

ESR experiments were performed in situ at temperatures up to 920 K to detect thermally induced radical oxygen anion species in the presence of oxygen, methane, or a reacting gas mixture. Signals attributable to O^- or $[A^+O^-]$ centers were photoinduced at 78 K but rapidly disappeared at higher temperatures (temperatures below 300 K). This result indicates that O^- centers are not sites for methane activation by selective dimerization catalysts.

TPD experiments indicate that the alkali components after extended reaction exist in the form of (probably molten) carbonate salts on MgO and CaO catalysts. Minor, perhaps fractional, monolayer quantities of oxygen and hydroxyl species were also shown to be present on the working catalysts. Other TPD experiments presented tantalizing evidence for an organic intermediate which was stable at temperatures below 550 K, but which decomposed into methane at 750 K in the absence of oxygen.

A picture of the working alkali-promoted alkaline earth methane dimerization catalysts and the reaction mechanism is emerging from the present work and the numerous methane activation studies under way throughout the world. Recent evidence presented by the Texas A&M group[12-15] convincingly confirms that a free radical mechanism involving gas phase recombination of methyl radicals as a primary step can explain the hydrocarbon product distribution for oxidative methane dimerization. The initial step is the abstraction of a hydrogen atom by an active surface oxygen species with subsequent release of a methyl radical into the gas phase. The high exchange rates we observed between CD_4 and CH_4 suggest that the production of methyl radicals is relatively rapid. Methyl radicals are easily oxidized so that the catalyst surfaces must have a very low concentration of reducible oxygen. The working catalyst may be passivated by the formation of a molten or glassy layer of alkali

carbonate over MgO or CaO surfaces. The carbonate layer may contain surface oxygen or hydroxyl species. The location (gas/alkali carbonate interface, bulk alkali carbonate, or alkali carbonate/alkaline earth oxide interface) and the nature (O^-, O_2^-, or O^{-2}) of the active site is still uncertain. Additional research now under way should clarify both the mechanism and nature of the active site for the initial methane activation step.

ACKNOWLEDGEMENT

This work has been sponsored by a grant from the Gas Research Institute and affiliated industrial cosponsors of GRI's Methane Reaction Science program.

REFERENCES

1. R. Pitchai and K. Klier, Catal. Rev. -Sci. Eng. 28, 13 (1986).

2. G. Jean, V. Allenger, and M. Ternan, "Natural Gas: Alternative Sources of Liquid Fuels" in Proceedings of the 37th Canadian Chemical Engineering Conference, Montreal, Quebec, May 18-20, 1987.

3. N. W. Green and R. V. Ramanathan, "Conversion of Natural Gas to Transport Fuels," AIChE Reprint, 1988 Spring National Meeting.

4. D. J. Driscoll, W. Martir, J.-X. Wang, and J. H. Lunsford, J. Amer. Chem. Soc. 107, 58 (1985).

5. T. Ito, J.-X. Wang, C.-H. Lin, and J. H. Lunsford, J. Amer. Chem. Soc. 107, 5062 (1985).

6. C.-H. Lin and J. H. Lunsford, J. Phys. Chem. 90, 534 (1986).

7. T. Matsuda, Z. Minami, Y. Shibata, S. Nagano, H. Miura, and K. Sugiyama, J. Chem. Soc., Faraday Trans. I 82, 1357 (1986).

8. C. A. Jones, J. J. Leonard, and J. A. Sofranko, Energy and Fuels 1, 12 (1987).

9. C. A. Jones, J. J. Leonard, and J. A. Sofranko, numerous U.S. patents including 4443644-9, 4444984, 4523050, 4547611 assigned to Atlantic Richfield Company.

10. G. E. Keller and M. M. Bhasin, J. Catal. 73, 9 (1982).

11. L. Quanzhi and Y. Amenomiya, Appl. Catal. 23, 173 (1986).

12. T. Ito and J. H. Lunsford, Nature 314, 721 (1986).

13. D. J. Driscoll and J. H. Lunsford, J. Phys. Chem. 89, 4415 (1985).

14. J.-X. Wang and J. H. Lunsford, J. Phys. Chem. 90, 5883 (1986).

15. K. D. Campbell, E. Morales, and J. H. Lunsford, J. Amer. Chem. Soc. 109, 7900 (1987).

STUDIES OF THE GAS PHASE AND Li/TiO_2 CATALYZED OXIDATIVE COUPLING OF METHANE

G.S. Lane and E.E. Wolf

Department of Chemical Engineering
University of Notre Dame
Notre Dame, Indiana 46556

ABSTRACT

The oxidative coupling of CH_4 was studied in the absence of catalysts and using a series of lithium-promoted TiO_2 catalysts by co-feeding CH_4 and O_2. Under some operating conditions, significant gas phase oxidative coupling can occur in the absence of catalysts. The general trend dicated by the gas phase kinetics is that the hydrocarbon selectivity falls as conversion increases. In the catalytic study, the degree of promotion was studied by varying the Li loading from 0 to 31.7% on the rutile phase of TiO_2. Generally, increasing the Li loading reduces the combustion capacity of the catalyst, lowers CH_4 conversion, and increases hydrocarbon selectivity. A 16.2% Li/TiO_2 catalyst had CH_4 conversions around 15% with hydrocarbon selectivities about 75% measured after 2 hours time-on-stream. X-ray diffraction, x-ray photoelectron spectroscopy, and differential thermal analysis were used to characterize the catalyst.

INTRODUCTION

Oxidative coupling of methane has been demonstrated using cyclic feeds(1-3), and co-feeding methane and oxygen (4-9), on a variety of metal oxide catalysts. Little attention has been paid to the gas phase reactions that can occur, even though it has been established that the mechanism involves the formation of CH_3 radicals. One of the objectives of the work reported here was to establish the role of the methane oxidative coupling gas phase reactions. The second objective was to determine the effect of Li on a lithium-titania catalyst system in relation to the gas phase results. The rutile phase of titania was chosen because our previous work indicated that the support imparted special oxygen transfer capacity to Pt supported on rutile (10). Lithium has been shown to be an effective promoter for the oxidative coupling of methane (6), and for this reason it was chosen to promote the titania catalysts. Characterization techniques involving XRD, XPS, and DTA were used to relate the role of Li with the activity results.

EXPERIMENTAL

A detailed description of the experimental apparatus has been presented elsewhere (11), thus only a brief description is given here. The activity measurements were carried out in a single pass flow reactor (0.95 O.D., 15 cm long) made of fused silica. A resistive furnace was specially designed to minimize non-isothermalities. Experiments were also performed in a reactor filled with quartz chips and in a stainless steel reactor. Activity measurements were conducted by co-feeding methane, O_2 and He as a diluent. Typical operating conditions were as follows : i) temperature 600-800°C, ii) contact time 0.25 to 1.05 g s/ml, and iii) feed mole ratio of methane to oxygen of 2:1 to 37:1. The reactor effluent concentrations were measured by gas chromatography using carbosphere and Hayesep Q columns in parallel. A different reactor was used for each catalyst sample due to the apparent formation of lithium silicates on the reactor walls.

The catalyst were prepared by wet impreganation using Li_2O dissolved in deionized water to give lithium loadings of 0.0, 1.0, 3.8, 6.7, 11.0 16.2, and 31% on the rutile-titania support (12). XRD analysis was conducted using a Cu K-alpha radiation, and XPS analysis were conducted on a HP-5950 ESCA spectrometer with an Al anode.

RESULTS AND DISCUSSION

Conversion and selectivity (amount of methane converted to a product) results for the gas phase studies are shown in Figs. 1a and 1b at various reactant partial pressures and in Figs. 2a and 2b at various temperatures. Depending on operating conditions; gas phase results yielded selectivities varying from 65% at 2% conversion, to 29% at 32% conversion. Results obtained when the reactor was filled with quartz chips were similar to the gas phase results, indicating that the quartz reactor walls were not responsible for the gas phase results.However, activity measurements conducted in a stainless steel reactor resulted in 100% oxygen conversion and complete combustion of methane to CO_2.

It is clear from Figs.1a and b and 2a and b that as conversion increases, selectivity to C_2 decreases.This trend is valid when other variables, such as contact time or oxygen and methane partial pressures, are changed, and it appears to be a generic relationship. A detailed comparaison of the conversion versus selectivity in the gas phase and catalytic results has been made showing that about half of the published results are below our gas phase results, whereas the other half are above (11). This indicates that in some of the catalytic studies the catalysts promoted combustion of the gas phase products to CO_2.

Results obtained with a 1% Li catalyst are shown in Figs 1c and 1d at various reactants partial pressures and in Figs. 1c and 2d at various temperatures. It can be seen that the catalyst promotes the combustion of C_2 and CO to CO_2. Under the various conditions shown in Fig. 1-2, c-d, the C_2 yield obtained in the presence of the 1% Li/TiO_2 catalyst is lower than in the gas phase.

Figures 3(a) to 3(c) display conversion, selectivity, and yield (conversion times selectivity), obtained with catalysts with different Li loadings, with a Li/MgO catalysts, and without catalysts. The results were obtained under the same operating conditions consisting of 250 mg of sample, dilution ratio of 0.4 (to minimize gas phase results), 100 cc/min total feed flow rate, methane to oxygen feed ratio of 4, 800°C,and after 2 hrs. of time-on-stream. The results in Fig. 3 show that as Li loading increases up to 11%, oxygen conversion decreases leading to an increase in selectivity. Further addition of Li results in an increase in conversion and selectivity, resulting in the highest yield for the 16.2% catalysts. Past the 16% loading the conversion decreases again lowering the yield.

XPS and XRD analysis have been conducted on the 16% catalysts at room temperature. However, DTA analysis indicates that there is a phase transition at about 750°C; consequently, the results at room temperature might not be relevant at the reaction conditions. The room temperature results indicate that increasing Li loading decreases the concentration of surface oxygen which is reponsible for the oxidation of reaction intermediates. Work is underway to characterize the catalyst at reaction conditions, and ascertain the nature of the surface species responsible for the increase in selectivity.

ACKNOWLEDGEMENTS

Financial support of the Amoco Research Center, Naperville, Il, is gratefully acknowledged.

REFERENCES

1. Keller, G. E., and Bhasin, M. J., J. Catal. 73, 9-19 (1982).
2. Labinger, J. A., and Ott, K. C., J. Phys. Chem. 91, 2682-84 (1987).
3. (a) Sofranko, J. A., Leonard, J. J., and Jones, C. A., J. Catal. 103, 302-10 (1987). (b) Jones, C. A., Leonard, J. J., and Sofranko, J. A., J. Catal. 103, 311-19 (1987).
4. (a) Aika, K.-I., T. Moriyama, N. Takasaki, and E. Iwamatsu, J. Chem. Soc., Chem. Commun. 1210-11 (1986).
5. Hinsen, W., W. Bytyn, and M. Baerns, 8th Int. Cong. on Catal. Proc. III, 581-92 (1984).
6. Ito, T., J.-X. Wang, C.-H. Lin, and J. H. Lunsford, J. Am. Chem. Soc. 107, 5062-68 (1985).
7. Kimble, J. B., and J. H. Kolts, Energy Prog. 6, 226-29 (1986).
8. (a) Lin, C.-H., K. D. Campbell, J.-X. Wang, and J. H. Lunsford, J. Phys. Chem. 90, 534-37 (1986). (b) Lin, C.-H., T. Ito, J.-X. Wang, and J. H. Lunsford, J. Am. Chem. Soc. 109, 4808-10 (1987).
9. (a) Otsuka, K., Q. Liu, M. Hatano, and A. Morikawa, Chem. Lett. 467-68 (1986). (b) Otsuka, K., Q. Liu, M. Hatano, and A. Morikawa, Chem. Lett. 903-06 (1986). (c) Otsuka, K., K. Jinno, and A. Morikawa, J. Catal. 100, 353-59 (1986).

10. Lane G. S., and E. E. Wolf, J. Catal. 105, 386-404 (1987).
11. Lane G. S., and E. E. Wolf, J. Catal. In press.
12. Lane G. S., and E. E. Wolf, Proc. 9th Int. Congress on Catalysis, Calgary (1988).

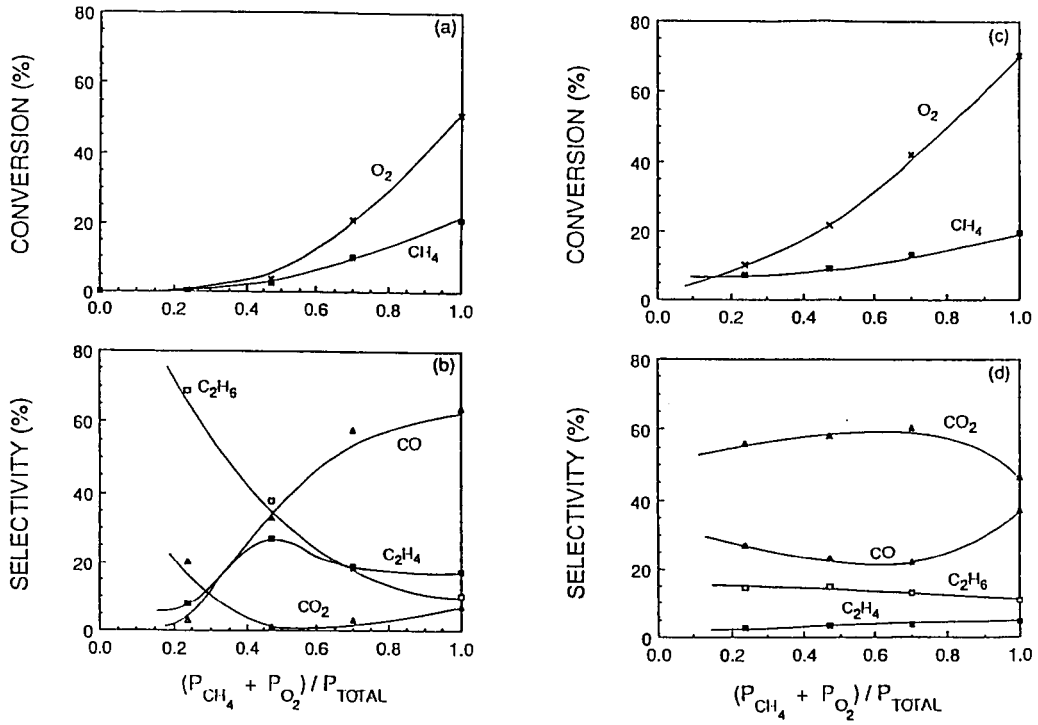

Fig. 1. Effect of dilution on conversion and selectivities at 750°C with a CH_4/O_2 feed mole ratio of 2 and a total flow rate of 50 cc/min. (a) and (b) represent results from a homogeneous study, and (c) and (d) represent results for a 1.0% Li/titania catalyst (250 mg sample).

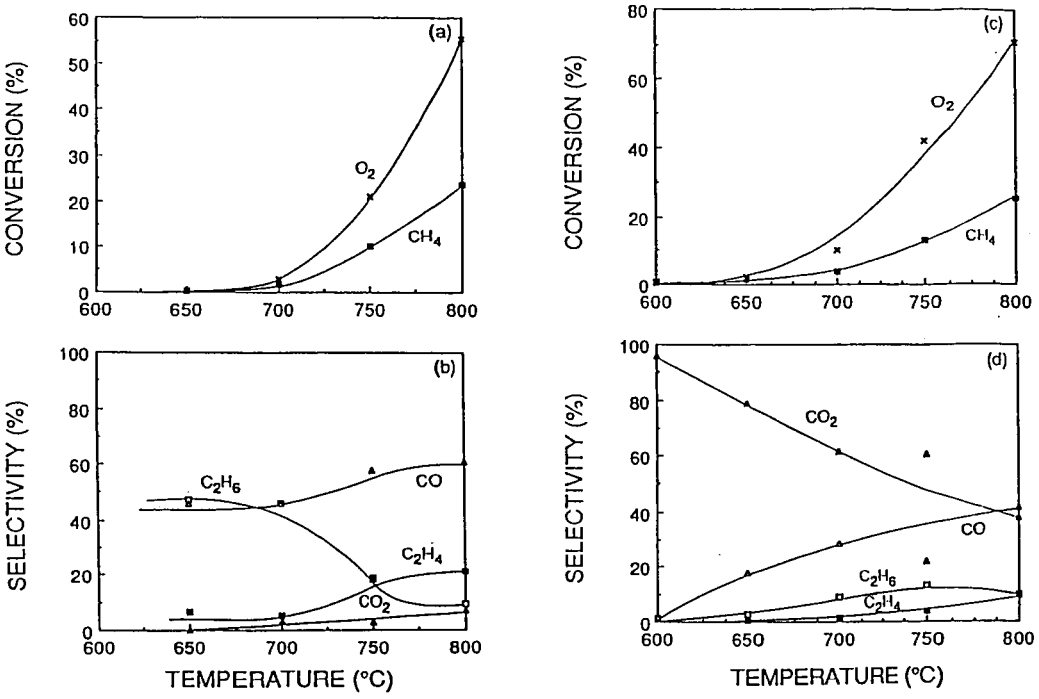

Fig. 2. Comparison of the effects of temperature on conversion and selectivity for a feed flow rate of 50 cc/min, CH_4 and O_2 partial pressures of 0.47 and 0.23, and a dilution ratio of 0.7. (a) and (b) represent results from a homogeneous study, and (c) and (d) represent results for a 1.0% Li/titania catalyst (250 mg sample).

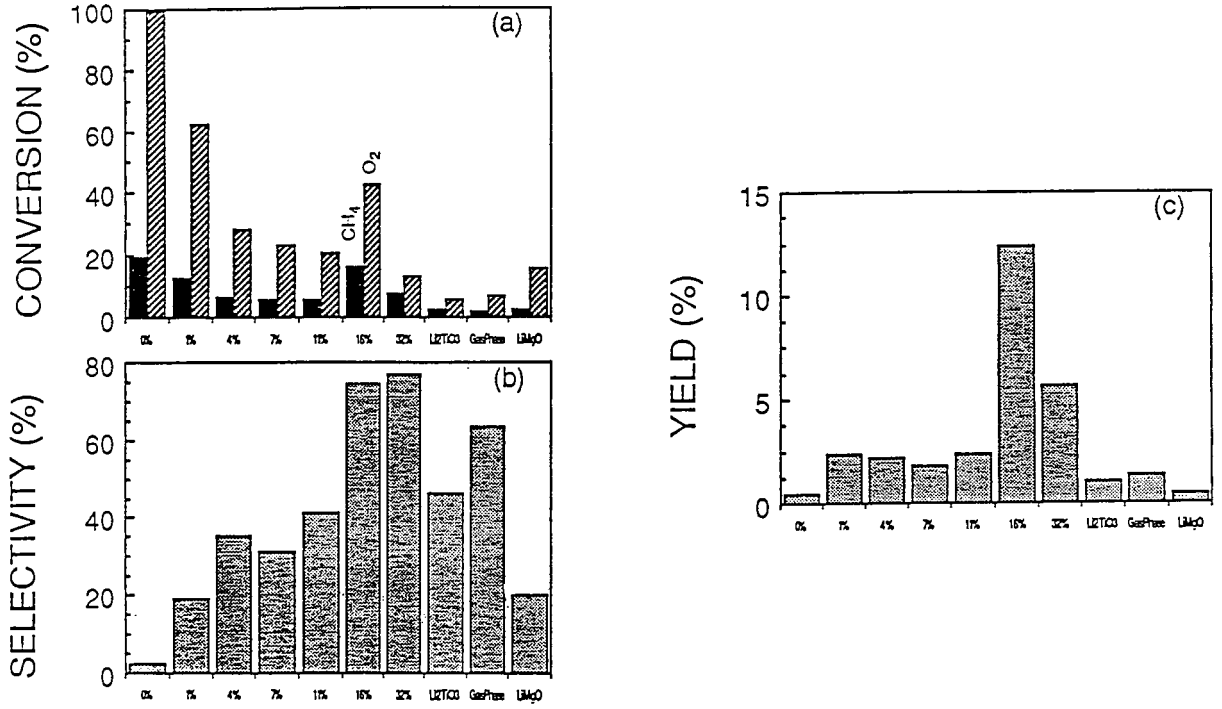

Fig. 3. Comparison of conversions, selectivities, and yields of several catalysts. The results represent samples taken at 800°C and 2 hours time-on-stream with a CH_4/O_2 feed mole ratio of 4, a total flow rate of 100 cc/min, a 250 mg catalyst sample, and a reactant partial pressure of 0.4.

"Kinetics and Mechanism of Methane
Oxidative Coupling over Samarium Oxide"

M. -Y. Lo, S. N. Kamat, and G. L. Schrader

Department of Chemical Engineering and
Ames Laboratory - USDOE
Iowa State University
Ames, Iowa 50011

Introduction

The direct conversion of methane to higher hydrocarbons is a promising process for the chemical utilization of methane, which is a major component of natural gas. Although many metal oxides (1,2) have proven to be active and selective for the direct conversion of methane to form C_2 hydrocarbons, there has been no general agreement on the mechanism of methane coupling. Lunsford and co-workers (3) studied the oxidative coupling of methane over Li/MgO and a series of rare earth oxide catalysts. Their results suggested that methyl radicals are formed during methane activation and the coupling of methyl radicals in the gas-phase is the major route for C_2 hydrocarbons formation. On the other hand, Carreiro and Baerns (4) and Asami et al. (5) studied the oxidative coupling of methane over lead oxo-salts and PbO/MgO catalysts, respectively. Their results suggested that ethane is formed from the coupling of adsorbed methyl radicals on the catalysts surface.

In addition, the types of oxygen species used for the activation of methane or for the subsequent reactions of activated methane are not very well defined. Lunsford and co-workers (3) suggested that O^- is responsible for the activation of methane and O^{2-} and/or $O_2(g)$ are used for carbon oxides formation on Li/MgO catalysts. Otsuka and Nakajima (6) suggested that adsorbed O_2 is responsible for the activation of methane and $O_2(g)$ is responsible for the formation of carbon oxides over Sm_2O_3.

Lo et al. (7) studied the adsorption of methanol, methyl iodide and methane over Sb_2O_4/SiO_2 using NMR spectroscopy. They observed the formation of methoxy species over the catalyst surface; this intermediate is the precursor for carbon dioxide formation.

The purpose of the present study is to use samarium oxide as a model catalyst to investigate the mechanism of methane coupling at atmospheric pressure using oxygen as the oxidant.

Experimental Procedure

Catalysts preparation

Samarium oxide (Sm_2O_3) catalysts were prepared from various samarium oxides and salts. Different calcination temperatures were employed also.

(1) Hydrothermally (HT) treated samarium oxide was prepared by placing Sm_2O_3 (Aldrich 99.9%) in a beaker containing deionized water. Residues obtained after evaporization of the water were calcined at 800°C for 16 h and 800°C for 4 h.

(2) Samarium oxide was heated to 1100°C for 22 h.

(3) Samarium nitrate hexahydrate was calcined at 900°C for 1 h.

XRD was used to determine the phases present. Surface areas were determined from BET measurements using N_2 as the adsorbate at 77 K.

Reaction studies

Methane oxidation was studied using a laboratory scale fixed-bed reactor system which could be operated in either flow or pulse modes. The reactor consisted of a 7 mm ID and 19 mm length quartz tubes which act respectively as the pre-heating and catalytic zone of the reactor. The 7 mm ID tube was fused to a 6 mm OD, 1 mm ID capillary quartz tube in order to reduce the extent of post-catalytic reaction giving rise to combustion products.

Blank experiments were performed at a temperature range of 600°C to 775°C with quartz wool placed in the reactor. Catalytic tests and kinetic studies were performed using the flow mode of the reactor system at atmospheric pressure. 0.2 to 0.8 g_1 of catalyst was used, and the flow rate ranged from 100 to 300 cc min^{-1}. Excess CH_4 was used in the reactant mixtures such that $CH_4/O_2 \geq 3$. Effluent gases were analyzed using an on-line gas chromatograph with a thermal conductivity detector. CO, O_2, and CH_4 were analyzed using a molecular sieve 5Å column and O_2(CO), CO_2, CH_4, C_2H_6, C_2H_4 and H_2O were analyzed using a Porapak Q column. Pulse experiments were performed using the pulse mode of the reactor system at a total flow rate of 25 cc min^{-1} with or without gas-phase oxygen. Pulse experiments using CH_3I or CH_3OH as reactants involved injection of either reactant at the reactor inlet.

Results and Discussion

The XRD powder patterns for the catalysts prepared in this study are shown in Figure 1. The catalyst prepared by hydrothermally treated Sm_2O_3 shows the presence of two phases, B (monoclinic structure) and C (cubic structure) phases (8,9). The C phase was the major component of this catalyst. The catalyst prepared by calcining Sm_2O_3 at 1100°C for 22 h shows the presence of the B phase only, and the catalyst prepared by calcining $Sm(NO_3)_3 \cdot 6H_2O$ at 900°C for 1 h shows the presence of the C phase only. These results suggested that the phase composition of the catalyst is dependent on the salt used and the calcination temperature employed.

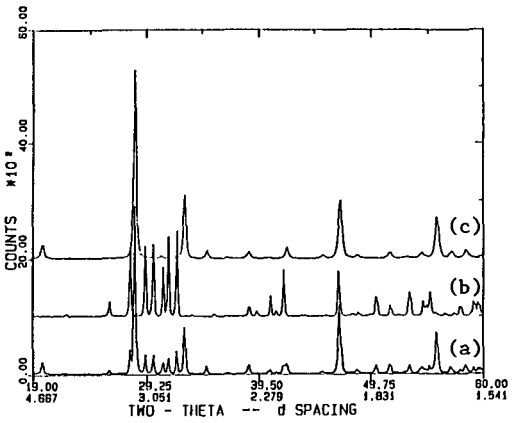

Figure 1. XRD powder patterns of samarium oxide prepared by (a) HT treatment of Sm_2O_3 (B and C phases), (b) Sm_2O_3 calcined at 1100°C for 22 h (B phase), (c) $Sm(NO_3)_3 \cdot 6H_2O$ calcined at 900°C for 1 h (C phase).

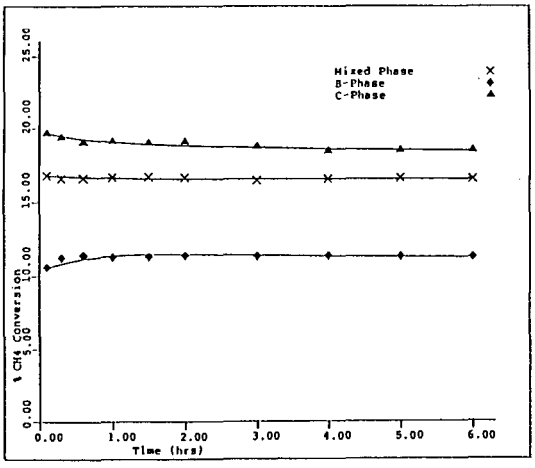

Figure 2. Time dependence on methane conversion over Sm_2O_3 catalysts prepared in this study at 750°C, $CH_4/O_2/He$ = 58/12/115.

Blank experiments revealed that the conversion of methane was less than 1% with carbon oxides being the only products. This suggests that the reaction of methane over samarium oxide is surface initiated.

Table 1 shows the activity of methane coupling over untreated (used as obtained from Aldrich Chemical Co.) and hydrothermally treated Sm_2O_3 at steady state. The conversion of methane are practically the same for both catalysts. In addition, although the selectivity to CO is higher for the untreated catalyst, the total yield to carbon oxides and to C_2 hydrocarbons are constant for both catalysts. These data suggest that the two catalysts behave quite similar towards methane coupling. One possible explanation to this similarity is that the untreated catalyst has been on stream (CH_4/O_2 = 3) for several hours at 700°C. During this time period, the catalyst is continually exposed to water.

Figure 2 shows the conversion of methane over the three Sm_2O_3 catalysts prepared in the present study. Among the three catalysts tested, C-phase Sm_2O_3 is the most active and B-phase Sm_2O_3 is the least active for methane coupling. Figure 3 shows the selectivity to C_2 hydrocarbons over the three catalysts prepared. This figure shows that the HT-treated Sm_2O_3 catalyst gives the highest C_2 selectivity and B-phase Sm_2O_3 gives the lowest C_2 selectivity. In conclusion, C-phase Sm_2O_3 and HT-treated Sm_2O_3 catalysts show a similar C_2 yield for methane coupling. Since most methane coupling studies over Sm_2O_3 catalysts employ mixed phase Sm_2O_3 (B and C phases). The present study will employ HT-treated Sm_2O_3, which consists of B and C phases, as the test catalyst for kinetic and mechanism study.

Figure 4 shows the effect of CH_4/O_2 ratio on methane conversion and product distribution for methane coupling over Sm_2O_3 at 750°C. High conversions of methane and high selectivity to carbon dioxide are obtained at low CH_4/O_2 ratios. On the other hand, high CH_4/O_2 ratios favor the formation of C_2H_6 in the expense of methane conversion.

Figure 5 shows the activity of methane coupling as a function of CH_4/O_2 time on stream over HT-treated Sm_2O_3. No appreciable changes in either CH_4 conversion or product selectivities are observed after the catalyst has been used for 20 h. This suggests that the present Sm_2O_3 catalyst is much more stable than the other unpromoted low melting metal oxides (such as lead oxide) in which catalyst deactivation due to catalyst volatility is a serious problem.

Rate laws of the form:

$$\frac{d[\text{product}]}{dt} = k[CH_4]^m[O_2]^n$$

were determined for the formation of the principal products (CO, CO_2 and C_2H_6) in kinetic studies. Nonintegral reaction orders in both methane and oxygen were obtained for the formation of CO and C_2H_6. These results suggest that the rate-determining step for C_2H_6 formation is the reaction between methane and adsorbed oxygen (0.9 order in CH_4 and 0.6 order in O_2

Table I. Activity of methane coupling over untreated and hydrothermally treated Sm_2O_3 at 700°C, CH_4/O_2 = 3.

Catalysts	% CH_4 Conversion	% Selectivity			
		CO	Co_2	C_2H_4	C_2H_6
Untreated Sm_2O_3	21.9	17.1	38.0	20.9	24.0
HT treated Sm_2O_3	21.2	11.7	46.2	19.9	22.2

Table II. Product distribution of methane coupling over Sm_2O_3 as a function of the # of the pulse at 800°C, $O_2/CH_4/He$ = 2-0/5-7/130 with 0.4 g of catalyst.

# of pulse	Rate of product formation (μmole/min g)			
	CO	CO_2	C_2H_6	C_2H_4
1	17.2	101.1	6.8	14.6
2	19.7	90.9	6.7	14.0
3	17.2	87.7	6.4	13.8
4[a]	--	--	--	--
5	10.7	79.9	4.5	13.1
6	9.8	56.4	3.8	11.0
7	13.5	42.2	3.2	11.0
8	23.2	38.9	2.7	10.6
9	24.9	37.2	2.2	8.9
10	21.4	27.9	3.0	8.9
reoxidation, 11 (20 cc)[b]	22.2	104.8	6.9	13.3
reoxidation, 12 (10 cc)	21.5	70.9	7.2	13.1
reoxidation, 13 (5 cc)	20.9	46.9	6.8	9.1

[a]Molecular sieve 5A column was used to analyze the products formed from this pulse experiment to determine whether all O_2 are consumed during this pulse. It was found that all O_2 are consumed during all pulse experiments.

[b]Reoxidation was done by passing O_2 pulses through the catalyst until no O_2 uptake has taken place, the value in the parenthesis reflects the flow rate of oxygen used during pulse exit.

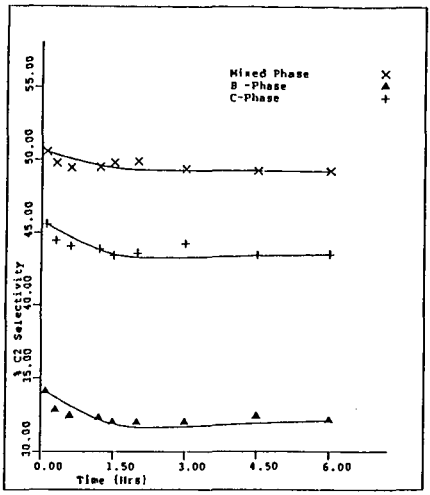

Figure 3. Time dependence on C_2 hydrocarbons selectivity over Sm_2O_3 catalysts prepared in this study at 750°C, $CH_4/O_2/He$ = 58/12/115.

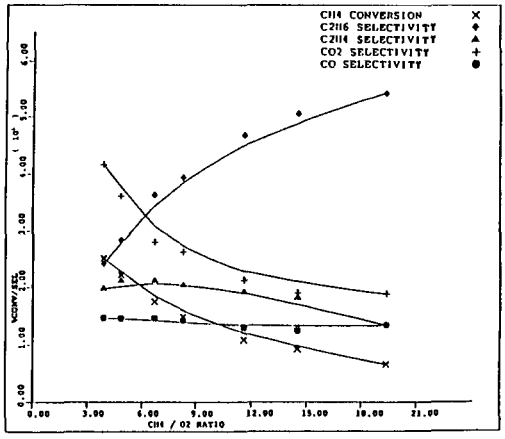

Figure 4. Effect of CH_4/O_2 ratio on methane coupling over HT treated Sm_2O_3 (B + C phases) at 750°C, total flow = 174 cc min^{-1}.

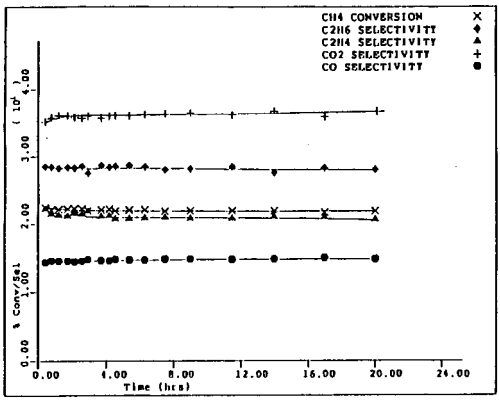

Figure 5. Time dependence on methane coupling over HT treated Sm_2O_3 (B + C phases) at 750°C, $CH_4/O_2/He$ = 58/12/115.

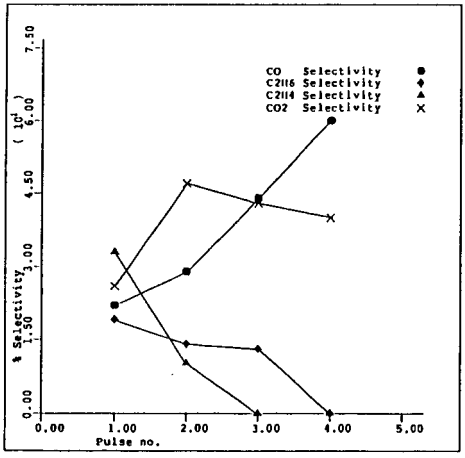

Figure 6. Product distribution in pulsed conversion of methane over HT treated Sm_2O_3 at 800°C in the absence of oxygen. Pulse size = 0.5 mL, CH_4/He = 57/130.

for a CH_4/O_2 ration ranging from 4.5 to 18). Rate dependences for CO_2 formation were first order in oxygen and a negative order in methane. This suggests that gas-phase oxygen or adsorbed molecular oxygen (or both) are used for CO_2 formation. In addition, the inhibition effect of CH_4, as indicated by the negative order, may be one reason why a 93% selectivity to C_2 hydrocarbons is obtained at very high CH_4/O_2 ratios, i.e., CH_4/O_2 = 45 (2).

The types of oxygen used for methane activation as well as the subsequent reactions of activated methane was investigated by using the pulse reaction studies. Figure 6 shows the product distribution obtained for the pulse reaction with CH_4 as the only reactant. Consecutive CH_4 pulses led to an immediate decrease in the formation of both C_2H_6 and C_2H_4. No C_2H_4 is observed after the second pulse and no C_2H_6 is observed after three pulses. The total amount of oxygen used for the formation of oxygenates during the first three pulses is less than one monolayer of oxygen (assuming an oxygen packing density of 1×10^{19} atoms/m^2). This suggests that only surface oxygen species are used for the formation of C_2 hydrocarbons. This result is in good agreement with the kinetic data in which the rate-determining step for C_2H_6 formation is found to be the reaction between gaseous methane and adsorbed monoatomic oxygen. This also suggests that the mobility of bulk oxygen to the surface is slow compared with the rate of C_2H_6 formation.

Table II provides the product distribution for the pulse experiments performed by co-feeding methane and oxygen ($CH_4/O_2/He$ = 5.7/2/13) to the reactor. Despite the fact that a high O_2/CH_4 ratio was used, the rate of products formation declined as the pulse experiment progressed. This suggests that adsorbed oxygen species is involved in the formation of products. If only gas-phase oxygen were required we would expect to observe a constant rate of product formation.

The results also show that the decrease in the rate of CO_2 formation is much faster than the rate of the replenishment of oxygen species on the surface of the catalyst. This result is in good agreement with the kinetic data in which the rate of CO_2 formation is reoxidation limited.

The rate of formation of C_2H_6 and C_2H_4 also decreased as the pulse number increased, but to a lesser extent compared to the decrease in the rate of CO_2 formation. However, when the catalyst is reoxidized with O_2 prior to CH_4/O_2 pulses, the rate of C_2H_6 formation is independent to the partial pressure of oxygen in the reactant (pulses #11 to 13). This indicates that the catalyst is partially reduced at steady state since a partial dependency on O_2 partial pressure is observed in kinetic studies.

In addition, since the replenishment of oxygen species for CO_2 formation is slow and is the rate-determining step for CO_2 formation, suppression in this replenishment of oxygen species may lead to an increase in C_2 yield. This also explains why a 93% in C_2 selectivity is obtained by Otsuka *et al.* (2) when CH_4/O_2 = 45 was used. In such experiments, replenishment of surface oxygen for CO_2 formation is suppressed.

It is generally accepted that the breaking of a C-H bond of methane is the rate-determining step in methane coupling. As a result, methyl radical or radical-like intermediates are formed. The details on the subsequent steps of these intermediates are not very clear yet. The use of methanol or methyl iodide as reactants, in conjunction with the pulse technique, has permitted the subsequent steps following methane activation to be probed. The major products formed from methanol and methyl iodide are methane, carbon dioxide and carbon monoxide. Less than 10% of C_2 hydrocarbons are formed in both reactions. These results suggest that methoxy species is a common intermediate formed from both methanol and methyl iodide, as well as methane. This methoxy species will form either carbon oxides or methane, plus ethane in cases where methane is the reactant, depending on the availability of surface oxygen. Since less than 10% of C_2 hydrocarbon are formed, it seems reasonable to conclude that the coupling of gas-phase methyl radical is a major pathway for ethane formation during methane coupling.

References

(1) G. E. Keller and M. M. Bhasin, J. Catal. 73, 9 (1982).
(2) K. Otsuka, K. Jinno and A. Morikawa, Chem. Lett., 499 (1985).
(3) (a) K. D. Campbell, E. Morales and J. H. Lunsford, J. Am. Chem. Soc., 109, 7900 (1987);
(b) K. D. Campbell, H. Zhang and J. H. Lunsford, J. Phys. Chem., 92, 750 (1988).
(4) J.A.S.P. Careiro and M. Baerns, React. Kinet. Catal. Lett., 35, 349 (1987).
(5) K. Asami, T. Shikada, K. Fujimoto and H. Tominaga, Ind. Eng. Chem. Res., 26, 2348 (1987).
(6) K. Otsuka and T. Nakajima, J. Chem. Soc., Faraday Trans., 83, 1315 (1987).
(7) M.-Y. Lo, S. K. Agarwal and G. Marcelin, to be published, Catal. Today.
(8) L. Pauling, Z. Krist., 69, 415 (1928).
(9) R. M. Douglass and E. Staritzky, Anal. Chem., 28, 552 (1956).

Oxidative Coupling of Methane on a Mixed Oxide Catalyst.

Ananth Annapragada and Erdogan Gulari
Department of Chemical Engineering
University of Michigan, Ann Arbor, MI-48109.

We have developed a family of catalysts for the oxidative coupling of methane which achieve high activities and selectivities at temperatures lower than those currently in the literature. Typical figures are: At 575 °C, GHSV = 28800 Hr^{-1}, CH_4/O_2 = 2, total conversion = 11%, C_2 selectivity = 43%. In this paper, we plan to present the development of the catalyst, and our results on the identification of the active components. In addition we will also discuss our steady state, pulse and TPR experiments which have lent some insight into the mechanism of the reaction.

Our steady state activity measurement experiments identified that the catalyst was active both in unsupported and supported form. In general, the unsupported catalyst was more difficult to activate than the supported catalysts. Also, the unsupported catalyst had a much lower range of active compositions than the supported catalyst. We attribute this to the possible existence of a wider distribution of crystal phases in the supported catalyst. The fact that the most active compositions in both supported and unsupported catalysts occured at the same composition of active components led us to believe that a characterization of the active species in the unsupported catalysts would give us some information about the active species in the supported catalysts. X-ray diffraction and ESCA studies identified a unique species in the active unsupported catalysts. However, this material in pure form was not active as a methane coupling catalyst. We concluded that some complex interaction between this species and the others in the active catalyst was the cause for the activity.

One of the problems we encountered during steady state studies on the catalyst was the fact that a catalyst composition which was active on one occasion was not necessarily active on another occasion under identical conditions. In general, active compositions would achieve a high level of activity approximately 45% of the time. This indicated the existence of multiple steady states either in the in-situ preparation of the catalyst or in the reaction itself. TPR studies indicated

that temperature hysteresis and multiple steady states did indeed exist for the coupling reaction in the vicinity of our operating conditions. Surface titration experiments on the catalysts operating in each of the two steady states indicated a difference in the way oxygen was incorporated into the catalyst during operation at the higher steady state.

Steady state activation energy measurements and suitably designed pulse experiments revealed that the reaction possibly occured by the following steps:

(1) Hydrogen abstraction from the methane to form CH_3- species.

(2) Coupling of the CH_3- species to C_2H_6.

(3) Pyrolysis of the Ethane to Ethylene.

(4) Oxidation of the Ethane and Ethylene to CO and CO_2.

At this point we can only speculate, but we believe that the first two steps occur on the surface of the catalyst, while the last two occur in the gas phase. We attribute the success of this catalyst to its ability to abstract hydrogen from methane at a temperature low enough to support reversible oxygen incorporation into the catalyst.

ELECTROCHEMICAL STUDIES OF OXYGEN ACTIVITY DURING THE OXIDATIVE COUPLING OF METHANE

By
Jeffrey W. McKown and Howard M. Saltsburg

Department of Chemical Engineering
University of Rochester, Rochester, NY 14627

When studying the kinetics of heterogeneous catalytic reactions, it is crucial to be able to measure the surface concentrations under actual reaction conditions. Unfortunately, there are virtually no techniques currently available which permit the measurement of these surface concentrations under the atmospheric pressures and high temperatures that most catalytic reactions occur. In this work we report the measurement of the thermodynamic activity of oxygen on the surface of a Li promoted MgO catalyst during the oxidative coupling of methane. This measurement provides additional information which may be utilized in the description of the different reactions responsible for the formation of the coupling and deep oxidation products.

The measurement of the thermodynamic activity of oxygen on catalytic metal films was first reported in 1976 by Vayenas and Saltsburg in a study of the oxidation of SO_2 over Pt (1,2). An electrochemical cell consisting of two porous catalytic Pt films separated by an oxide conducting solid electrolyte was utilized in these oxygen activity measurements. It has been shown that the oxygen activity on the metal films is related to the measured EMF through the Nernst equation. The surface oxygen activity is directly related to the surface oxygen concentration and its measurement subsequently provides information about reactions involving the surface oxygen.

This technique has been extended by McKown (3) so that the thermodynamic activity of oxygen on metal oxide catalysts may be measured under reaction conditions. It was demonstrated that an electrochemical based oxygen sensor similar to that utilized by Vayenas and Saltsburg was capable of measuring a mobile oxygen species on the oxide catalyst surface. In this manner, the effect that the oxidative coupling of methane reaction is having on the surface oxygen species may be monitored.

The oxygen activity on a Li promoted MgO catalyst was monitored along with overall conversion and selectivity for a variety of reaction conditions. It was found that in the presence of the coupling reaction, the measured surface oxygen activity was always lower than its equilibrium value. Furthermore, the extent of deviation from oxygen gas-surface was observed to be a function of reaction conditions. It was deduced that a reaction involving the mobile surface oxygen was responsible for the lowered steady state amount of surface oxygen. The magnitude of this deviation from equilibrium between oxygen in the gas and on the catalyst surface must then be related to the rate of reaction depleting the mobile surface oxygen.

As the selectivity for the formation of the C_2 products increased, the deviation from equilibrium between oxygen in the gas and oxygen on the catalyst surface was also observed to increase. Since an increased deviation from gas-surface equilibrium indicates an increased rate of reaction involving surface oxygen, it was concluded that the production of the C_2 products, C_2H_4 and C_2H_6, must involve a mobile surface oxygen species. Similar arguments can be employed to deduce that the C_1 products, CO and CO_2, must be formed primarily by a reaction with oxygen from the gas.

Lunsford et. al. (4,5) were able to characterize the active center responsible for the activation of the CH_4 molecule in the Li promoted MgO catalyst using ESR. We have combined their active site characterization with our oxygen activity measurements in a mechanism which is based heavily on experimental observations.

We have demonstrated the ability to measure a quantity which is directly related to the surface oxygen concentration on a metal oxide catalyst under actual reaction conditions. This technique has provided vital information about the types of reactions responsible for the selectivity in the oxidative coupling of methane.

The authors would like to thank the Petroleum Research Fund for partial support of this research.

LITERATURE CITED

1. Vayenas, C., Ph.D. Thesis, University of Rochester (1976).
2. Vayenas, C., Saltsburg H., *J.Cat.*, **57**, 296 (1979).
3. McKown, J.W., Ph.D. Thesis, University of Rochester.
4. Ito, T., Wang, J., Lin, C., Lunsford, *JACS*, **107**, 5062-5068 (1985).
5. Wang, J., Lunsford, J., *J. Phys. Chem.*, **90**, 5883-5887 (1986).

THE PARTIAL OXIDATION OF METHANE AND ETHANE ON WELL-CHARACTERIZED VANADIUM OXIDE SURFACES

K. Lewis, T. Oyama, and G. A. Somorjai
Department of Chemistry and Materials and
Chemicals Sciences Division
Lawrence Berkeley Laboratory
University of California
Berkeley, California 94720

Vanadium oxide ordered thin films were grown by condensing vanadium metal onto gold single crystal surfaces then oxidizing it. Films of V_2O_5 could also be produced by condensing V_2O_5 onto gold. After characterization by various surface science techniques, chemisorption studies were carried out to study the bonding of CH_4, C_2H_6 and O_2. A high pressure cell was then used to carry out partial oxidation studies and the results were correlated with those obtained on silica supported high surface area V_2O_5 catalyst.

SYMPOSIUM ON CATALYTIC AND RELATED CHEMISTRY OF METHANE

PRESENTED BEFORE THE DIVISION OF FUEL CHEMISTRY INC.

AMERICAN CHEMICAL SOCIETY

LOS ANGELES MEETING, SEPTEMBER 25-30 1988

SELECTIVE OXIDATION OF METHANE TO FORMALDEHYDE OVER VARIOUS CATALYSTS

By

G. N. Kastanas, G. A. Tsigdinos and J. Schwank

University of Michigan, Department of Chemical Engineering, Ann Arbor, Michigan 48109

INTRODUCTION

The conversion of methane into useful intermediate oxidation products instead of complete oxidation to CO_2 or partial oxidation to CO is one of the most challenging problems for catalysis research (1). Oxidative coupling leading to the formation of ethane and ethylene from methane (2), (3), (4) and production of oxygenates as methanol and formaldehyde (5) , (6), (7), (8) are the two main directions pursued so far and several promising systems have emerged although with low yields. The ultimate goal is to obtain useful intermediates as higher hydrocarbons and/or oxygenates from the main source of methane, the natural gas.

RESULTS AND DISCUSSION

Activity of Vycor- Quartz reactor tubes

Vycor glass has proven to be active in the n-butene isomerization at room temperature (9) as well as in the adsorption of ammonia at 150 °C (10). It was generally believed that the surface hydroxyl groups played an important role in the adsorption, being capable of forming hydrogen bonds with the adsorbates. Sheppard and Yates studied the interaction of various molecules with Vycor glass by infrared spectroscopy (11) . In the case of methane a new band, not present in the gas phase spectrum appeared, and it was attributed to physical adsorption. Similar infrared spectroscopy results were obtained in a study of the adsorption of methane on ZSM-5 zeolites by Yamazaki et al (12). Cheaney and Walsh (13) observed a high activity of Vycor glass tubes in the combustion of methane. They attributed the activity to the deposition of a silicic acid layer on the glass

surface during the manufacture of the Vycor glass which included a treatment with HF. When silica tubes were coated with silicic acid, the high CH_4 combustion activity of the Vycor tubes could be reproduced (13).

Throughout the course of our work a small amount of ethane , from 0.14 mol % to 1.25 mol % based on methane was present in the feed stream. Table 1 summarizes the total conversion of methane and the selectivities of the various products obtained in our work over quartz and Vycor glass tubes. At a CH_4/O_2 molar ratio of about 1 and over the temperature range of 893 to 993 K both tube surfaces produced C_2H_4 , C_2H_6 , HCHO and CO_2. The formaldehyde was identified by Gas Chromatography and Mass Spectrometry. Under the reaction conditions used here, CO was observed only over Vycor glass at temperatures > 940 K. The CO production occurred mainly at the expense of HCHO. At a given temperature, the total methane conversion, over Vycor glass was much higher than the one over quartz. At similar conversions (0.41% at 928 K for Vycor glass and 0.37% at 993 K for quartz) the CO_2 selectivity over Vycor glass was much lower than the one observed over quartz whereas the HCHO selectivity was somewhat higher. The very substantial differences in activity and selectivity between Vycor and quartz reactors despite identical flow conditions and reactor geometries imply that gas interactions sensitive to the nature of the tube surfaces occur. However , in view of the high temperatures, a contribution of gas phase reactions cannot be ruled out.

The residence time has a very significant effect on the product distribution. Fig. 1 illustrates this effect for a quartz reactor at 993 K where the residence time was increased from 3.3 s to 13.2 s by reducing the flowrates by a factor of four while keeping the CH_4 / O_2 ratio close to 1. The total methane conversion increased from 0.3% to 2.52% . At a residence time of 3.3 s the formaldehyde selectivity was 60% and the combined C_2H_4 and C_2H_6 selectivity was 27%. The remaining 13% consisted of CO_2. The short residence time quartz runs did not produce any CO. At the long residence time run of 13.2 s CO was generated at the expense primarily of HCHO. This implies that long residence times increase the probability of CO formation via the decomposition of HCHO, a reaction sequence analogous to that observed in the combustion of methane (14) . Similar residence time effects were observed in the Vycor reactors.

The methane to oxygen ratio is another important factor influencing the product distribution. Oxygen rich mixtures strongly favor the overall rate of methane reaction and the rate of CO formation (at the expense of formaldehyde). In view of the blank activity of the quartz, an upper temperature limit of 893 K was imposed on runs with catalyst powders placed into quartz reactors.

Activity of silica based compounds

Various silica based compounds in powder form, including silicic acid, Cab-O-Sil, and Ludox gel exhibited similar trends of methane conversion as the empty Vycor and quartz reactors, although at much lower temperatures. Methane to oxygen ratios lower than one enhanced the activity of these catalysts, in accordance with the behavior observed in the Vycor brand and quartz tubes. Short residence times favored the selectivity of HCHO .

Table 2 compares the overall rate of methane reaction and the selectivity over the various silica compounds for a CH_4 /O_2 ratio of close to1 at a temperature of 893 K. The rate of reaction is reported in two different ways, based on the weight and the surface area of the catalysts as determined after the reaction.

TABLE 1

Conversion and selectivity achieved over Vycor and quartz U tubes at CH_4 / O_2 =1.14

	T(K)	% total methane conversion	% Selectivity				
			C_2H_4	C_2H_6	HCHO	CO	CO_2
Vycor	893	0.26	2	15	81	-	2
	913	0.31	3	13	81	-	3
	928	0.41	4	17	76	-	3
	943	0.95	4	12	44	35	5
	958	1.44	4	15	40	37	4
	973	2.26	5	17	34	41	3
	993	3.93	7	19	27	45	2
quartz	963	0.13	8	13	62	-	17
	993	0.37	9	18	60	-	13

Flowrates : 10% CH_4 in Ar=29.7 cm^3 STP /min, O_2=2.6 cm^3 STP/min. P= 205 kPa

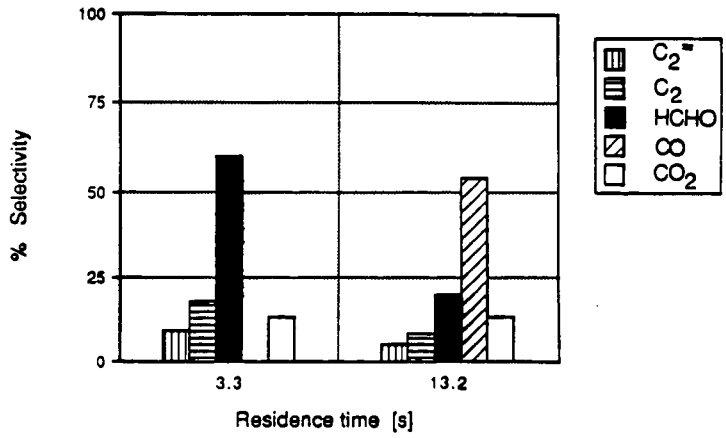

FIGURE 1 CH_4 oxidation over empty quartz reactors. Effect of the residence time on the product distribution at 993 K and CH_4 / O_2 close to 1

TABLE 2

Activity and selectivity of various silica compounds at 893 K and CH_4 / O_2 close to 1

Compound	Pressure [kPa]	Overall CH_4 reaction rate [mol / g s]	Overall CH_4 reaction rate [mol / m^2 s]	Surface area after reaction [m^2 / g]	% Selectivity C_2H_4	HCHO	CO	CO_2
Silicic acid	218[a]	1.98 E-7[c]	0.72 E-9	274	1	23	66	10
	340[b]	2.6 E-7	0.95 E-9	274	7	47	37	9
	515[b]	4.2 E-7	1.53 E-9	274	1	26	63	11
Cab-O-Sil	308[b]	2.75 E-7	1.44 E-9	191	1	30	44	24
Ludox gel	377[b]	0.9 E-7	0.87 E-9	105	1	27	67	5

[a] Flowrates: 10% CH_4 in Ar=29.7 cm^3 STP / min, O_2=2.6 cm^3 STP / min. [b] Flowrates: 10% CH_4 in Ar= 46.8 cm^3 STP / min, O_2=5.2 cm^3 STP / min. [c] 1.98E-7 corresponds to $1.98X10^{-7}$

All three catalysts produced C_2H_4, HCHO, CO and CO_2 . From the silicic acid runs , a trend emerged of increasing rate of methane reaction with increasing pressure. On a weight basis, silicic acid and Cab-O-Sil were more active than Ludox gel. When normalized on a surface area basis the differences in reaction rates became less pronounced. Therefore, it is very likely that the high per weight activities of silicic acid and Cab-O-Sil can be attributed to their high surface areas . A similar surface area effect could also explain the relatively high blank activity of empty Vycor glass reactors compared to the quartz reactors. Vycor glass is much more porous than quartz, and consequently, Vycor has a higher surface area.

Figure 2 shows the Arrhenius plots for the overall rate of CH_4 reaction as well as for the rates of formation of C_2H_4, HCHO, CO and CO_2 over silicic acid at a pressure of 585 kPa . The temperatures were randomly selected within the range of 783 - 893 K . Very good linear fit of the Arrhenius plots was achieved excluding the possibility of substantial catalyst deactivation from one run to the next. In the case of formaldehyde, however , at temperatures higher than 853 K a deviation from linearity was observed in the Arrhenius plot, probably due to secondary reactions of formaldehyde to CO and CO_2. The apparent activation energies for the overall rate of methane reaction and the formation of the various products are summarized in Table 3. For comparison, the apparent activation energy values for methane oxidation in empty Vycor glass tubes were also determined . The 95% confidence intervals used to estimate the activation energy error margin are also given in Table 3.

The apparent activation energies over silicic acid were generally lower than those over Vycor glass. On both silicic acid and Vycor glass , the apparent activation energy values for formaldehyde were very low and had within experimental error the same value.

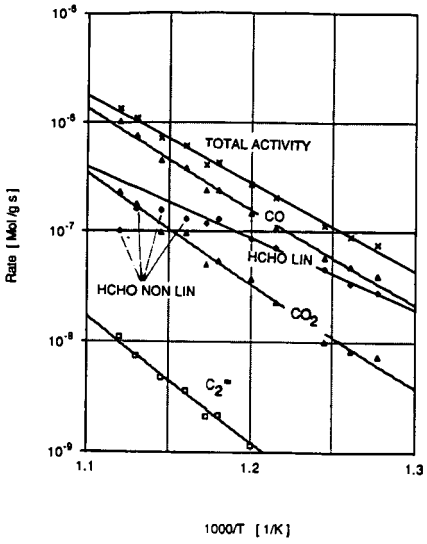

FIGURE 2 Arrhenius plots for silicic acid at 585 kPa and 783-893 K. Flowrates : 10% CH_4 in Ar=39.8 cm^3 STP / min, O_2=4 cm^3 STP / min . The plot for HCHO is divided into a linear (HCHO LIN) and non linear portion (HCHO NON LIN)

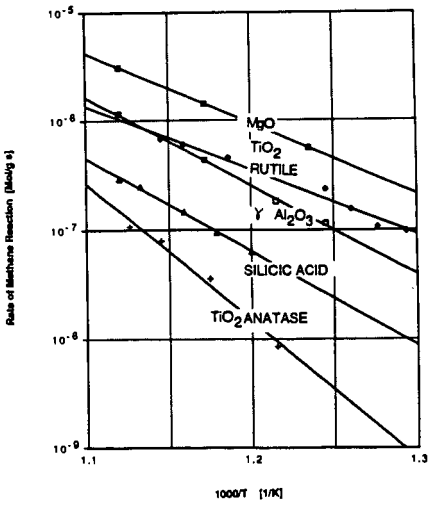

FIGURE 3 Arrhenius plots for the methane reaction rates over MgO (P=205 kPa, CH_4/O_2=1), Gamma Al_2O_3 (P=294 kPa, CH_4 / O_2=0.1), Silicic acid (P=380 kPa, CH_4/O_2=1), TiO_2 rutile (P=515 kPa, CH_4/O_2=1) and TiO_2 anatase (P=510 kPa, CH_4/O_2=1)

TABLE 3

Apparent activation energies for the rate of methane reaction and rates of product formation over silicic acid (at 585 kPa, 783 -893 K) and Vycor glass (at 205 kPa, 893-993 K).

	Silicic acid [kJ/mol]	Vycor glass [kJ/mol]
Overall CH_4 Reaction	154 ±10	217 ± 49
C_2H_4	213 ±18	299± 39
C_2H_6	(not formed)	236 ±59
HCHO	125 ±15 (linear portion of plot)	123 ±19
CO	171 ± 15	264 ± 34
CO_2	184 ±18	(non linear)

This might imply that once the methane molecule is activated the formation of formaldehyde is not dependent on the nature of the catalytic surface and probably occurs in the gas phase. The difference in the activation energy for CO , however, suggests that the subsequent oxidation and/or decomposition of formaldehyde is sensitive to the nature of the catalytic surface or reactor walls.

The deactivation characteristics of silicic acid were also studied by monitoring its activity over a long time period. The methane oxidation activity maintenance was excellent over a period of 16 hrs at 863 K.

Effect of catalyst acidity

In order to investigate the effect of catalyst acidity on methane oxidation, MgO, gamma Al_2O_3 as well as two forms of TiO_2 , rutile and anatase, were selected for a comparison with silicic acid. Figure 3 shows the rates of the overall methane reaction over these materials in the form of Arrhenius plots. The basic MgO was the most active catalyst. The rates over gamma alumina and rutile were of the same order of magnitude. The lowest rates were obtained over the anatase. Under our reaction conditions, only the moderately acidic silicic acid and the anatase produced formaldehyde. The formaldehyde yields over the anatase, however, were much lower than the ones over the silicic acid. Gamma Al_2O_3 and MgO do not seem to preserve formaldehyde, yielding instead deep oxidation products CO and CO_2. Rutile drives the reaction to complete oxidation, producing almost exclusively CO_2 . The very substantial difference between the activity the rutile and anatase TiO_2 forms could be attributed to different oxygen adsorption characteristics, possibly induced by the open structure of the rutile (15).

In the case of the gamma Al_2O_3 and MgO , the CO_2 selectivity increased with temperature at the expense of CO, whereas for silicic acid the CO_2 selectivity remained almost unchanged at 10 to 13 %. As a consequence,

silicic acid appears to be very promising for the conversion of methane into products besides CO_2, because it suppresses the CO_2 production at higher temperatures and higher conversions

Effect of small amounts of ethane on the selective methane oxidation over silicic acid and quartz glass.

Gesser et al (16) as well as Foster (17) in their reviews of early work on the oxidation of methane to methanol report that whenever natural gas or mixtures of methane and ethane were used instead of pure methane the oxidation reaction was triggered at lower temperatures . Ito et al (2) found that an increase of the ethane concentration over a methane oxidative coupling catalyst (Li^+ / MgO) improved the ethylene production. Westbrook and Pitz (18) reported that traces of ethane and propane shorten the ignition time of methane mixtures with air.

We have further investigated the effect of the ethane on the methane conversion and selectivity by varying the amount of ethane in the feed . Figure 4 shows the % selectivity of the various products versus the % CH_4 conversion for silicic acid at the temperature range of 833 to 893 K. Conditions (1) and (2) correspond respectively to 0.14 mol % and 1.25 mol % of ethane in the feed stream (based on methane) . The increase in the ethane percentage in the feed enhances the ethylene, HCHO and CO_2 formation and suppresses the CO production. The most dramatic increase occurs in the ethylene selectivity and thus it would be very reasonable to attribute the ethylene formation almost exclusively to the ethane. The improvement in the formaldehyde selectivity could be due to the fact that the ethane and/or ethylene interactions with the surface inhibit the destruction of formaldehyde. At a conversion level of 5 % the increase of the ethane percentage in the feed from 0.14% to 1.25 % improves the selectivity of useful products (ethylene and formaldehyde) from 30% to 38%.

Runs of varying ethane concentration were performed over quartz tubes at 913 K and 445 kPa. The results obtained are shown on Figure 5. It is clear that the ethane in the feed has a very dramatic effect in the conversion of methane. By increasing the mol percent of ethane from 1.25% to 5.2 % based on methane, the conversion of methane nearly doubled from 1.8% to 3.2 % . The ethane conversion also increased from 10% to 40 % and always remained higher than the methane conversion. At the highest ethane mol percent of 8.9% complete conversion of ethane (90 %) and a 34.4% conversion of methane occured. High conversions favored the CO and CO_2 formation, at the expense of formaldehyde and ethylene.

Ethylene is considered as a primary product of the ethane combustion formed via the oxidative dehydrogenation of the $C_2H_5\cdot$ radicals, in an analogous way that formaldehyde is a primary product of the methane combustion formed from the oxidation of $CH_3\cdot$ radicals (14). Therefore, the same silica surfaces that produce formaldehyde from methane can lead to the formation of ethylene from ethane. The conversion of ethane was always three to five times higher than the conversion of methane and this is in qualitative agreement with the experimental values of Bohme and Fehsenfeld (19) where it was reported that the probability for the first hydrogen abstraction increases with the size of the hydrocarbon chain. The ethane molecule apart from forming $C_2H_5\cdot$ radicals by hydrogen abstraction is also likely to act as a source of $CH_3\cdot$ radicals formed via C-C bond breakage. Experimental data show that the rate of formation of $CH_3\cdot$ radicals from ethane in this way is two orders of magnitude higher than the rate of formation of these radicals from methane (20). Therefore the $C_2H_5\cdot$, $CH_3\cdot$ as well as the $H\cdot$ radicals, which are generated from ethane easier than from methane could activate methane or

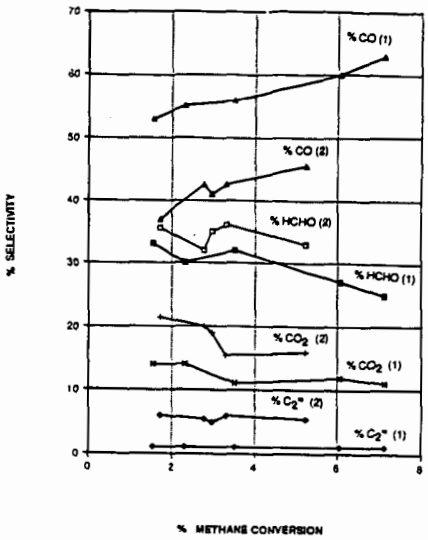

FIGURE 4 % Selectivity of the various products vs % CH_4 conversion over silicic acid in the temperature range of 833 to 893 K as a result of the variation of the ethane concentration in the feed. (1): 0.14 mol % ethane based on methane, flowrates 10% CH_4 in Ar 31 cm^3 STP /min, oxygen 3 cm^3 STP /min, at 380 kPa and over 535 mg of catalyst. (2) : 1.25 mol % ethane based on methane, flowrates 10% CH_4 in Ar 50 cm^3 STP /min, oxygen 5 cm^3 STP /min, at 360 kPa and over 504 mg of catalyst.

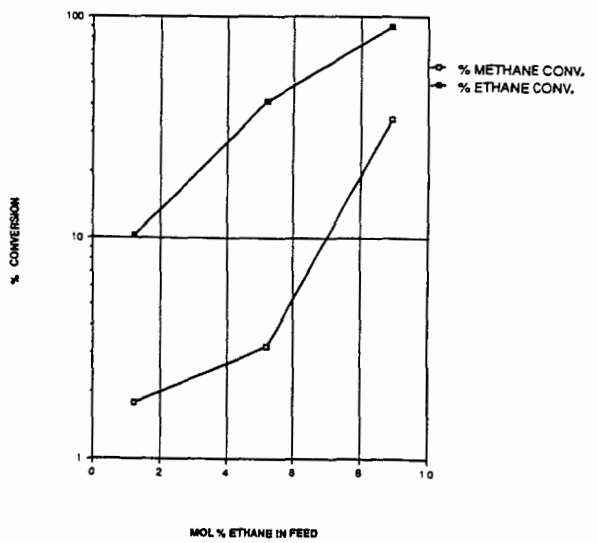

FIGURE 5 Methane and ethane conversions achieved over quartz glass at 913 K and 445 kPa as a function of the mol % ethane based on methane and ethane . Molar ratio of C to O_2 from 0.988 to 1.043.

even interfere in the process of the chain propagation occuring during the methane oxidation-combustion.

Methane oxidation over MoO_3 WO_3 and H_3BO_3 co-gels with Ludox silica

Ammonium heptamolybdate, ammonium metatungstate and H_3BO_3 were dissolved in Ludox colloidal silica. The pH was then adjusted either with nitric acid or with ammonium hydroxide and high surface area co-gels up to loadings of 12% by weight of MoO_3, WO_3 and H_3BO_3 on SiO_2 were prepared. Loadings of up to 5% by weight of MoO_3 led to complete oxidation of methane to CO_2 under an increased overall activity. Loadings of 5% by weight of WO_3 did not have any significant effect neither in the methane oxidation activity of the plain Ludox nor in the product distribution. A mechanical mixture of 5% by weight MoO_3 with Ludox exhibited almost identical activity and selectivity results as the 5% co-gel of MoO_3 . This may suggest that at the high loadings used in the co-gels with Ludox MoO_3 may be present as a bulk phase.

As shown on Table 4 the boric acid co-gels dramatically improved the yields of formaldehyde over the plain silicas. It appears that while silica is responsible for the primary activation of methane, boron preserves the formaldehyde from further oxidation and / or decomposition to CO.

TABLE 4

Effect of boron in the activity and selectivity of Ludox silica at 903 K.

Compound	%Overall conversion	% Selectivity			
		HCHO	$C_2^=$	CO	CO_2
Ludox silica gel	5.2	8	13	55	24
7% H_3BO_3 / Ludox silica co-gel	4.9	47	12	34	7

Flowrates: 10% CH_4 in Ar=49.3 STP / min, O_2=5 cm^3 STP / min. P= 480 kPa. Ethane in feed: 1.25 mol% based on methane.

ACKNOWLEDGEMENTS

Financial support of this work through the Gas Research Institute under GRI Contract 5086-260-1324 is gratefully acknowledged.

LITERATURE CITED

1. R. Pitchai and K. Klier, Catal. Rev.-Sci. Eng., 28 , 13 (1986).
2. T. Ito, J.-X. Wang, C.- H. Lin, and J. H. Lunsford, J. Am. Chem. Soc., 107 , 5062 (1985).
3. K. Otsuka, K. Jinno and A. Morikawa, J. Catal., 100 , 353 (1986).
4. J. A. Sofranko, J. J. Leonard and C. A. Jones, J. Catal., 103 , 302 (1987).
5. H.- F. Liu, R. - S. Liu, K. Y. Liew, R. E. Johnson, and J. H. Lunsford, J. Am. Chem. Soc., 106 , 4117 (1984).
6. M. M. Khan and G. A. Somorjai , J. Catal., 91 , 263 (1985) .
7. K. Otsuka and M. Hatano, J. Catal. , 108 , 252 (1987).
8. N. D. Spencer, J. Catal. , 109 , 187 (1988).
9. L. H. Little, H. E. Klauser, and C. H. Amberg, Can. J. Chem., 39 , 42 (1961).
10. N. W. Cant, and L. H. Little, Can. J. Chem. , 42 , 802 (1964) .
11. N. Sheppard and D.J.C. Yates, Proc. Roy. Soc. London, A 238 , 69 (1956).
12. T. Yamazaki, I. Watanuki, S. Ozawa and Y. Ogino, Nippon Kagaku Kaishi, 8 , 1535 (1987).
13. D. E. Cheaney and A.D. Walsh, Fuel, 35, 238 (1956).
14. D. J. Hucknall, Chemisrty of Hydrocarbon Combustion, Chapman and Hall, 1985.
15. A. F. Wells, Structural Inorganic Chemistry, 5th Ed., Oxford University Press, Oxford, 1987.
16. H. D. Gesser, N. R. Hunter and C. B. Prakash, Chem. Revs. , 85 , 235 (1985).
17. N. R. Foster, Appl. Catal., 19 , 1 (1985).
18. C. K. Westbrook and W. I. Pitz, Combustion Science and Technology, 33 , 315 (1983).
19. D. K. Bohme and F. C. Fehsenfeld, Can. J. Chem., 47 , 2717 (1969).
20. W. C. Gardiner, Combustion Chemistry , Springer-Verlag, Heidelberg, 1985.

Effect of Loading and Support on the Activity and Selectivity of Partial Oxidation of Methane, I. Lee and K. Y. Simon Ng, Department of Chemical Engineering, Wayne State University, Detroit, Michigan 48202

The major component of our vast natural gas reserves is methane. Most of the methane produced nowadays is simply used as fuel, with only a small fraction used in the water-gas process. In order to utilize our gas reserves fully, it is desirable to turn methane into more valuable oxygenated products. Even though methane is a simple molecule, it is one of the most difficult hydrocarbons to oxygenate, due to its highly symmetric character.

A number of patents have been claimed on technologies for converting methane to methanol, but there is still no commercial oxidation process utilizing the direct oxidation mechanism. Recently, a considerable amount of research has been undertaken to identify a selective catalyst system. Two recent reviews by Pitchai and Klier (1) and by Foster (2) have summarized the research on partial oxidation reported in the literature. It is to be noted that most research work (3-8) has focused on evaluating the catalytic potential of different compounds, but the role of supports, the functions of promoters, and the effect of catalyst morphology have not been studied in detail. There are indications that catalyst morphology can have a significant impact on selectivities (1). Even though Liu et al. (4) used nitrous oxide and Pitchai et al. (1) used oxygen as oxidant, they both observed that low loading catalyst showed high selectivity. Catalyst morphology has been found to depend on the metal loading, method of preparation, support, and promoter addition (9). Based on the above literature survey, we have focused our efforts on searching for a selective catalyst through support interaction, and to understand the nature of active sites for partial oxidation of methane on different supported catalysts. In this paper, we report our findings in the activity and selectivity of molybdenum- and vanadium-based catalyst on silica, silica-titania, and titania support.

EXPERIMENTAL

Supports

Three types of catalyst supports were studied. The titania oxide was P-25

from Degussa, with a surface area of 50 ± 5 m^2/g. The silica was from Kodak. Both supports were used as received, without further treatment. The 1:1 ratio of titania-silica mixed oxide support was made using the method of homogeneous co-precipitation. Sodium metasilicate was first dissolved in double-distilled water and acidified to pH 1 with hydrochloric acid. Equimolar of titanium tetrachloride was then added and followed by neutralization using urea. The mixture was then heated at 90 °C for 6 hours. The precipitate was filtered and washed with warm distilled water. The mixed oxide was dried at 120 °C for 24 hours, followed by calcination at 600 °C for 1 hour.

Catalyst

The catalysts were prepared by the conventional impregnation method. The molybdenum-based catalysts were prepared by dissolving the desired amount of ammonium heptamolybdate in double-distilled water, and the PH was adjusted to 10 using ammonium hydroxide. For vanadium-based catalysts, the desired amount of vanadium pentoxide was dissolved in an aqueous solution of oxalic acid. The solution was then impregnated on the support. The resulting mixture was stirred thoroughly and was dried at 120 °C for 2 hours, followed by calcination at 500 °C for 24 hours.

Reactor System

A 6mm I.D. quartz U-tube reactor, with a reduction of I.D to 2mm immediately following the catalyst bed, was used. The reactor design, which allows fast removal of products from the furnace, is intended to minimize the gas phase oxidation reactions. A K-type thermocouple with an Omega temperature controller was used to control the reactor temperature to ± 0.1 °C. A typical of 0.1 g of catalyst was used. The catalyst was first heated at 500 °C in helium for 1 hour, and with CO in helium for another 30 minutes. The reactor temperature was then lowered to 400 °C for 30 minutes in helium, and was subsequently increased to the reaction temperature and the reactant gases introduced. Total gas flow rate is 8 c.c./minute unless stated otherwise. The compressed gases used -- methane

(99.99%), nitrous oxide (99.0%), oxygen (99.99%), helium (99.995%), hydrogen (99.9%), nitrogen (99.9985%), and carbon monoxide (99.9%) -- were from Air Products and were used as received. The mass flow rates of reactants were controlled by Tylan mass flow controllers to ± 1.0 % . Water was introduced in form of steam using a Havard syringe pump. The whole system is heat-traced with heating wire, and insulated to prevent possible condensation of products and reactants. The products were analyzed using an HP-5890A gas chromatograph equipped with TCD and FID detectors. A 20 ft. Hayesep A column and a 5 ft. Hayesep Q column were used to separate the products.

RESULTS and DISCUSSION

Table 1 shows the conversion and selectivity of molybdenum-based catalysts with different loadings on the silica, silica-titania and titania supports using nitrous oxide as oxidant at 600 °C. On blank silica, there was a small conversion of 0.9% but no formaldehyde was observed. For the silica-supported molybdenum catalysts, both the 1% and 3% loading catalysts gave almost identical conversion (7.5%), indicating that the 3% catalyst may already contain bulk-like molybdenum species that are relatively inactive. The low loading catalyst gave a higher selectivity (42.7%) towards formaldehyde than the 3% catalyst (32.5%), which is consistent with the selectivity trends reported previously (3-5). Our results are comparable to the results of Liu et al. (14% conversion and 15% combined selectivity towards methanol and formaldehyde) and Khan et al. (2.6% conversion and 56% selectivity), taking into consideration of the conversion-selectivity relationship (7). However, the conversion-selectivity relationship is different when a different support is used. On a titania-silica support, the catalyst has a slightly higher conversion (10.2%), but the selectivity is much lower (7.2%). When supported on pure titania, the conversion of methane drops significantly, and no observable formaldehyde was detected. It is apparent from this result that on different supports, the nature of active sites is very different for partial oxidation. It is also suggested that silica plays an important role in the reaction mechanism, as evident from the fact

that mixed oxide support showed some selectivity.

Table 2 shows the effect of temperature on conversion and selectivity. For the blank silica using oxygen as oxidant, no conversion was observed at 500 °C. Conversion of 0.1% with 53.8% selectivity was observed for 600 °C, and conversion of 0.6% with 48% selectivity was observed for 650 °C. The 650 °C data was almost identical with Spencer's results (7). As we will see later, the selectivity is very different when water is added along with the reactants. When nitrous oxide was used as oxidant, a higher conversion (0.9%) was observed at 600 °C, indicating that nitrous oxide is a stronger oxidant compared to oxygen. Surprisingly, no formaldehyde was detected. For the 1.7% Mo/SiO_2 catalyst, the conversions are 0.9%, 2.3%, 7.5%, 34.6% at 500 °C, 550 °C, 600, and 650 °C respectively. The corresponding selectivities are 79.3%, 73.5%, 42.7% and 4.1%. There is a strong conversion-selectivity relationship, as reportedly previously. A similar temperature dependence was also observed for the $TiSiO_2$-supported catalyst. However, at comparable conversions, the selectivity is much lower compared to the silica-supported catalysts.

The performance of vanadia-based catalysts at 600 °C using nitrous oxide as oxidant was shown on Table 3. With 2% of vanadia on silica, a conversion of 31.5% and selectivity of 51.0% were observed. The yield was calculated to be 132.2 g/kgcat hr., which is significantly higher then yields reported in the literature. It should be noted that for pure silica the conversion was found to be only 0.9% and no formaldehyde could be detected. Unlike the molybdenum-based catalyst, a 15% selectivity towards formaldehyde was observed when supported on titania. Interestingly, no formaldehyde was observed for the $TiSiO_2$-supported catalyst, even though it showed a conversion similar to the titania-supported catalyst. It is apparent that the nature of the active site for vanadium-based catalysts is quite different from molybdenum-based catalysts, and that the effects of the support on the nature of the active site are not the same.

Table 4 shows the effect of temperature on conversion and selectivity on

vanadium-based catalysts. The conversion was found to increase, as expected, as a function of temperature; however, the selectivity did not show the same conversion-selectivity behavior as the molybdenum-based catalysts. The selectivity increases from 44% at 3% conversion (500 °C) to 51% at 31.5% conversion (600 °C). However, at 650 °C, only carbon oxides were detected. For $TiSiO_2$-supported catalysts, no formaldehyde was detected for the temperature range (500-650 °C) tested. The titania-supported vanadium catalyst showed a 15% selectivity only at 600 °C, indicating that there is a narrow temperature range that can be used to produce formaldehyde.

The effect of water added as reactant and the effect of contact time on the conversion and selectivity is shown in Figures 1 and 2 for silica and vanadia-silica. The results are consistent with those reported in the literature. The conversion is generally lowered when water is added, with the exception of pure silica at 650 °C using oxygen as oxidant. The selectivity towards formaldehyde was generally improved. A more comprehensive study is continuing in this laboratory to elucidate the effect of water on product selectivity. When the contact time was reduced by 50%, the conversion was reduced from 13% to 7.5%, but the selectivity increased from 5.0% to 11.6%. With water added as reactant, a similar trend was observed. The conversion was reduced form 11.8% to 4.3% and the selectivity increased from 6.3% to 24.3%.

The effect of oxidant for vanadium-based catalysts is summarized in Table 5. For pure silica, oxygen appears to be a better oxidant, with 82% selectivity (with water as reactant) as compared to nitrous oxide (0 % selectivity). However, for the vanadia catalyst, N_2O is obviously a better oxidant than oxygen, especially at a higher reaction temperature (600 °C).

CONCLUSION

The nature of the support has a dramatic effect on the catalytic activities and selectivities of molybdenum- and vanadium-based catalysts. However, the extent of support influence is different for the two catalyst systems, suggesting different

levels of support interaction and possibly different reaction mechanisms. There is a distinct conversion-selectivity relationship for the Mo/SiO_2 catalyst. However, this is not observed with the V_2O_5/SiO_2 catalysts. Thus high conversion with reasonably high selectivity seems to be possible with the vanadium catalyst to produce a high yield. Addition of water reduces conversions but improves selectivities in most cases. Nitrous oxide is found to be a better oxidant for V_2O_5/SiO_2 catalyst. However, for blank silica, oxygen gives a high selectivity towards formaldehyde, which suggests that modified silica can be a promising approach to partial oxidation of methane.

ACKNOWLEDGEMENT

Financial support of this research by American Natural Resources and by the Institute for Manufacturing Research of Wayne State University is gratefully acknowledged. The authors would like to thank Mr. Sendjaja Kao for preparing the mixed-oxide support and Miss Carolyn Parks for measuring the B.E.T. surface area.

REFERENCES

1. Pitchai, R., and Klier, K., Catal. Rev.-Sci. Eng., 28(1), 1(1986)

2. Foster., N.R., Applied Catalysis., 19, 1(1985).

3. Liu, R.S., Iwamoto, M., Lunsford, J.H., J. Chem. Soc., Chem. Commun., 78(1982).

4. Liu, H.F., Liu, R.S., Liew, K.Y., Johnson, R.E., and Lunsford, J.H., J.Am. Chem. Soc., 106, 4117(1984).

5. Khan, M.M., and Somorjai, G.A., J. Cat., 91, 263(1985).

6. Zhen, K.J., Khan, M.M., Mak, C.H., Lewis, K.B., and Somorjai, G.A., J. Cat., 94, 501(1985).

7. Spencer, N.D., Submitted to J. Cat.

8. Otsuka, Kiyoshi., and Hatano, Masahru., J.Cat., 108, 252(1987).

9. Ng, K.Y.S., and Gulari, E., J.Cat., 92, 340(1985)

Table 1

Molybdenum - Based Catalyst at 600 °C

(W / F = 0.0125 g min / cc)

$CH_4:N_2O:He$ = 1:4:2 Total flow rate = 8 cc/ min

Catalyst	Conversion	Selectivity (%)			Yield (g/kgcat hr)
		HCHO	CO	CO_2	(HCHO)
SiO_2	0.9	0	50.4	49.6	0
Mo/SiO_2 (1.7%)	7.5	42.7	43.8	13.5	20.2
Mo/SiO_2 (3%)	7.4	32.5	54.7	12.8	15.6
$Mo/TiSiO_2$ (1.7%)	10.2	7.2	65.7	27.1	5.6
Mo/TiO_2 (3%)	2.2	0	77.7	22.3	0
Mo/TiO_2 (5%)	1.7	0	70.2	29.8	0

Table 2

Effect of Temperature on Conversion and Selectivity

(W/F = 0.0125 g min / cc)

$CH_4:N_2O:He$ = 1:4:2 Total flow rate = 8 cc/ min

Catalyst	Oxidant	Temp(°C)	Conversion	Selectivity(%)			Yield (g/kgcat hr)
				HCHO	CO	CO_2	HCHO
SiO_2	O_2	500	0	0	0	0	0
		600	0.1	58.3	24.1	17.6	1.3
		650	0.6	48.0	45.4	6.6	5.7
	N_2O	600	0.9	0	50.4	49.6	0
Mo/SiO_2	N_2O	500	0.9	79.3	10.5	10.2	3.9
		550	2.3	73.5	19.6	7.0	9.3
(1.7%)		600	7.5	42.7	43.8	13.5	20.2
		650	34.6	4.1	63.5	32.4	6.8
$Mo/TiSiO_2$	N_2O	550	3.7	0	83.9	16.1	0
		600	10.2	7.2	65.7	27.1	5.6
(1.7%)		650	20.6	1.1	56.5	42.4	1.2

Table 3

Vanadium - Based Catalyst at 600 °C

(W/F = 0.0125 g min / cc)

CH_4:N_2O:He = 1:4:2 Total folw rate = 8 cc / min

Loading(wt %)	Conversion	Selectivity (%)			Yield (HCHO)
		HCHO	CO	CO_2	g/kgcat hr
SiO_2	0.9	0	50.4	49.6	0
V_2O_5/SiO_2 (2%)	31.5	51.0	35.4	13.6	132.2
$V_2O_5/TiSiO_2$ (2%)	11.4	0	73.4	26.6	0
V_2O_5/TiO_2 (2%)	13.7	15.0	34.0	51.0	15.8

Table 4

Effect of Temperature on Conversion and Selectivity

(W/F = 0.0125 g min / cc)

CH_4:N_2O:He = 1:4:2 Total flow rate = 8 cc/ min

Catalyst	Temp (°C)	Conversion	Selectivity (%)			Yield (HCHO)
			HCHO	CO	CO_2	(g/kgcat hr)
V_2O_5/SiO_2	500	3.0	44.0	43.4	12.6	9.7
	600	31.5	51.0	35.4	13.6	132.2
(2 %)	650	42.8	0	62.8	37.2	0
$V_2O_5/TiSiO_2$	500	2.3	0	76.9	23.1	0
	600	11.4	0	73.4	26.6	0
(2 %)	650	25.6	0	53.7	46.3	0
V_2O_5/TiO_2	500	1.3	0	71.7	28.3	0
	600	13.7	15.0	34.0	51.0	15.8
(2 %)	650	24.2	0	27.4	72.6	0

Table 5

Effect of Oxidant

(W / F = 0.0125 g min / cc)

$CH_4:N_2O:He$ = 1:4:2 , $CH_4:O_2:He$ = 4:1:2 Total flow rate = 8 cc/min

Loading	Temp	Oxidant	Conversion	Selectivity(%)			Yield(HCHO)
(Wt %)	(°C)			HCHO	CO	CO_2	g/kg cat hr
SiO_2	600	O_2	0.1	58.3	24.1	17.6	1.3
	600	N_2O	0.9	0	50.4	49.6	0
V_2O_5/SiO_2	500	O_2	0.2	38.5	42.5	19.0	1.4
(2 %)	500	N_2O	3.0	44.0	43.4	12.6	9.7
	600	O_2	13.0	5.0	69.1	25.9	14.4
	600	N_2O	31.5	51.0	35.5	13.5	132.2

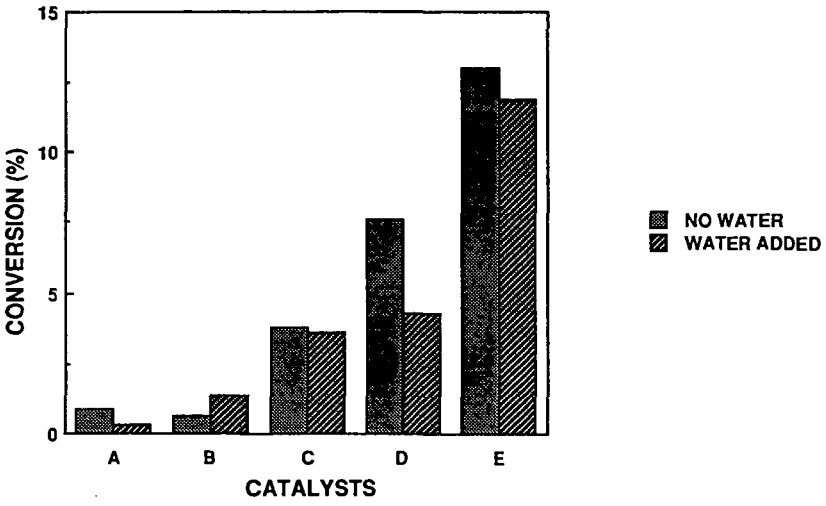

FIGURE 1. EFFECT OF WATER ON CONVERSION

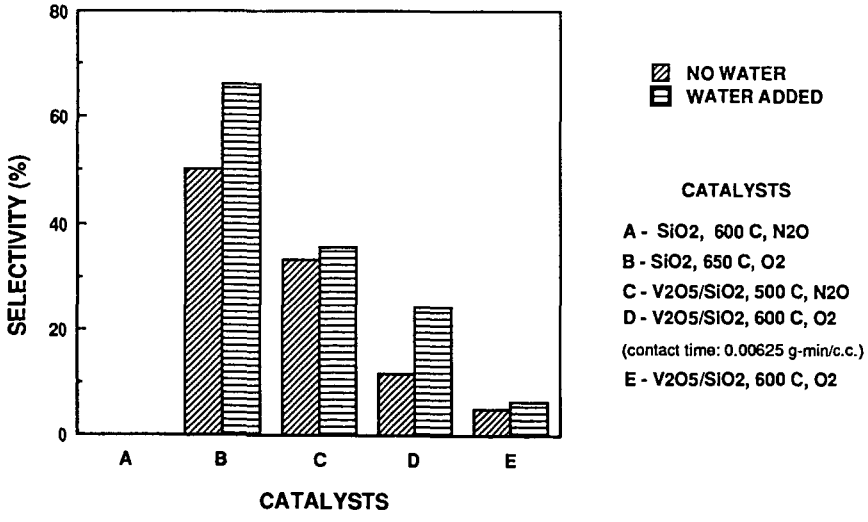

FIGURE 2. EFFECT OF WATER ON FORMALDEHYDE SELECTIVITY

Pages 413 thru 420 have intentionally been left blank.

ACS National Meeting -
Los Angeles, September 25-30, 1988
Division of Fuel Chemistry
Catalytic and Related Chemistry of Methane

Conversion of Methane into Ethylene, Acetylene and Ethane by the CCOP Process: Control of Product Selectivities

by

S.M. Senkan*, D. Dang, M.K. Abdelaal, and M. Qun
Department of Chemical Engineering
Illinois Institute of Technology
Chicago, Illinois 60616

* To whom correspondence should be addressed.

ABSTRACT:

The oxidative pyrolysis of CH_3Cl, representing the second stage in the Chlorine-Catalyzed Oxidative-Pyrolytic (CCOP) conversion of methane into C_2 hydrocarbons have been studied in the presence of CH_4 in a flow reactor operating at 0.7 atm and 900-950 C. The effects of temperature, mixture composition, in particular the concentration of O_2, and residence times on CH_3Cl conversion and selectivity towards the formation of C_2 products have been explored experimentally. The role of CH_4 and other operational variables in effecting rates and selectivities will be discussed in view of our current understanding of the detailed chemical kinetic aspects of the CCOP process.

INTRODUCTION:

Chlorine-Catalyzed Oxidative-Pyrolysis (CCOP) process was recently developed as a practical method to convert methane, the major component in natural gas, into more valuable products such as acetylene and ethylene (Senkan 1987a). In the CCOP process CH_4 is chlorinated to form chlorinated methanes (CM) first, followed by the oxidative pyrolysis of CM to form C_2 products such as C_2H_4, C_2H_2, C_2H_6, C_2H_3Cl, synthesis gas (CO and H_2), and HCl in the second step. The process developed ameliorates the problem of formation of carbonaceous solid deposits inherent with the earlier chlorine-catalyzed methane conversion processes which took place in the absence of oxygen (Gorin 1943, Benson 1980, Weissman and Benson 1984). The HCl produced can either be converted back to chlorine via the well-known Deacon reaction and recycled, or can be used to oxychlorinate methane to form CMs, thus completing the catalytic cycle for

chlorine (Senkan 1987b).

In previous studies we reported experimental product distributions for the oxidative pyrolysis of isolated CH_3Cl in the presence of an inert (argon) carrier gas (Granada et al. 1987). In parallel, a detailed chemical kinetic mechanism for the oxidative pyrolysis of CH_3Cl was also developed and validated (Karra and Senkan 1988a).

As discussed in these earlier studies the selectivity for C_2H_4 can be substantially high, e.g. about 40%, at low conversions of CH_3Cl. However, it decreases rapidly with increasing conversion, rendering acetylene as the major product beyond 30% conversion of CH_3Cl. Since C_2H_4 is a more desirable product, the identification of proper process conditions that will favor its formation clearly are of interest (C&E News 1987).

Pyrolysis of CH_3Cl in the presence of CH_4 increases C_2H_4 production over C_2H_2 as demonstrated by Weissman and Benson 1984. However, in the absence of O_2, the process also leads to the formation of significant levels of carbonaceous deposits, in particular coke, which is undesirable.

In this communication we present results on the oxidative pyrolysis of CH_3Cl conducted in the presence of CH_4, in which coke formation is avoided. The effects of temperature, O_2 concentration and residence times on the conversion of CH_3Cl and product distributions are discussed based on experiments conducted at 0.7 atm, 900-950 C, and for a CH_3Cl/CH_4 ratio of about 0.25. In addition, the role of these process variables on conversion and selectivity is discussed based on our current understanding of the detailed chemical kinetic aspects of the CCOP process.

EXPERIMENTAL:

The experimental facility used has been discussed in detail previously (Granada et al. 1987), thus only a brief summary will be presented here. The

experiments were conducted in a 2.1 cm ID quartz tube which was placed in a 3-zone Lindbergh furnace. The first zone of the furnace, which is about 15 cm long, was used to preheat methane which served as a reactive carrier gas. Mixtures of CH_3Cl/O_2 were then introduced into pre-heated methane using an air-cooled probe through radially directed injection holes. Small amounts of nitrogen (3-5%) also were introduced into the feed mixture as an internal reference gas.

Gases used were acquired either from the Matheson Co. (Joliet, IL) or from Bennet Welding Supply Co. (Bensenville, IL), and had the following reported purities: CH_3Cl:99.5% as liquid, CH_4:99.97%, O_2:99.6% extra dry, and N_2:99.99%. They were used directly from the cylinders, and their flow rates were controlled by the combined use of two-stage regulators, rotameters and needle valves. The needle valves were maintained under critical flow conditions to establish uncoupled flow rates. A mechanical vacuum pump was then used to remove the reaction products from the system. The pressure in the reactor was kept slightly below atmospheric pressure (about 0.70 atm) in all the experiments to prevent toxic gases from leaking into the laboratory, and was monitored continiously by a capacitance transducer (MKS Baratron, Burlington MA).

Mean gas flow velocities in the reactor were in the range 1-10 m/s, suggesting that laminar flow conditions were present. However, the deviation from ideal plug flow behavior would be in the range 10-15%, the same order of magnitude as the other experimental errors (Cathonnet et al. 1981).

Gas samples were withdrawn continiously using a vacuum pump through a warm-water-cooled quartz sampling probe positioned centrally at the downstream end of the reactor, and then through a heated sample loop in the gas-chromatograph (Hewlett-Packard 5880A). The pressure in sampling lines and the loop was kept at about 0.25 atm to minimize the condensation of species, in particular H_2O and HCl. Following the establishment of steady sampling conditions, that were

determined in prior experiments by studying the variation of mixture composition as a function of sampling time, the sampling loop was automatically switched on-line with the helium carrier gas. Gas separation and detection were then accomplished by Porapak N (0.31 cm diameter by 1.8 m long) and by molecular sieve 5A (0.31 cm diameter by 1.8 m long) columns (both acquired from Alltech Assoc., Deerfield IL), and by the thermal conductivity detector, respectively.

Gas analysis was accomplished using standard gas chromatographic methods (GC). For reactants, i.e. CH_3Cl, CH_4, O_2, and N_2, GC response factors were obtained directly by analyzing the reactor effluents in the absence of reaction, i.e. at low temperatures. For reaction products, such as C_2H_4, C_2H_2, C_2H_6, C_2H_3Cl, and CO a certified calibration mixture (Matheson Co., Joliet IL) was used. For this calibration, a gas mixture having a composition reasonably close to those encountered in the experiments was acquired. Consequently, we estimate that the mole fractions obtained in this study should be accurate within $\pm$ 5%. Species mole fraction profiles were then obtained by moving the sampling probe relative to the stationary injection probe.

Carbon balances for each measurement were made by using the following definition:

$$\% \text{ Carbon balance} = \frac{(\text{gas-phase carbon}/N_2)_{\text{reaction mixture}}}{(\text{gas-phase carbon}/N_2)_{\text{feed mixture}}} * 100$$

and they were better than 95% for all the experiments.

RESULTS:

The major species quantified directly by GC were the reactants CH_3Cl, CH_4, O_2, and N_2 as the tracer gas, and the major carbon-containing products C_2H_4, C_2H_2, C_2H_6 and CO. Since only trace levels of CO_2 form in the CCOP process, it was neglected in the final product analysis. Unlike the oxidative pyrolysis of CH_3Cl, which leads to substantial C_2H_3Cl formation, very little C_2H_3Cl formed in

the current experiments when an excess CH_4 was present.

Before presenting any results a number of issues must be discussed concerning the experiments. First, as we noted previously even small amounts of O_2 in the mixture suppresses the extent of formation of carbon in the system, and this effect is most dramatic with regard to coke formation. On the other hand, when O_2 feed was deliberately cut off, rapid coking, manifested by the formation of black deposits on the inner surface of the reactor walls, was observed.

Second, although CH_4 actively participates in the process, and dramatically increases the concentration of C_2H_4 relative to C_2H_2, the precise quantification of the extent by which CH_4 contributes to this phenomena was rendered difficult in the present studies because of CH_4 reformation from CH_3Cl and experimental errors. For example, the absolute concentrations of C_2 products formed in the experiments were of the same order of magnitude as the uncertainties in the measurements of CH_4 concentrations. Consequently, we report selectivities based on the amount of CH_3Cl reacted. This appears reasonable because CH_4 is expected to form as a major product in the oxidative pyrolysis of CH_3Cl even in the presence of excess methane based on detailed chemical kinetic calculations (Senkan 1988).

In order to systematically explore the effects of each of the process variables on CH_3Cl conversion and on product selectivities, we conducted experiments in which independently adjustible variables were changed one at a time. In Figure 1 the influence of temperature on carbon containing product concentrations in the CCOP process are illustrated for a mixture with the following pre-reaction composition: CH_3Cl 15.9%, CH_4 75.9%, O_2 4.12%, and N_2 3.98%. Nominal residence times were about 330 ms. In this and subsequent figures lines have been drawn through experimental data points (indicated by symbols) to indicate trends.

The compositions shown in this figure represent conditions at a fixed position near the exit of the reactor, and therefore do not precisely correspond to identical residence times. However, since the differences in temperatures between these experiments were at most 50 K, residence times are expected to be different by at most 5% due to temperature effects, well within normal experimental error limits. Product (carbon) selectivities, determined relative to CH_3Cl reacted, similarly are presented in Figure 2, together with the percent conversion of CH_3Cl.

As seen in Figure 1, temperature has the most dramatic effect on the concentration of CO, with CO mole percent increasing exponentially with reaction temperature. In contrast, the concentrations of all the C_2 products varied more gradually with temperature. These results can be explained in view of the detailed chemical kinetic mechanism for the CCOP process developed recently (Karra and Senkan 1988a), and will be discussed in a future publication (Senkan 1988).

The effects of O_2 concentration on rates and selectivities are presented in Figures 3 and 4, respectively. These results similarly were obtained by sampling gases near the exit of the reactor corresponding to a nominal residence time of about 330 ms. The reaction temperature was 920 C, and the following O_2-free pre-reaction composition was used: CH_3Cl 20.6%, CH_4 74.8%, and N_2 4.56%. The concentration of O_2 in these experiments were changed by changing the flow rate of O_2 entering the reactor, while maintaining the flow rates of other gases constant. Consequently, the data points presented in Figures 3 and 4 also do not precisely correspond to same residence times. However, since O_2 represents at most 7% of the reaction mixture, differences in residence times are not expected to be different by more than this amount, again within experimental error limits. As evident from Figures 3 and 4, O_2 concentration directly effects the

level of CO formed in the system, while its impact on C_2 products is more subtle.

Since the CCOP process must proceed under non-flame conditions, the levels of O_2 in the mixture must be selected carefully (1987a). In this regard it is important to recognize that although the presence of some O_2 in the mixture is essential to prevent coke formation, an excess O_2 concentration is also undesirable because of the onset of flame reactions. The onset of flame reactions are characterized by the formation of excessive levels of CO, CO_2, H_2O and soot. The formation of excessive H_2O, in particular, causes operational problems because of its condensation together with HCl on cold surfaces at the exit of the reactor.

In Figures 5 and 6 the concentration and selectivity profiles along the reactor are presented for a mixture with the following pre-reaction composition: CH_3Cl 19.78%, CH_4 71.62%, O_2 4.23%, and N_2 4.37%. These profiles were obtained at 920 C, and by moving the sampling probe along the reactor. The distance along the reactor was measured relative to the point of injection of the CH_3Cl/O_2 mixture into preheated CH_4. In this experiment, the total number of moles in the system remained essentially the same, i.e. the absolute concentration of N_2 measured by GC was constant, thus residence times were directly proportional to distance along the reactor. Since the mean gas velocity in the reactor was 1.15 m/s, the data presented in Figures 5 and 6 correspond to residence times ranging from 173 to 312 ms at the exit of the reactor.

ACKNOWLEDGEMENT:

This research was supported, in part, by funds from the U.S. Environmental Protection Agency, Grant No:R812544-01-0, and IIT IWERC Project No:8605.

REFERENCES:

Cathonnet, M., Boettner, J.C., James, H., "Experimental Study and Numerical Modeling of High Temperature Oxidation of Propane and n-Butane", 18th Symp. (Int'l) on Combustion, p.903, The Combustion Institute, Pittsburgh (1981).

Benson, S.W., "Conversion of Methane", US Patent 4,199,533, 1980.

Chemical and Engineering News, December 13, p.28, 1987.

Colket, M.B., "The Pyrolysis of Acetylene and Vinylacetylene in a Single-Pulse Shock Tube", Twenty First Symposium (International) on Combustion, p.851, The Combustion Institute, Pittsburgh 1988.

Dean, A.M., "Predictions of pressure and temperature effects upon radical addition and recombination reactions", J. Phys. Chem., v.89, p.4600 (1985).

Frenklach, M., Clary, D.W., Gardiner, W.C., and Stein, S.E., "Detailed Kinetic Modeling of Soot Formation in Shock-Tube Pyrolysis of Acetylene", Twentieth Symposium (International) on Combustion, p.887, The Combustion Institute, Pittsburgh (1984).

Granada, A., Karra, S.B., and Senkan, S.M., "Conversion of CH_4 into C_2H_2 and C_2H_4 by the Chlorine-Catalyzed Oxidative-Pyrolysis (CCOP) process: Oxidative pyrolysis of CH_3Cl", Ind. Chem. Eng. Res., 1987, 26, 1901.

Gorin, E., "Conversion of normally gaseous hydrocarbons", US Patent 2,320,274, 1943.

Karra, S., and Senkan, S.M.,"A Detailed Chemical Kinetic Mechanism for the Oxidative Pyrolysis of CH_3Cl", Ind. Eng. Chem. Research, in press 1988a.

Karra, S.B., and Senkan, S.M., "Analysis of the Chemically Activated CH_2Cl/CH_2Cl and CH_3/CH_2Cl Recombination Reactions at Elevated Temperatures using the Quantum-Rice-Rampsperger-Kassel (QRRK) Method", Ind. Eng. Chem. Research, v.27, p.447 (1988b).

Senkan, S.M. "Production of Higher Molecular Weight Hydrocarbons from Methane", US Patent 4,714,796, 1987a.

Senkan, S.M., "Conversion of methane into higher molecular weight hydrocarbons by the Chlorine-Catalyzed Oxidative-Pyrolysis (CCOP) process", Chem. Eng. Prog., 1987b, 12, 58.

Senkan, S.M., "Detailed Chemical Kinetic Modeling of the CCOP Process: Formation of C_3 and C_4 Species", in preparation (1988).

Weissman, M., and Benson, S., "Pyrolysis of Methyl Chloride, a Pathway in the Chlorine-Catalyzed Polymerization of Methane", Int. J. Chem. Kinetics., v.16, p.307 (1984).

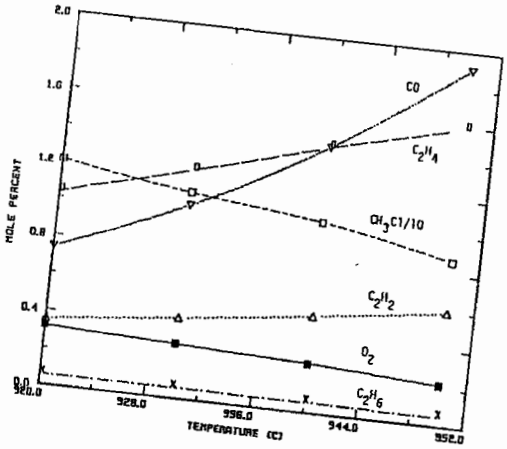

Figure 1. The effects of temperature on the concentration of species at a nominal residence time of 330 ms.

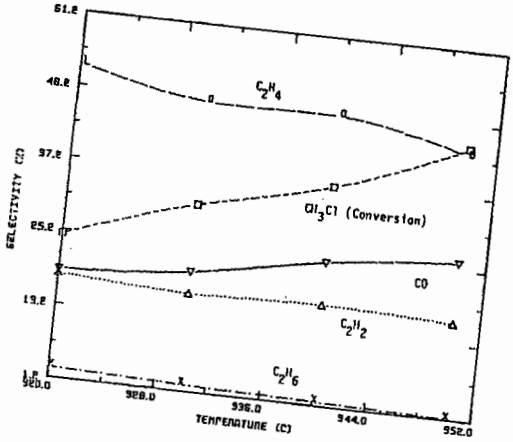

Figure 2. The effects of temperature on conversion and product selectivities at a nominal residence time of 330 ms.

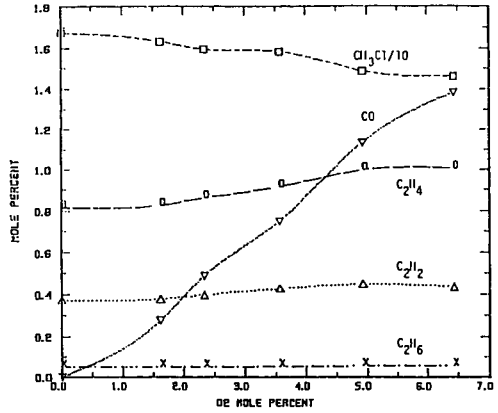

Figure 3. The effects of O_2 concentration on the concentration of species at 920 C and a nominal residence time of 330 ms.

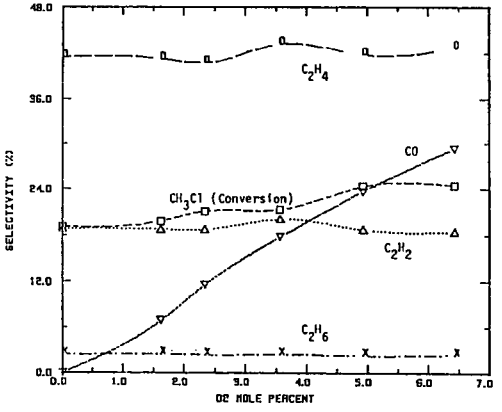

Figure 4. The effects of O_2 concentration on conversion and product selectivities at 920 C and a nominal residence time of 330 ms.

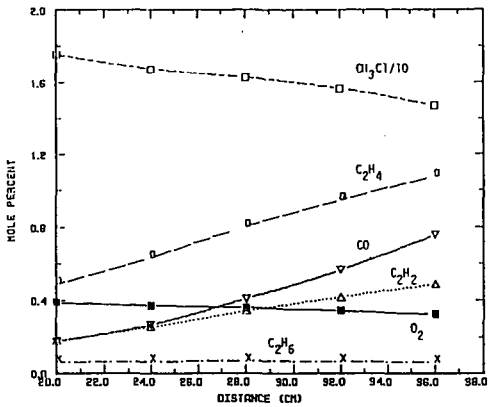

Figure 5. The effects of residence time on the concentration of species at 920 C.

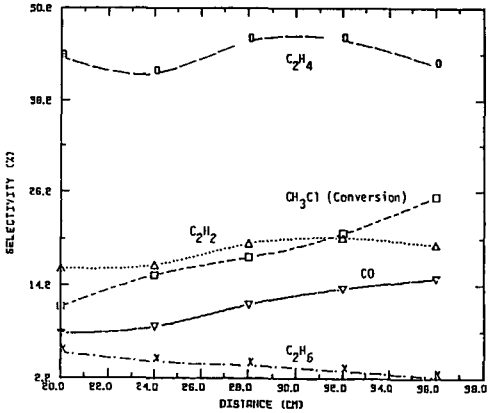

Figure 6. The effects of residence time on conversion and product selectivities at 920 C.

DIRECT METHANE CONVERSION - AN ASSESSMENT

David Gray and Glen Tomlinson
The MITRE Corporation
McLean, VA

and

John Shen
U.S. Department of Energy
Washington, D.C.

Worldwide proven reserves of natural gas are estimated to be approximately 3500 trillion cubic feet of which the U.S. has approximately 6 percent[1]. Gas production and consumption worldwide are about 63 trillion cubic feet annually. In 1985 the U.S. produced about 27 percent of this (i.e., about 17 trillion cubic feet)[1]. In terms of energy, natural gas consumption represents about half of the total petroleum consumed and natural gas reserves are being discovered at twice the rate of petroleum. This trend indicates the increasingly important role that gas will play in the future energy supplies of the world.

Large quantities of this natural gas are located in remote areas, isolated rom centers of commerce and population. No distribution network exists for its transportation. In fact, gas associated with petroleum is often flared rather than utilized. Transportation costs of remote natural gas are a relatively expensive part of the final delivered price. Therefore, most natural gas is consumed in the country where it is produced. Liquefied natural gas (LNG) terminals and vessels can bring remote gas to market. In 1985, 30 percent (1.7 trillion cubic feet) of natural gas traded internationally was transported as LNG and this percentage is growing[2]. For shorter distances, remote gas can be compressed (CNG) and transported using tankers with pressurized containers. Alternatively, depending on the economic conditions, on-land and subsea pipelines can be constructed to transport the remote gas.

A potentially attractive option, currently being practiced in New Zealand, is to convert the gas on-site to readily transportable liquids like methanol or liquid hydrocarbons. These liquids can then be transported using coventional tankers. The New Zealand plant produces 14,500 barrels per day of gasoline, which are shipped to a refinery for blending into the New Zealand gasoline pool[3]. The option of on-site conversion of gas to liquids not only allows for easier transportation but also produces a more valuable energy commodity, i.e. a liquid transportation fuel in the case of higher hydrocarbons, or a petrochemical feedstock, gasoline additive or turbine fuel in the case of methanol. In a world where requirements for liquid transportation fuels are paramount, natural gas will increasingly be used to fulfill this role.

Methane, the major consituent of natural gas, is also a by-product of Fischer-Tropsch and other synthesis processes for the production of liquid fuels and chemicals from synthesis gas. This methane must be reformed back to synthesis gas if only liquid products are required; this process is both thermally inefficient and expensive. Thus, alternative processes for converting this methane by-product into liquids will also be a benefit to indirect liquefaction technology.

Conventional transformation of natural gas to methanol and liquid hydrocarbons involves the reforming of the natural gas to synthesis gas followed by catalytic synthesis to produce methanol. If hydrocarbons are required, the methanol can be

further processed using Mobil's Methanol-to-Gasoline (MTG) technology to produce high octane gasoline[4]. This conventional process is a complex processing sequence involving the highly endothermic steam reforming reaction followed by exothermic methanol synthesis.

If it were possible to convert methane directly to methanol or higher hydrocarbons with high conversion and selectivity, both the steam reforming and methanol synthesis steps could be eliminated. This direct conversion approach has the potential for considerable savings in cost if technically sound processes can be developed. Interest in direct methane or natural gas conversion has recently intensified worldwide. Several approaches to this are being researched at oil companies and in programs funded by the Department of Energy or the Gas Research Institute. The more technically advanced processes are those that operate in the temperature range 600-800°C.

This paper assesses the technical potential of some of these high temperature direct methane conversion approaches being researched by various groups. These new approaches are then compared to the conventional technology for converting methane to gasoline by utilizing steam reforming, methanol synthesis and Mobil's Methanol-to-Gasoline (MTG) technology[5]. The direct methane conversion approaches analyzed in this report are Oxidative Coupling, Partial Oxidation, and Oxyhydrochlorination. Computer simulation has been used to model the technical performance of conceptual commercial plants that utilize these direct methane conversion approaches. In addition, the conventional technology has been simulated with the same size plant to provide a baseline to which the new approaches could be compared. These analyses were based on the thermodynamics of the reactions and the reported yields and selectivities for each process. Results are reported on the basis of the efficiency of the lower heating value (LHV) of the product. LHV of the product is the heating value of the product divided by the heating value of the reactant. Sensitivity studies have been conducted for some of the new approaches to identify the levels of performance necessary for these direct conversion techniques to be technically as efficient as the baseline conventional technology.

Data on Oxidative Coupling have been obtained from open literature sources that document the results from Atlantic Richfield (ARCO)[6-8]. Partial oxidation data have been obtained from published results of H. Gesser et al. of the University of Manitoba[9-14]. Preliminary results of the Oxyhydrochlorination of methane have been obtained from the Pittsburgh Energy Technology Center (PETC)[15].

In the analysis of Oxidative Coupling, the system used was the redox mode. In this approach, methane is contacted with a solid oxidant, in this case manganese oxide on silica. This oxidant provides lattice oxygen for the oxidative coupling of the methane and the manganese is reduced to a lower oxidation state. The solid is then transferred to a regeneration reactor where it is reoxidized. The reoxidized solid is then transferred back to the oxidative coupling reactor where it reacts again with the methane. The products from the oxidative coupling reactor, which are predominantly C_2+ olefins, are then sent to a ZSM-5 polymerization reactor where they undergo oligomerization to form gasoline.

For analysis of Partial Oxidation, methane is reacted with pure oxygen at pressures of 65 bar in a glass-lined, non-catalytic reactor to produce methanol and carbon oxides. The methanol is then sent to an MTG unit, as in the baseline case, to give high octane gasoline as a final product.

In Oxyhydrochlorination, methane is reacted with oxygen and hydrogen chloride over a copper chloride catalyst[16]. The analysis assumes a process in which the

products formed are cooled to remove water and hydrogen chloride, and the methyl chlorides produced are sent to a ZSM-5 reactor where they undergo polymerization to form gasoline and liberate hydrogen chloride. The first stage data used gave a 25 percent conversion of methane per pass and a selectivity to mono- and dimethyl chlorides of 81 percent with a molar ratio of mono- to dichloride of approximately 4 to 1. Complete oligomerization of the mono- and dichlorides was assumed to occur over the second stage ZSM-5 reactor to give a stoichiometric mixture of C_6 hydrocarbons and toluene.

Table I summarizes the known process parameters and calculated conversion efficiencies for the new direct methane conversion approaches and the baseline technology considered in this analysis. Using the preliminary data available, the computer simulations of the new approaches all show overall system efficiencies that are not greatly different from the conventional technology. Using ARCO data for the 15 percent Mn/SiO_2 system that gave a methane conversion per pass of 26 percent for a C_2+ selectivity of 60 percent, an LHV product efficiency of 56 percent was obtained for the Oxidative Coupling approach. ARCO showed that promotion of this system with sodium pyrophosphate increased C_2+ selectivity to about 70 percent. Our analysis shows that LHV product efficiency increases to 64 percent at this higher selectivity level. For Partial Oxidation, using the best available data[9-14], an overall product efficiency of 59 percent was obtained. It was assumed that a product selectivity to methanol of 83 percent was obtained at a per pass methane conversion of 8 percent. For Oxyhydrochlorination, using the assumptions mentioned above, the overall product efficiency was estimated to be 65 percent.

Oxidative Coupling looks promising provided that the selectivity to CO and CO_2 can be maintained at a level of about 25 percent. The design of a practical high pressure redox reactor system needs to be addressed. The excess waste heat from the system, which is of good quality, also needs to be effectively utilized. If this can be done with the current selectivities, then the overall system efficiency including the potentially recoverable heat would be around 70 percent.

Partial Oxidation would appear to be a potentially attractive alternative, based on our estimates of efficiency, provided that high methanol selectivities can be achieved. However, the results from the University of Manitoba are considerably better than have been achieved elsewhere; they may be a function of the particular reactor dimensions used in the experiments. This requires further investigation.

Based on efficiency, Oxyhydrochlorination looks very attractive. However, this analysis has assumed very favorable polymerization potential for the methyl chlorides over ZSM-5, which has yet to be demonstrated in practice. Of greater potential concern for this technology, however, is the severe materials corrosion problems that exist with the handling and recovery of wet hydrogen chloride.

To further evaluate the process potential of these new technologies, additional research and development is needed together with economic analyses to quantify the expected cost savings associated with the elimination of steam reforming and methanol synthesis.

Acknowledgement:

This work was funded by Sandia National Laboratories, which is supported by the U.S. Department of Energy under Contract DE-AC04-76DP00789.

References:

1. Oil and Gas Journal, December 30, 1985, p. 66.

2. Leibson, I., S. T. Davenport and M. H. Muenzier, "Costs to Transport Natural Gas," Hydrocarbon Processing, April 1987, p. 47.

3. Fox, Joseph M., "The Fixed-Bed Methanol-to-Gasoline Process Proposed for New Zealand," paper presented at the Australian Institute of Petroleum, Coal Gasification Conference, Adelaide, March 2, 1982.

4. Haggin, J., "Methane-to-Gasoline Plant Adds to New Zealand Liquid Fuel Resources," Chemical and Engineering News, June 22, 1987, p. 22.

5. Kuo, J. C. W., Gasification and Indirect Liquefaction. Chapter 5 from The Science and Technology of Coal and Coal Utilization, edited by B. R. Cooper and W. A. Ellingson, Plenum Publishing Corp., 1984.

6. Jones, A. C., J. J. Leonard and J. A. Sofranko, "The Oxidative Conversion of Methane to Higher Hydrocarbons Over Alkali-Promoted Mn/SiO_2," Journal of Catalysis, 103, 311-319, 1987.

7. Jones, A. C., J. J. Leonard and J. A. Sofranko, "Fuels for the Future: Remote Gas Conversion," Energy and Fuels 1, 12-16, 1987.

8. Sofranko, J. A., J. J. Leonard and C. A. Jones, "The Oxidative Conversion of Methane to Higher Hydrocarbons," Journal of Catalysis, 103, 302-310, 1987.

9. Gesser, H. D. and N. Hunter, "The Direct Conversion of Methane to Methanol by Controlled Oxidation," Chemical Reviews 85 (4), August 1985, p. 235.

10. Gesser, H. D., N. R. Hunter, L. A. Morton, P. S. Yarlagadda and D. P. C. Fung, "The Direct Conversion of Methane to Methanol by a High Pressure Partial Oxidation Reaction," American Chemical Society, Division of Fuel Chemistry, Preprints 32 (3), 255, 1987.

11. Hunter, N. R., et al., "The Direct Conversion of Methane to Methanol," Proceedings of the VI International Symposium on Alcohol Fuels Technology, Ottawa, May 21-25, C-14, Vol. 11-147, 1984.

12. Hunter, N. R., et al., "The Direct Conversion of Natural Gas to Methanol by Controlled Oxidation at High Pressure," Proceedings of the 35th Canadian Chemical Engineering Conference Category, Oct. 6-9, 1985.

13. Hunter, N. R., et al., "The Direct Conversion of Natural Gas to Alcohols," presented at the VII International Symposium on Alcohol Fuels, Paris, Oct. 20-23, 1986.

14. Yarlagadda, P. S., et al., "Direct Catalytic Conversion of Methane to Higher Hydrocarbons," Fuel Science and Technology Int. 5(2), 169-183, 1987.

15. Taylor, C. E. and R. P. Noceti, "Conversion of Methane to Gasoline-Range Hydrocarbons," American Chemical Society, Division of Fuel Chemistry, Preprints 32 (3), 307, 1987.

16. Pieters, W. J. M., E. J. Carlson, E. Gates and W. C. Conner, U.S. Patent, 4,123,389 (1978).

TABLE 1
SUMMARY OF DIRECT METHANE CONVERSION APPROACHES
FOR PRODUCTION OF GASOLINE

	BASELINE TECHNOLOGY	OXIDATIVE COUPLING	PARTIAL OXIDATION	OXYHYDRO-CHLORINATION
Number of Stages	3	2	2	2
Stage 1	Steam Reforming	Oxidative Coupling	Partial Oxidation	Oxyhydrochlorination
Catalyst	Nickel	Mn/SiO_2	None	CuCl/KCl on Silica
Temperature (°C)	800-900	815	458	340
Pressure (Bar)	7-20	35	65	15
CH_4 Conversion Per Pass	---	26	8	25
Overall CH_4 Conversion %	90	99	95	93
Selectivity	---	50% to C_2+	83% to CH_3OH	77% to CH_3Cl
Stage 2	Methanol Synthesis	Olefin Oligomerization	Methanol-to-Gasoline	Methyl Chloride Oligomerization
Catalyst	Cu/Zn	ZSM-5	ZSM-5	ZSM-5
Temperature (°C)	250-300	370	320	400
Pressure (Bar)	80-100	27	22	12
Stage 3	Methanol-to-Gasoline	None	None	None
Catalyst	ZSM-5			
Temperature (°C)	320			
Pressure (Bar)	22			
Overall LHV Efficiency %	59	56	59	65

The Oxidation of Methane on Silica-Supported Heteropoly Oxometalates

S. Ahmed, S. Kasztelan and J.B. Moffat
Department of Chemistry and
Guelph-Waterloo Centre for
Graduate Work in Chemistry
University of Waterloo
Waterloo, Ontario, Canada
N2L 3G1

Abstract

The conversion of methane with nitrous oxide is shown to be catalyzed by silica-supported heteropoly oxometalates of Keggin structure, in particular 12-molybdophosphoric acid (HPMo). The activity of the HPMo catalysts is related to the presence of a thermally sensitive species whose degradation products are considerably less active in the oxidation of methane. The thermally sensitive species are identified as the heteropoly anions which are stabilized on the silica support.

Introduction

In many countries, supplies of natural gas are more plentiful than those of crude oil, often necessitating the importation of crude oil while, at least in some cases, natural gas is exported. While the heat released per carbon atom in oxidation is higher with methane than with any other hydrocarbon, methane suffers from the disadvantage of its gaseous state under ambient conditions. Further, although decreases in free energy are observed for the successive elimination of hydrogen atoms, the complete oxidation of methane is thermodynamically more spontaneous than any processes associated with the partial elimination of hydrogen. Consequently, while natural gas, whose predominant component is methane, has found considerable use as a fuel in stationary applications, it has seen relatively little use in motorized vehicles, nor as a feedstock in the production of chemicals.

Interest in the conversion of methane to more amenable substances has resulted in research efforts on the partial oxidation and oligomerization of the gas. A number of excellent recent reviews are available (1-4). The studies of partial oxidation by Lunsford and co-workers on Mo/SiO_2 (5) and
Somorjai and co-workers on Mo/SiO_2 and V/SiO_2 (6) and that on oxidative coupling with transition metal oxides by Sofranko and coworkers (7-8) are particularly noteworthy.
In this laboratory studies of the surface, structural and catalytic properties of heteropoly oxometalates have been in progress for a number of years. Heteropoly oxometalates are ionic solids with discrete anions of cagelike structure. The anions of Keggin structure have a central atom such as, for example, phosphorus or silicon, surrounded by four oxygen atoms arranged tetrahedrally. Twelve octahedra with, for example, tungsten or molybdenum at their centres envelope the central tetrahedron and share oxygen atoms with each other and with the former (Fig. 1).

Semiempirical extended Huckel calculations have predicted that the solid heteropoly acid containing tungsten as peripheral metal element has more acidic protons than that with molybdenum (9). In addition, the oxygen atoms in the latter anions should be more labile than those in the former anions. Indeed, methanol is converted to hydrocarbons on tungsten-containing heteropoly oxometalates but to CO and CO_2 on those containing molybdenum (10). Photoacoustic FTIR studies have shown that polar molecules such as ammonia (11), pyridine (12) and methanol (13) are able to enter the bulk structure of the heteropoly oxometalates but nonpolar species apparently cannot do so. The acidic proton has been shown to protonate the methanol molecule and at elevated temperatures the C-O bond undergoes a scission and the heteropoly anions are methylatedapparently at the terminal oxygen atoms (14).

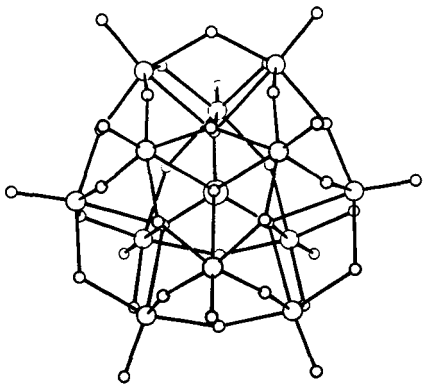

Fig.1 Heteropoly Oxometalate Anion of Keggin Structure

In the present work the oxidative conversion of methane with nitrous oxide is studied on various heteropoly oxometalates, but primarily 12-molybdophosphoric acid ($H_3PMo_{12}O_{40}$, abbreviated to HPMo).

Experimental

Since methane cannot enter the bulk structure of the heteropoly oxometalates and the parent heteropoly acids have low surface areas, it is necessary to support the acids on a high area solid, in the present case silica (Davison Grade 407). An incipient wetness technique is employed to load the solid. A fixed-bed continuous flow reactor with on-line gas chromatograph (HP 5890) was employed for the catalytic studies (15-17).

Results

Table 1 provides a comparison of the results for various supported heteropoly oxometalates as well as supported molybdenum and vanadium catalysts. It is evident that the molybdenum-containing heteropoly oxometalates produce higher conversions and better selectivities to partial oxidation products than those containing tungsten. For comparison samples of molybdenum and of vanadium on silica have been prepared by the method of Liu (5) and the results are included in Table 1.

Table 1

Conversion and Selectivity[a]

Catalyst[b]	Conversion		Selectivity			
	CH_4	N_2O	CO	CO_2	CH_2O	CH_3OH
HPMo (20.0)	5.1	36.4	65.0	22.5	12.0	0.5
HPW (26.2)	0.4	3.2	56.0	44.0	τ	nd
HSiMo (19.9)	2.5	17.0	58.6	32.3	8.7	0.4
HSiW (26.2)	0.4	2.8	44.0	56.0	τ	nd
V (1.66)	8.9	59.1	81.8	14.5	3.5	0.2
Mo (3)	0.4	3.3	57.0	31.0	12.0	τ

a Reaction Conditions: T_R = 843 K, W = 0.35 g, F = 30 ml min^{-1} CH_4 (67%), N_2O (33%)

b Figures in brackets refer to loading of the silica support in wt%.

The remaining of the results reported here pertain to silica-supported HPMo. As expected the selectivity to partial oxidation products increases with decreasing contact time until a maximum is reached. A maximum is also observed for the selectivity to CO while the CO_2 selectivity shows a minimum. The production of CO_2 is found to increase with reaction temperature while that of CO and formaldehyde decreases. The selectivity to partial oxidation produces and the conversion have been shown to be inversely related.

It is of interest to consider the evidence for the participation of the heteropoly oxometalate in the conversion process. The conversion and selectivity in the oxidation of methane with nitrous oxide on silica-supported HPMo remain relatively unchanged for pretreatment temperatures up to approximately 773 K (Figures 2A and 2B). However at higher temperatures the conversion decreases markedly while the production of CO and CO_2 remains constant up to approximately 900 K. For temperatures higher than 900 K the production of H_2CO and CO decreases while that of CO_2 increases with all three apparently approaching that found with the support above.

Experiments in which the pretreatment temperature was held at that for which thermal degradation is occurring (823 K) and the duration of pretreatment varied (Fig. 2C and 2D) show a relatively gradual decrease in the conversion of methane and a small loss of HPMo while CO increases slightly in quantity and the production of CO_2 and H_2O decreases slowly. It is evident that the activity of the HPMo catalysts is related to the presence of a thermally sensitive species whose degradation products are considerably less active in the oxidation of methane.

The rates of reaction are found to be strongly dependent on the loading of HPMo on silica (Fig. 3). The rates increase approximately linearly (except for that of methanol) and reach maxima at a loading of approximately 120 μ mol of heteropoly anions per gram of support. This corresponds to a coverage of approximately 1000 Å/anion, to be compared with an estimate of 100 $Å^2$ for the cross-sectional area of the heteropoly anion. It seems reasonable to assume, at least tentatively, that each anion is isolated on the silica support surface.

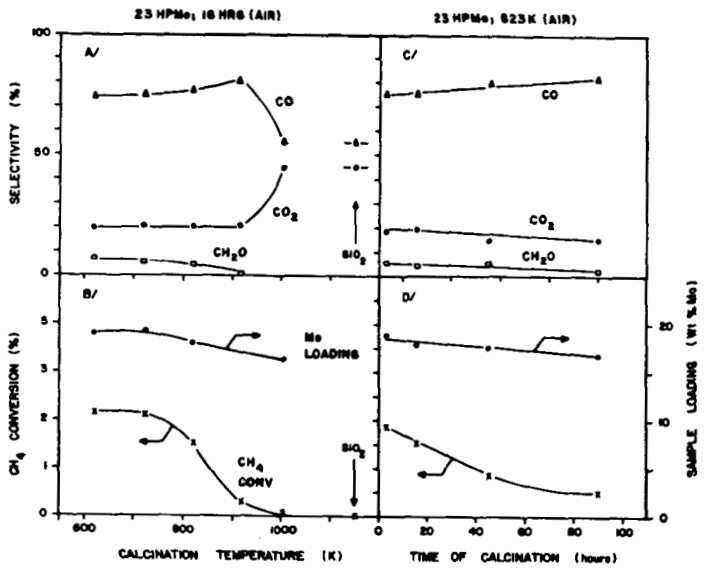

Fig.2 Effect of the temperature of pretreatment during 16 h (left) and of the time of calcination at 823 K under air (right) on the CH_4 conversion, selectivity, and Mo loading of the 23-HPMo catalyst. Reaction conditions: CH_4 (67%), N_2O (33%), T_R = 843 K, W = 0.5 g, F = 30 ml min^{-1}. Symbols: (Δ) CO, (○) CO_2, (□) CH_2O, (X) CH_4 conversion, (●) Mo loading.

Infrared spectra show that the supported HPMo retains the heteropoly anion structure up to temperatures as high as 973 K, suggesting that the silica is, in addition to providing a high area support for the HPMo, also acting to provide a thermal stabilization for the HPMo.

Acknowledgements

Part of this work was done under contract to Energy, Mines and Resources (Canada). The financial support of the Natural Sciences and Engineering Research Council of Canada is also gratefully acknowledged.

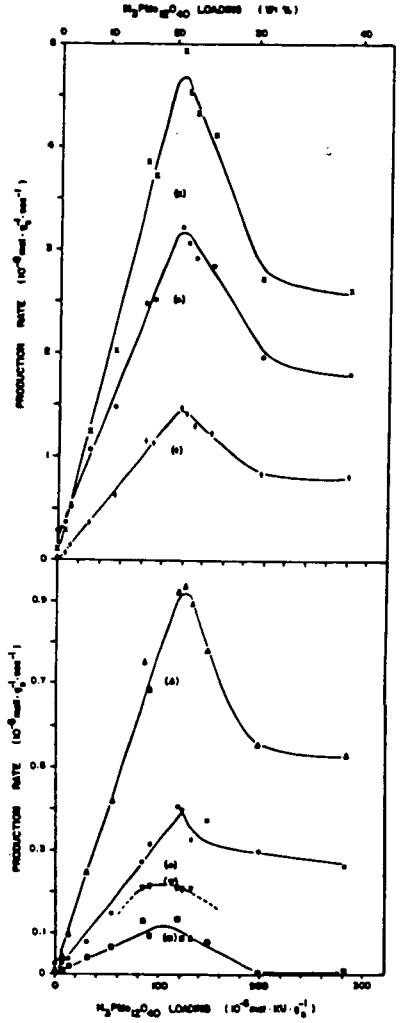

Fig. 3 Effect of the HPMo loading of the support on the production rate of the different products of the $CH_4 + N_2O$ reaction at 843 K. Reaction conditions: CH_4 (67%), N_2O (33%), W - 0.5 g, F = 30 ml min^{-1}, Symbols: (X) N_2, (+) total carbon detected, (●) H_2O, (▽) CH_3OH, (Δ) CO, (○) CO_2, (□) CH_2O.

References

1. C.A. Jones, J.J. Leonard and J.A. Sofranko, Energy and Fuels, 1 (1987) 12.

2. R. Pitchai and K. Klier, Catal. Rev.-Sci. Eng., 28 (1986) 13.

3. H.D. Gesser, N.R. Hunter and C.B. Prakash, Chem. Rev., 85 (1985) 235.

4. N.R. Foster, Appl. Catal., 19 (1985) 1.

5a) H.F. Liu, R.S. Liu, K.Y. Liew, R.E. Johnson and J.H. Lunsford, J. Amer. Chem. Soc. 106 (1984) 4117.

b) L. Mendelovici and J.H. Lunsford, J. Catal., 94 (1985) 37, and references contained therein.

6. K.J. Zhen, M.M. Khan, C.H. Mak, K.B. Lewis and G.A. Somorjai, J. Catal., 94 (1985) 501.

7. J.A. Sofranko, J.J. Leonard and C.A. Jones, J. Catal., 103 (1987) 302.

8. C.A. Jones, J.J. Leonard and J.A. Sofranko, J. Catal., 103 (1987) 311.

9. J. B. Moffat, J. Molec. Catal., 26 (1984) 385; Proc. 8th Iberoamerican Sympos. Catalysis, 1984, p. 349, Lisbon; Catalysis on the Energy Scene, Studies in Surface Science and Catalysis, S. Kaliaguine and A. Mabay (Eds.), 1984, Vol. 19, p. 77, Elsevier, Amsterdam; Catalysis by Acids and Bases, Imelik et al (Eds.), 1985, p. 157, Elsevier, Amsterdam.

10. H. Hayashi and J.B. Moffat in Catalytic Conversion of Synthesis Gas and Alcohols to Chemicals, (R.G. Herman, Ed.), Plenum, N.Y., 1984, and references contained therein.

11. J.G. Highfield and J.B. Moffat, J. Catal., 88 (1984) 177.

12. J.G. Highfield and J.B. Moffat, J. Catal., 89 (1984) 185.

13. J.G. Highfield and J.B. Moffat, J. Catal., 95 (1985) 108.

14. J.G. Highfield and J.B. Moffat, J. Catal., 98 (1986) 245.

15. S. Kasztelan and J.B. Moffat, J. Catal., 106 (1987) 512.

16. S. Kasztelan and J.B. Moffat, J. Catal., (in press).

17. S. Ahmed and J.B. Moffat, Applied Catal., (in press).

CONVERSION OF METHANE TO HIGHER HYDROCARBONS BY SUPPORTED ORGANOMETALLIC COMPLEXES

Robert B. Wilson, Jr. and Yee-Wai Chan
Inorganic and Organometallic Program
SRI International
Menlo Park, CA 94025

ABSTRACT

Novel highly dispersed metal catalysts were prepared by attaching metal clusters to inorganic oxides. The hydridoruthenium complexes (containing one, four or six ruthenium atoms) were first reacted with triethylaluminum, which releases one equivalent of ethane per hydride to give a novel aluminum-containing complex. These complexes were then anchored to the support (alumina, zeolite 5A, or Y-zeolite) by reaction with acidic sites, in which another equivalent of ethane was released. These catalysts were active in the conversion of methane to C_2 and higher hydrocarbons at 750°C using a fixed-bed down-flow reactor under anaerobic condition. Up to 50% selectivity for higher hydrocarbons was observed with the alumina supported hexameric ruthenium clusters. The zeolite supported tetrameric cluster produced less coke than the other catalysts apparently due to the cluster being located inside the zeolite supercage.

INTRODUCTION

Research on the technique of surface confinement to produce novel catalysts for a wide variety of processes is continuing in many laboratories.[1-4] We have been working on the development of novel catalysts for converting methane to higher hydrocarbons. The catalysts are prepared by reacting organometallic complexes of transition metals with inorganic oxide supports to produce surface-confined metal complexes.[5] The metal complex is then decomposed to obtain very stable, highly dispersed catalysts. The increased activity of highly dispersed catalysts is desirable for activating the relatively inert methane and because highly dispersed catalysts are resistant to coking. The use of zeolitic supports will stabilize the highly dispersed catalysts which are confined inside the zeolite pores. The variables we studied include cluster size, supporting materials, and reaction conditions.

EXPERIMENTAL DETAILS

Synthesis of catalysts

The synthesis of these catalysts involves three steps. The first step is to synthesize the ruthenium cluster precursors. The second step is a novel approach developed in our laboratory that involves the reaction of the organometallic clusters with alkyl aluminum. The final step is to anchor these catalysts on supports by a chemical reaction between the hydroxy group of the support and the alkyl groups of the organometallic cluster to give a covalent chemical bond.

The organometallic complexes include a monoruthenium complex, $Ru(allyl)_2(CO)_2$; a tetrameric ruthenium cluster, $H_4Ru_4(CO)_{12}$; a hexameric ruthenium cluster, $H_2Ru_6(CO)_{18}$; and a mixed metal cluster, $H_2FeRu_3(CO)_{13}$; all were prepared according to literature procedures.[6,7] The hydrido clusters reacted with triethyl aluminum at room temperature (eq. 1). The reaction stoichiometries were determined by measuring the quantity of ethane produced.[5] These alkyl aluminum carbonyl ruthenium clusters were then used to react with acidic supports: -alumina, 5A molecular sieves, and LZ-Y 52 zeolite. The reaction stoichiometries were again determined by measuring the quantity of ethane produced (eq. 2).

$$H_4Ru_4(CO)_{12} + Et_3Al \xrightarrow[25^\circ C]{THF} (ET_2Al)Ru_4H_3(CO)_{12} + EtH \qquad (1)$$

$$(ET_2Al)Ru_4H_3(CO)_{12} + S\text{-}OH \xrightarrow[25^\circ C]{THF} S\text{-}O\text{-}Al(Et)Ru_4H_3(CO)_{12} + EtH \qquad (2)$$

The monomeric ruthenium complex reacted directly with the acidic support to release one equivalent of propylene. The tetraruthenium and the mixed iron-ruthenium clusters were also supported on magnesium oxide by the reaction of acidic hydride with the basic oxide. All support materials were in powder form except for the 5A molecular sieves which was 60-80 mesh.

General Procedure for testing catalysts

The activity of the catalysts were tested using a conventional fixed-bed down-flow reactor. In a typical run, the catalyst (0.5 g) was loaded into a stainless steel reactor (0.22 inch ID) under an inert atmosphere. The reactor was connected to the reactor system and purged with helium for 15 min. A helium diluted methane gas (contains 20% methane) was introduced through a mass flow controller to the reactor. A back pressure regulator was set at 50 psig and the methane flow rate was controlled by the mass flow controller. A thermocouple was immersed in the catalyst bed and connected to a temperature controller. The outlet gases were fed to a Carle 500 gas chromatography for sample analysis. The GC was programmed to separate light gases including hydrogen and hydrocarbons up to C_5. The C_6 and higher hydrocarbons and other polar compounds (C6+) were back flushed from the column to the detector. The calibration of C6+ was based on the area integration and referenced to the methane peak. Other components were calibrated with standard sample mixtures. Initial methane concentration was measured before and after each run at ambient temperature under the same conditions. Each sample run lasted for at least 15 h and the products were analyzed every hour. During the first 2 h of the reactions, we detected small amounts of CO, which was released from the decomposition of the metal complexes. The analytical data from the first 3 h of reactions were discarded and the subsequent 12 h data were averaged.

RESULTS AND DISCUSSION

The ruthenium catalysts were tested at 750°C under 50 psig pressure. Three different sizes of ruthenium clusters: monomer (Ru), tetramer(Ru4), and hexamer (Ru6) were supported on three different supports: -alumina, 5A molecular sieve, and Y-zeolite. The results are summarized in Table 1. We used a commercial ruthenium catalyst which is supported on alumina (obtained from Engelhard) for comparison. The amount of metal loading were based on elemental analyses (Galbraith Laboratory).

Effects of cluster size

The commercial ruthenium catalyst gave a very high conversion of methane (71.2%) but no hydrocarbon product was detected. Methane conversion on the monoruthenium catalysts were considerably lower than the ruthenium clusters (Ru_4 and Ru_6). In general, methane conversions depend on the type of support and decreased in the order of alumina, 5A molecular sieve, and zeolite. These results suggested that the methane conversion was related to the amount of surface bonded metal. On alumina, the metals are located on the surface while on 5A molecular sieves and on zeolite, increased amount of metal were located inside the zeolite pore. The differences of methane conversions were more obvious for the Ru_4 catalyst where the conversion decreased from 10.1 to 4.9 and to 1.7% on alumina, 5A molecular sieve, and Y-zeolite, respectively.

Our intention in using different supports is to confine the ruthenium cluster at different locations on or within the support. Hence, the Ru_4 and Ru_6 clusters are dispersed on the alumina surface but are partly confined inside the pores of zeolite supports. The pore size of 5A molecular sieve is too small for the Ru_6 cluster but should be large enough for the Ru_4 cluster after decomposition. Since the Y-zeolite has the largest pore (~ 17), most of the Ru_4 are located inside the zeolite pore.

Product selectivity

All the ruthenium catalysts produced thane and ethylene. The selectivity of C_2 hydrocarbons for Ru_4 clusters increased as the percent conversion of methane decreased. The Ru_6AL has the highest total hydrocarbon yield which probably due to the higher metal loading. The total hydrocarbon yield on Ru_6MS and Ru_6ZL are about the same but the the Ru_6ZL has a higher selectivity for C_2 product. Confining the metal cluster inside the zeolite cage may also limite the propagation of methane polymerization. The ruthenium monomers gave relatively low hydrocarbon yields indicating that polymerization of methane required more than one metal atom.

Table 1

ACTIVITY OF RUTHENIUM CATALYSTS ON METHANE DEHYDROGENATION[a]

Catalyst[b]	Ru(wt%)	Flow Rate (mL/min)	Methane Conver(%)	Selectivity[c] to H_2(%)	C_2(%)	C_{6+}(%)
Ru-com	0.50	50	71.2	151.0	--[d]	--
RuAL	0.35	10	3.0	139.9	2.8	--
RuMS	0.31	10	2.3	147.5	1.2	--
RuZL	0.37	10	1.7	177.5	2.6	--
Ru_4AL	0.61	100	10.1	78.6	1.62	--
Ru_4MS	0.49	100	4.9	146.6	3.52	--
Ru_4ZL	0.61	50	1.7	25.3	6.9	28.9
Ru_6AL	1.26	50	6.1	113.4	6.9	41.4
Ru_6MS	0.19	50	5.6	192.8	1.0	14.8
Ru_6ZL	0.20	50	3.6	161.9	3.6	10.0

[a]Reaction condition: temperature=750C, pressure=150 psig.
[b]Abbreviation: Ru-com=commercial ruthenium catalyst from Engelhard; Ru_4=$(C_2H_5)_2AlRu_4H_3(CO)_{12}$;$Ru_6$=$(C_2H_5)_2AlRu_6H(CO)_{18}$; Ru=Ru(Allyl)$(CO)_2$; AL=-alumina; MS=5A molecular sieve; ZL=LZ-Y-zeolite.
[c]Selectivities were calculated on converted methane. Selectivity to hydrocarbons are based on carbon number.
[d]Not detected.

Coking

The results listed in Table 1 show that more than on equivalent of hydrogen was produced per methane input, which suggests that some of the methane turned to coke. The elemental analyses listed in Table 2 showed that the Ru_4AL, Ru_4MS, Ru_6AL and Ru_6MS contained more carbon after reaction with methane. In contrast, the carbon content of the Ru_4ZL decreased after reactios. Thus, those catalysts having metal dispersed on the support surface (and therefore larger particle size) promote coke formation while the metals confined inside the zeolite cages have much reduced coking. For the Ru_4MS, the carbon content only increased slightly to 4.38% as compare to more than 20% for the Ru_4AL suggesting that at least a portion of the metal clusters are located inside the

cages of the molecular sieve. On Y-zeolite, the Ru_4 cluster in fact showed a decrease in carbon content indicating very low coking. The decrease is due to the decomposition of the ruthenium complexes, i.e. release of carbon monoxide.

Table 2

ELEMENTAL ANALYSES OF RUTHENIUM CATALYSIS FOR METHANE DEHYDROGENATION[A]

	Before Reaction			After Reaction		
Catalyst	%C	%H	%Ru	%C	%H	%Ru
Ru_4AL	5.09	1.04	0.61	26.50	0.40	0.57
Ru_4MS	1.46	1.13	0.49	4.38	0.46	0.64
Ru_4ZL	5.25	1.53	0.61	0.58	0.22	1.26
Ru_6AL	9.77	1.84	1.26	23.24	0.67	0.55
Ru_6MS	0.95	1.68	0.19	22.29	0.19	0.32

[a]Reaction with methane at 750C for 15 h.

Effect of reaction conditions

The effect of reaction temperature is similar for every catalyst. Higher methane conversion and product yield are obtained at higher temperature. These results are expected because polymerization of methane is thermodynamically unfavored process.[8] Increasing the reaction pressure has a similar effect on the methane conversion. However, the product selectivities for hydrogen and C2 hydrocarbons decrease but increases for C6+ hydrocarbons (Table 3). Highest selectivity is observed at 150 psig. As expected, increasing the space velocity lowers the methane conversion but increase the selectivity of hydrocarbon products.

Basic support and mixed metal cluster

Methane conversion on the magnesia supported ruthenium monomer and the $FeRu_3$ cluster are much higher than the zeolite supported analogs (Table 4). However, the product selectivities to hydrocarbons are lower.

Table 3

EFFECT OF REACTION PRESURE AND SPACE VELOCITY TO THE ACTIVITY OF Ru_6ZL[a] AT 750°C

Pressure (psig)	Flow rate mL/min	%CH_4 Conversion	%Selectivity[b] of H_2	C_2	C_{6+}
50	50	3.18	164.16	6.04	6.6
150	50	5.19	91.33	4.48	10.70
250	50	8.64	82.41	2.46	7.38
250	100	2.62	177.10	9.24	20.64

[a] Ru_6ZL = zeolite supported Ru_6 cluster, $C_2H_5AlRu_6H(CO)_{18}$.
[b] Selectivity was based on carbon number of hydrocarbon and the amount of methane reacted.

Table 4

CATALYTIC REACTIVITY OF ZEOLITE AND MAGNESIA SUPPORTED CATALYSTS FOR METHANE DEHYDROGENATION[a]

Catalysts	Temp(°C)	Methane Conversion(%)	Selectivity[b] C_2(%)	C_{6+} (%)
RuMgO	600	21.044	0.1	0.5
Ru_4MgO	750	4.04	6.9	49.2
$FeRu_3ZL$	600	3.07	1.9	18.5
$FeRu_3MgO$	600	8.87	0.1	--

[a] Reaction conditions: pressure=150psig, flow rate=20 mL/min, weight of catalyst=2 g, reactor O.D.-3/8in (S.S.).
[b] Selectivity to hydrocarbon is based on carbon number.
[c] Not detected.

For the mixed iron-ruthenium catalysts, magnesia support also increased the methane conversion. At 600°C, the methane conversion was 8.87% for $FeRu_3MgO$ and was 3.07% for $FeRu_3ZL$. At 750°C, methane conversion increased to 41.5% and 23.05% for $FeRu_3MgO$ and $FeRu_3ZL$, respectively. These catalysts behave similarly to the ruthenium monomers in that the hydrocarbon yields were lower on the magnesia supported catalyst.

Increased temperature has a similar effect on the methane conversion over $FeRu_3ZL$, but the methane conversion was lower than the MgO supported catalysts. At 750°C, the methane conversion was 23.05%. Hydrocarbon yields increased as the reaction temperature increased from 500° to 600°C and then declined at higher temperature. The maximum yield of C2 was 0.06% of the input methane and was 0.57% for C6+. Since the Ru_4ZL was essentially not active at 600°C, this low temperature reactivity of $FeRu_3ZL$ is obviously due to an effect of the mixed metal. Introduction of the iron to the metal cluster is advantageous to methane dehydrogenation activity. Figure 3 shows the effect of increasing temperature on methane conversion and on hydrocarbon yield. Highest hydrocarbon yield was obtained at 600°C. However, the hydrogen selectivity was 170% at this temperature which suggests coke formation.

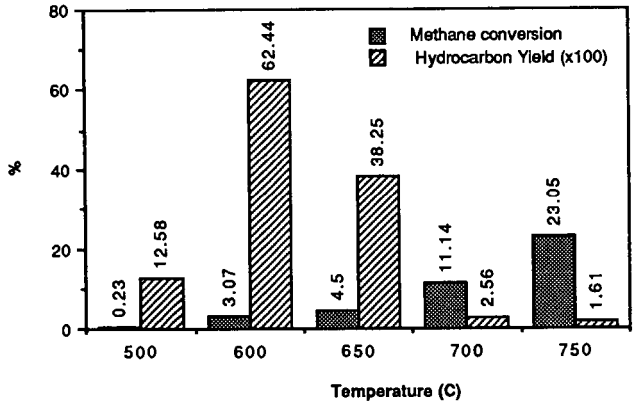

Figure 1. Activity of FeRu3ZL for methane reforming at various temperatures.

CONCLUSION

Most of the reports on catalytic conversion of methane to higher hydrocarbons are based on metal oxides by the oxidative coupling pathway. Few examples have been reported of direct methane dehydrogenation. Table 5 lists some of the literature results on both oxidative coupling and dehydrogenation together with our results.

It is difficult to truly compare the catalytic activities of the catalysts because the experimental condition are so different. However, based on the methane conversion and the selectivities of higher hydrocarbons, our catalysts are comparable. Interestingly, we have not detected any mid-ranged hydrocarbons (C_3-C_5). Mitchell and Waghorne reported the major product of alumina supported CaCrPt catalyst under anaerobic condition was benzene.[9] Jones et al. also observed small amounts of benzene produced from methane dehydrogenation over silica support GeO_2.[10] We have not yet identified our C_{6+} product, but it is possible that it contains benzene.

Table 5

COMPARISON OF THE ACTIVITIES OF CATALYSTS FOR METHANE DEHYDROGENATION

Catalyst	CH_4/O_2	Temp. (°C)	Press (atm)	GHSV (h^{-1})	CH_4 conv(%)	Selectivity to C_2	Selectivity to C_6
Li/MgO[a]	2	720	1	2754	37.8	50.3	N.R.[h]
CaCrPt/AL[b]	>200[j]	705	1	N.R.	27.64[i]	31.4	68.3
PbO/MgO[c]	6	750	1	8000	10.0	65.5	N.R.
Sm_2O_3[d]	6	750	1	3.8×10^7	6.5	60.0	N.R.
Sb_2O_3/SiO_2[e]	>200	800	1	600	0.25[i]	82.9	N.R.
GeO_2/SiO_2[f]	>200	700	1	860	0.22	57.1	3.3[k]
Ru_6AL[g]	>200	750	4.5	16000	6.06	6.9	41.4
Ru_4ZL[g]	>200	750	4.5	16000	1.74	6.9	28.9
Ru_4MgO[g]	>200	750	4.5	6200	4.04	6.9	49.2
$FeRu_3ZL$[g]	>200	600	4.5	6200	3.07	1.9	18.5

[a] T.Ito; J-X Wang; C-H, Lin; J.H. Lunsford, J. Am. Chem. Soc., 107, 5062 (1986).
[b] H.L.Mitchell, III; R.H. Waghorne; U.S. Patent No. 4239658 (1980).
[c] K.Asami; S. Hashimoto; T. Shikada; Chem. Letter 1233 (1986).
[d] K. Otsuka, T. Komatsu; Chem. Lett. 483 (1987).
[e] C.A. Jones, J.J. Leonard; J.A. Sofranko; U.S. Patent 4,443,644 (1984).
[f] C.A. Jones, J.J. Leonard; J.A. Sofranko; U.S. Patent 4,554,395 (1985).
[g] This work.
[h] Not reported.
[i] Cumulative result.
[j] No oxygen added.
[k] benzene.

References

1. M.E. Dry and J.C. Hoogendoorn, Catal. Rev., 23, 265 (1981).

2. D.L. King, J.A. Cusumano, and R.L. Garten, Catal. Rev., 23, 203 (1981).

3. H.C. Foley, S.J. D-Cani, K.D. Tau, K.J. Chao, J.H. Onuferko, C. Dybowski, and B.C. Gates, J. Am. Chem. Soc., 105, 3074 (1983).

4. J.P. Candlin and H. Thomas, "Supported Organometallic Catalysis", in Homogeneous Catalysis II, D. Forster and J.F. Roth, eds., Adv. Chem. Series, 132, 212-239 (1974).

5. Y.I. Yermakov, B.N. Kuznetsov, and V.A. Zakharou, "Catalysis by Supported Complexes," Vol.8, Studies in Surface Science and Catalysis, Elsevier, Amsterdam, (1981).

6. A.A. Bhattacharyya, C.L. Nagel, and S.G. Shore, Organometallics, 2, 1187 (1983).

7. G.L. Geoffroy and W.L. Gladfelter, J. Am. Chem. Soc., 99, 7565 (1977).

8. D.R. Stull, E.F. Westrum Jr., and G.C. Sinke, The Chemical Thermodynamic of Organic Compounds, Wiley, New York, (1969).

9. H.L.Mitchell, III; R.H. Waghorne; U.S. Patent No. 4239658 (1980).

10. C.A. Jones, J.J. Leonard; J.A. Sofranko; U.S. Patent 4,554,395 (1985).

PARTIAL OXIDATION OF METHANE USING SUPPORTED PORPHYRIN AND PHTHALOCYANINE COMPLEXES

Yee-Wai Chan and Robert B. Wilson, Jr.
Inorganic and Organometallic Program
SRI International
Menlo Park, California 94025

ABSTRACT

The catalytic oxidation of methane with molecular oxygen was investigated in a fixed-bed flow reactor with various anchored metal phthalocyanine (PC) and porphyrins (TPP) as the catalysts. These support organometallic species were stable at temperatures as high as 400°C. Methanol was formed from zeolite encaged RuPC, CoTPP, and MnTPP at 375°C. In contrast, a PdPC complex attached to magnesia produced ethane rather than methanol. The other surface-supported catalysts gave carbon dioxide and water as the sole observable products (by GC).

INTRODUCTION

Conversion of methane to useful chemicals by partial oxidation and oxidative dehydrogenation has received the attention of many researchers.[1] Our first approach to the goal of selective partial oxidation of methane was to synthesize zeolite encapsulated porphyrin and phthalocyanine complexes that mimic the oxygenase enzyme: Cytochrome P-450.[2-5] Porphyrins and phthalocyanines are potent oxidants that also allow control of the active form of oxygen, thereby leading to control of activity and selectivity. The use of zeolitic supports will enhance the stability and reactivity of the catalysts, and will discourage the secondary reactions that always pose problems in the oxidation of methane because the primary products are more easily oxidized than methane.

Our second approach to stabilize the phthalocyanine complex is by anchoring the complex on the surface of a support. Magnesium oxide is

known to generate methyl radicals from methane,[6] lithium promoted MgO has shown high selectivity to C_2 hydrocarbons on methane oxidation.[8,9] The metal oxo intermediate generated from the phthalocyanine and oxygen should react with methyl radicals faster than with methane. We prepared magnesium oxide supported catalysts by reacting the basic support with the acid form of tetrasulfophtha-locyanine (TSPC) complexes. The TSPC complexes were anchored to the MgO surface by ionic interaction between the sulfonate groups of the metal complex and the basic sites of MgO.

EXPERIMENTAL DETAILS

Preparation of Metal Ion Exchanged Zeolite

To a slurry of 500 g zeolite (LZ-Y52, Unioncarbide) and water (500 mL), a 1M aqueous solution of metal salt (500 mL, $FeCl_2$, $CoCl_2$, $MnSO_4$, or $Ru(DMSO)_2Cl_2$) was added dropwise. The zeolite slurry was stirred at a constant speed. The total addition time was approximately 1 h. The mixture was allowed to stir for 24 h. The exchanged powder was filtered, washed with water until the washing were free of chloride or sulfate and then dried at 150°C under vacuum for 48 h. Elemental analysis of Co-zeolite: C, 0.27; H, 0.91; Co, 4.76; Fe-zeolite: C, 0.26; H, 1.20; Fe, 4.89; Ru-zeolite: C, 1.16; H, 1.08, Ru, 0.95.

Preparation of zeolite encapsulated metallophthalocyanine

Metal exchanged zeolite (100 g) and 8 equivalent of 1,2-dicyano-benzene were added to 200 mL of nitrobenzene in a round bottom flask fitted with a reflux condenser and a mechanical stirrer. The mixture was heated to 180°C for 4 h under nitrogen until the solution changed color (dark green for Fe, dark blue for Co, brown for Mn and Ru). The zeolite was filtered, washed with methanol to remove nitrobenzene, and Soxhlet extracted with pyridine until the solution was clear. Excess pyridine was removed by Soxhlet extraction with methanol. The zeolite powder was then boiled in a 1 M solution of NaCl (reverse metal exchange) for 4 h, washed with water and acetone. The product was dried at 150°C under vacuum for 24 h.

Preparation of zeolite encapsulated tetraphenylporphyrin

Zeolite powder (200 g) was added to 1.8 L of acetic acid in a 2 L round bottom flask equipped with mechanical stirrer and an addition funnel which contained 46.5 mL pyrrol and 66.5 mL of benzaldehyde. The acetic acid was heated to boil. The pyrrol and benzaldehyde were added slowly. The reaction mixture was boiled for 0.5 h under air. The dark purple solid was filtered while the solution was still warm. It was then washed with large amount of acetone until the washing was colorless. The product was dried at 150°C under vacuum for 24 h.

Metal insertion of tetraphenylporphyrin in zeolite

A mixture of TPP zeolite (50 g) and metal salt (0.12 mole of $CoCl_2$, $FeCl_2$, $MnSO_4$, or $Ru_3(CO)_{12}$) was added to 200 mL of dimethyl sulfoxide in a three necked round bottom flask equipped with a mechanical stirrer, a reflux condenser, and a gas inlet adaptor. The reaction mixture was heated to reflux for 3 h. The product was washed with water and methanol. Excess metal salt was removed by boiling in a 1 M aqueous solution of NaCl for 2 h. The product was washed again with water and methanol and then dried at 150°C for 24 h.

Preparation of magnesia supported tetrasulfothalocyanines

The tetrasulophthalocyanine complexes were prepared via the reaction of monosodium salt of 4-sulfophthalic acid, urea, and metal salt in the presence of catalytic amounts of ammonium molybdate, and ammonium chloride at 180°C. The acid form of the complexes were obtained by acidification of the aqueous solutions with 2 N HCl. The resulting metal complex (0.5 g) was then dissolved in DMF (500 mL) , added to MgO powder (10 g), and stirred for 2 h. After washing with DMF and acetone, the catalysts were dried at 60° under vacuum overnight. Five catalysts: PdTSPCMgO, FeTSPCMgO, CuTSPCMgO, RuTSPCMgO, CoTSPCMgO, were prepared by this method.

General procedure for testing methane oxidation catalysts

The catalyst (3 g) was loaded into a stainless steel reactor (3/8" OD). The reactor was connected to the reactor system and purged with helium for 15 min. It was heated to 200°C under a slow flow of hydrogen for 2 h. Methane (10.3% in helium) and oxygen (5.2% in helium) were introduced to the reactor and the temperature was increased to 300°C or higher. Methane and oxygen were individually controlled by mass flow controllers. The reactor pressure was set at 50 psig via a back pressure regulator. A thermocouple was immersed in the catalyst bed and connected to a temperature controller that controls the furnace. The outlet gases were fed to a GC sampling value through heated stainless steel tubing (110°C).

RESULTS AND DISCUSSION

Phthalocyanine complexes are synthesized within the zeolite pore by first exchanging the metal ion into the pore, followed by template condensation.[10] We used Na-Y zeolite because it has large pores that allows the phthalocyanine complexes to fit in and contains exchangeable ions. Some of the phthalocyanines that absorbed on the zeolite surface were removed by extraction with pyridine and acetone. Excess metal ions were then back exchanged with sodium ions. Surface reflectance UV-Vis and FT-IR of the non-extracted catalysts evidenced the presence of phthalocyanine.

The zeolite encapsulated metalloporphyrins was synthesized by a modified method. The metal free ligand was first synthesized inside the zeolite cage by refluxing benzaldehyde, pyrrol, and the Na-Y zeolite (without metal exchange) in acetic acid. The surface attached porphyrin was extracted with methanol. The washings contain tetraphenylporphyrin as indicated by its UV-Vis spectrum.

The desired metal ion was inserted into the porphyrin by boiling the metal salt and the zeolite containing the porphyrin in dimethyl-

sulfoxide solution. The product was washed with water and then Soxhlet extracted with methanol to remove surface-bound TPP complex. Uncomplexed metal ions are removed by reverse ion-exchange with sodium chloride. However, the excess iron ions were not exchangeable by sodium ions and we have not attempted to remove the excess iron by another method. The FePCZL and the ReTPPZL thus contained excess iron ions. The metal loading (by weight) and the percent of super cages occupied by the metal complexes (calculated based on the results from elemental analyses) are listed in Table 1.

Table 1

METAL AND COMPLEX LOADING OF ZEOLITE ENCAPSULATED COMPLEXES

Catalyst [a]	Wt.% metal Loading	% Supercages Occupied
CoPCZL	1.53	60
FePCZL	4.15[b]	50
RuPCZL	0.97	20
MnPCZL	1.62	68
CoTPPZL	0.15	5
FeTPPZL	4.04[b]	8
RuTPPZL	0.13	2.5
MnTPPZL	0.12	4.3

[a] Pc = phthalocyanine, TPP = Tetraphenylporphyrin, ZL = zeolite.
[b] The iron complexes contained excess iron ions which can not be exchanged by sodium ions.

These zeolite catalysts were tested for methane oxidation at 375°C under 50 psig pressure. The results are averaged from data taken during the 15 to 20 h of the runs and are summarized in table 2. Three catalysts including RuPcZL, CoTPPZL, and MnTPPZL showed some reactivity toward the formation of methanol. As shown in table 5, the RuPcZL gave the highest selectivity of methanol. The methane conversions were generally below 10%. Carbon dioxide and water were always the major products.

Three control experiments were run using the blank zeolite, ruthenium exchanged zeolite (with triruthenium dodecacarbonyl), and ruthenium tetracarboxyphthalocyanine. The blank zeolite gave essentially no reactivity toward methane oxidation. Less than 0.5% of methane was oxidized to carbon dioxide. The ruthenium zeolite produced hydrogen, carbon dioxide and water with approximate 16% methane conversion. The RuTPPZL and FePcZL also gave hydrogen which suggest that these two catalysts behaved like the simple metal exchanged zeolite, because the excess metal ion in these two catalysts was not removed by the reverse ion exchange process. The productions of hydrogen were due to the catalytic ability of the zeolite adsorbed metal particles.

Table 2

ACTIVITY OF METHANE OXIDATION CATALYSTS

Catalyst	% Conv.of CH_4	H_2	% Selectivity of CO_2	H_2O	CH_3OH
Zeolite	0.5	---	100	---	---
RuZL	15.9	45	100	100	---
CoPcZL	6.3	---	100	100	---
FePcZL	18.2	1.2	100	42	---
RuPcZl	4.8	---	87	1	11.3
MnPcZL	9.6	---	80	65	---
CoTPPZL	1.9	---	94	120	5.8
FeTPPZL	1.9	---	100	73	---
RuTPPZL	8.4	50	99	146	---
MnTPPZL	1.8	---	95	126	3.5

Reaction conditions: Temperature=375C, Pressure=50psig, CH_4/O_2=4, GHSV=2600 h^{-1}.

Some of the catalysts were also tested at higher temperature under the same condition. The results were summarized in Table 3. Methane conversions were generally increased at higher temperature. Again, only

RuPcZL and CoTPPZL showed some activity toward methanol formation, but the yields were significantly decreased. These results indicated that the metal complexes decomposed at high temperature and therefore lost their activity. The characteristic blue green color of the phthalocyanines and the purple color of the porphyrins disappeared after the high temperature reactions. The decomposition of catalysts were confirmed by elemental analyses.

Table 3

ACTIVITY OF METHANE OXIDATION CATALYST AT HIGH TEMPERATURE

Catalyst	Temp. (°C)	% Conversion		% Selectivity			
		CH_4	O_2	H_2	CO_2	H_2O	CH_3OH
RuZL	500	20.8	99.0	110.0	89.3	---	---
FePcZL	500	22.7	87.2	15.9	100.0	45.0	---
RuPcZl	450	9.0	99.6	---	96.7	0.5	3.3
CoTPPZL	450	3.3	56.1	---	98.0	126.2	2.0
FeTPPZL	450	6.1	32.8	---	100.0	65.1	---

Reaction conditions: Pressure=50 psig, $CH_4/O_2 = 4$, GHSV = 2600 h^{-1}.

It has been noted that high levels of complex loading results in blocking the access of substrate to the metal center.[11] The zeolite encapsulated phthalocyanines prepared in this work contained relatively high complex loading. About half of the supper cages in the zeolite were filled with metal complex in the CoPCZL, FePCZL, and MnPCZL. The RuPCZL was the only catalyst that showed activity and it contained less metal complex than the others. We are not certain whether the lack of catalytic activity was due to the accessibility of methane to the active site of the catalyst or was truly an inactive metal complex since methane is a rather small molecule. In contrast, the TPP analog of RuPCZL was not active in converting methane to methanol but the CoTPPZL

and the MnTPPZL were active. Since all the zeolite encapsulated TPP complexes contained low complex loading, the nature of the metal complex should be responsible for the catalytic activity.

We tested four metal complexes of tetrasulfophthalocyanine supported on magnesium oxide (Pd, Fe, Ru, Cu). The metal loading and complex loading are listed in Table 4. Interestingly, the palladium catalyst (PdTSPCMgO) produced ethane from the oxidation of methane at 375°C instead of methanol (Table 5). Although the selectivity was low (2.8%), oxidative coupling of methane to ethane at such low temperature is unusual. Increasing the reaction temperature to 400°C, increased methane conversion and decreased ethane selectivity. Further increases of the temperature to 450°C decomposed the complex. All other catalysts tested gave only products of complete oxidation, ie. CO_2 and H_2O.

Table 4

METAL LOADING AND COMPLEX LOADING OF THE MAGNESIUM OXIDE SUPPORTED CATALYSTS

Catalyst	Metal loading (Wt%)[a]	Complex loading (mol/100g)[b]
FeTSPCMgO	0.24	0.052
RuTSPCMgO	0.45	0.047
PdTSPCMgO	0.18	0.026
CuTSPCMgO	0.37	0.054

[a]Based on elemental analysis.
[b]Mole of complex were calculated based on the carbon weight from the elemental analyses.

Table 5

ACTIVITY OF MgO SUPPORTED METHANE OXIDATION CATALYSTS[a]

Catalysts	Temp. (°C)	%Conversion of Methane	%Selectivity[b] CO_2	%Selectivity[b] C_2H_6
PdTSPCMgO	375	1.4	97.2	2.8
	400	2.6	97.8	2.2
	450	5.7	99.7	0.3

[a]Condition: Pressure = 1 atm, CH_4/O_2 = 10, GHSV = 5000 h^{-1}.
[b]Selectivity was calculated based on carbon number.

CONCLUSION

To the best of our knowledge, this is the first observation of methanol production from partial oxidation of methane using cytochrome-P450 mimic. Encapsulating the porphyrin and phthalocyanine complexes inside the zeolite cages precludes the intermolecular reactions which leads to the problem of catalyst deactivation. Anchoring the metal complexes on the support surface also prevents such bimolecular self destruction. Oxidative coupling of methane is usually observed at temperature much higher (>700°C) than what we observed for PdTSPCMgO (375°C). Many questions remained to be answered including improving product selectivity.

References

1. R. Pitchai and K. Klier, Catal. Rev.-Sci. Eng., 28(1), 13-88 (1986).

2. J. T. Groves and D. V. Subramanian, J. Am. Chem. Soc., 106, 2177 (1984).

3. J. P. Collman, T. Kodadek, S. A. Raybuck, and B. Meunier, Proc. Natl. Acad. Sci. USA, 80, 7039 (1983).

4. D. Mansuy, P. Battioni, and J-P. Renaud, J.C.S. Chem. Commun., 1255 (1984).

5. A. M. Khenkin and A. A. Shteinman, J.C.S. Chem. Commun., 1219 (1984).

6. T. Ito, T. Tashiro, T. Watanabe, K. Toi, and I. Ikenmoto, Chem. Lett., 1723 (1987).

7. D. L. Driscoll, W. Martir, J.-X. Wang, and J. H. Lunsford, J. Am. Chem. Soc., 107, 58 (1985).

8. E. Iwamatsu, T. Moriyama, N. Takasaki, and K.-I. Aika, J.C.S. Chem. Commun., 19 (1987).

9. T. Ito, J.-X. Wang, C.-H., Lin, J. H. Lunsford, J. Am. Chem. Soc., 107, 5062 (1986).

10. G. Meyer, D. Wohrle, M. Mohl, and G. Schulz-Ekloff, Zeolites, 4, 30 (1984).

11. N. Herron, G. D. Stucky, and C. A. Tolman, J.C.S. Chem. Commun., 1521 (1986).

BIOCONVERSION OF METHANE TO METHANOL BY METHYLOBACTERIUM ORGANOPHILUM.

LORI E. PATRAS AND ALICE TANG

UNOCAL
SCIENCE AND TECHNOLOGY DIVISION
BREA, CALIFORNIA

INTRODUCTION

Large reserves of natural gas have stimulated the development of processes that can convert methane to more valuable chemicals such as methanol. Commercial routes to methanol involve three steps. First synthesis gas is generated from natural gas or naphtha at 15-30 atmospheres and 840-900 °C. The synthesis gas is converted to methanol using a copper catalyst which requires the process condition of 300-350 psig and 250-270 °C. The methanol is then distilled to desired purity. Many bacteria and fungi grow on methane at ambient temperature and pressure. In this study we attempt to develop a low severity route from methane to methanol, involving a biochemical catalyst.

Methylobacterium organophilum was grown in a methane-oxygen controlled atmosphere water bath shaker apparatus to study the bioconversion of methane to more valuable chemicals such as methanol. To optimize production of methanol from the metabolism of methane by Methylobacterium organophilum, we tested the effects of culture enrichment and inhibitors.

EXPERIMENTAL

Methylobacterium organophilum was purchased from the American Type Culture Collection (ATCC #27886). For all studies, excepted when noted, ammonium mineral salts (AMS) medium was used.

All growth experiments were conducted under a methane atmosphere, in a controlled atmosphere water bath shaker apparatus. Liquid cultures were grown in 250 ml Erlenmeyer flasks at 30 °C on the rotary shaker (150-200 rpm) at pH 6.8 with methane as the only carbon source for growth (unless otherwise stated). The atmosphere of the incubator shaker was normally continuously gassed with 65% methane, 20% oxygen, and 15% nitrogen.

Cell densities were measured by monitoring the absorbance at 660nm by Sargent-Welch model SM spectrophotometer. The cells were harvested by centrifugation and dry cell weights were determined after drying the cell paste in a vacuum oven.

Cell free culture broth was analyzed for methanol by gas chromatography. The cells were removed by centrifugation followed by filtration.

RESULTS AND DISCUSSION

Methylobacterium organophilum is a facultative methylotroph; it can grow not only on C-1 compounds but also on multicarbon compounds as the sole sources of carbon and energy. Figure 1 shows the growth of M. organophilum on one-carbon and multicarbon substrates.

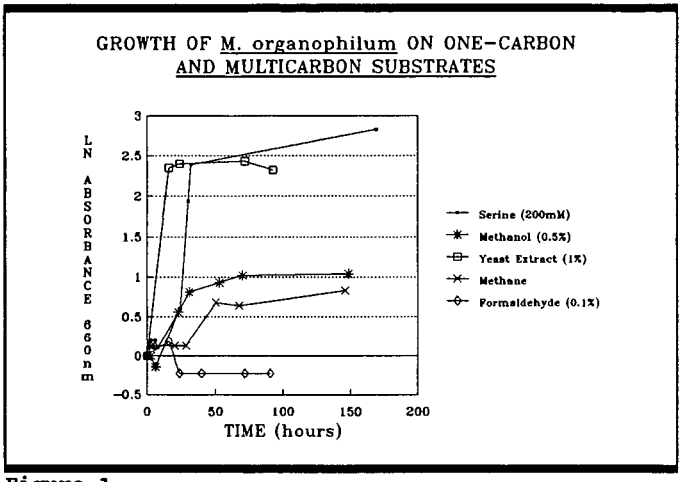

Figure 1

The specific growth rate on methane is lower than the other substrates. This is expected since the solubilities in water of the other substrates are higher than the solubility of methane in water.

Another important characteristic of M. organophilum is the type II intracytoplasmic membrane. Cultures previously grown on a multicarbon substrate for growth and energy required several transfers grown on methane before accumulating methanol. This "inactive" state of the microbe may be explained by the fact that it is necessary for the bacterium to possess an intracytoplasmic membrane for methane metabolism to occur. The literature reports that M. organophilum contains an intracytoplasmic membrane when grown on methane but this membrane is not present during growth on higher substrates such as methanol and glucose (1).

Methylobacterium organophilum oxidizes methane by a special C-1 oxidation pathway (see below).

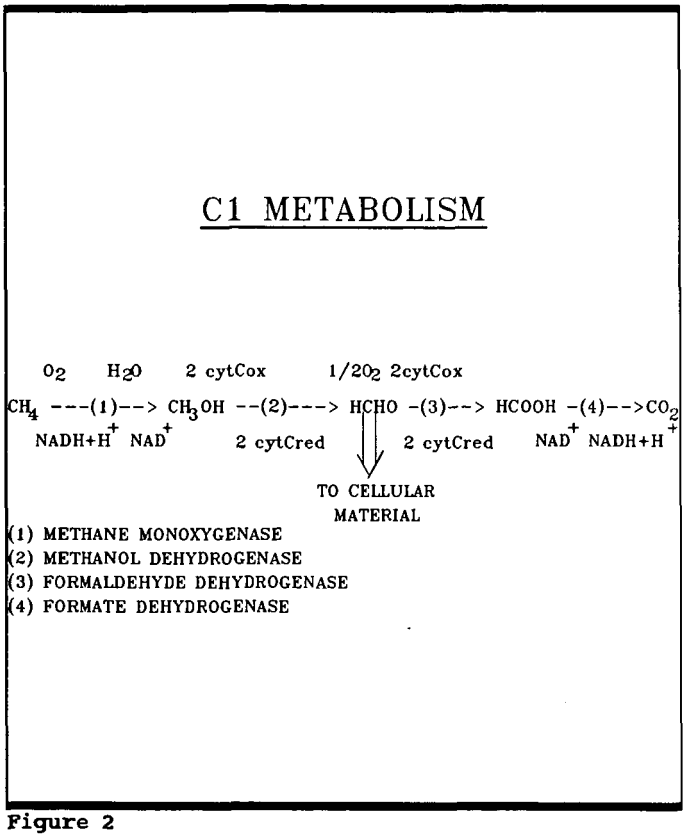

Figure 2

Biomass is produced through formaldehyde assimilation. The mechanism of the reaction CH_4 -----> CH_3OH involves atmospheric oxygen incorporated directly into the methane molecule with the aid the enzyme, monooxygenase. The hydrogen requirement is supplied by the conversion of formic acid to carbon dioxide implying that methane oxidation is a function of successive oxidations. This presents a problem if methane oxidation is stopped at methanol because the regeneration of NAD+ would be lost.

High biomass cultures of M. organophilum were tested for methanol accumulation while growth was monitored (see below).

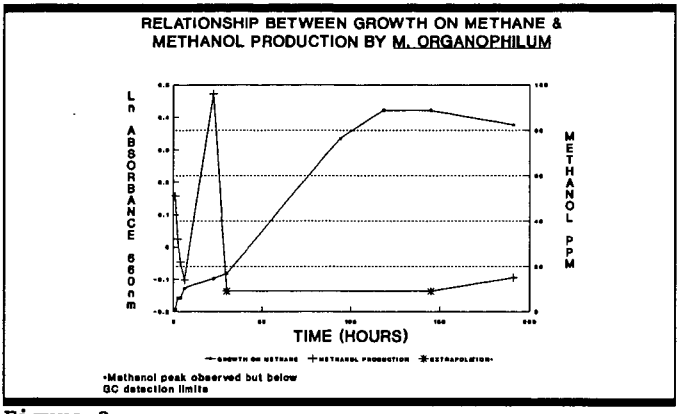

Figure 3

It appears that methanol accumulates during non-growth periods from methane oxidation. This is expected since during growth, the methanol is further metabolized for cell growth and energy. During initial incubation, methanol production was low (1.1 mmoles/gDCW.Hr).

The effect of iodoacetic acid on methanol production was studied. Cultures of M. organophilum were tested for methanol accumulation during growth on methane in the presence of iodoacetic acid (see below).

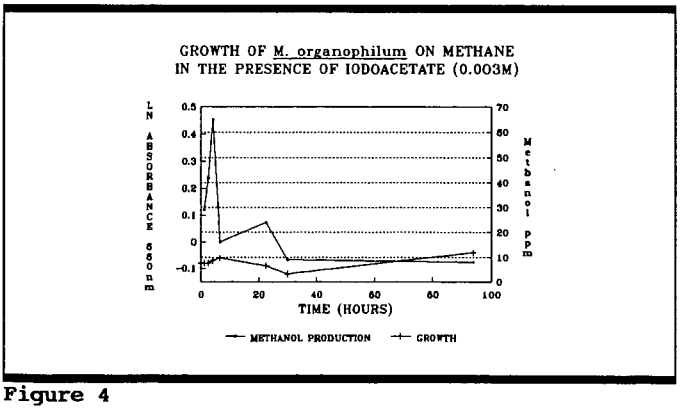

Figure 4

Iodoacetic acid inhibited growth but did not inhibit further oxidation of methanol. Iodoacetic acid had no effect on methanol accumulation at the described conditions.

Culture enrichment was also studied to increase the methanol production rate. M. organophilum was grown on serine in the presence of methane. Serine is an intermediate metabolite in the pathway of methane oxidation to cellular material. By adding high concentrations of serine (200mM) in a culture of M. organophilum growing on methane, the equilibrium of the organism may shift. Creation of a metabolic block through manipulation of the environment (the addition of serine) may bring accumulation of metabolites preceeding the block. Methane (the original carbon source) is the starting material for bioconversion (Figure 5).

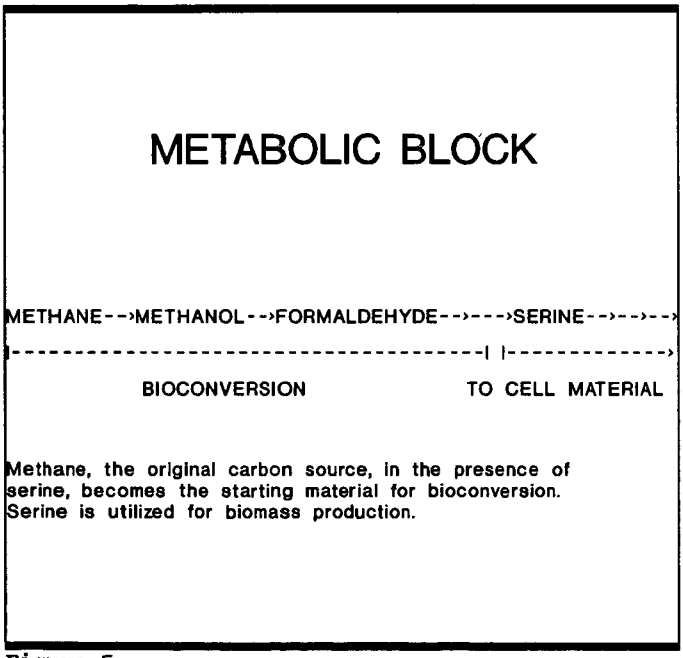

Figure 5

During growth on methane and serine, accumulation of formic acid and acetic acid were seen during growth. Volumetric rates were 0.1g/l.hr and 0.3g/l.hr for formic acid and acetic acid, respectively.

Figure 6 shows that regulation in M. organophilum is obvious during growth on more than one carbon substrate in the medium.

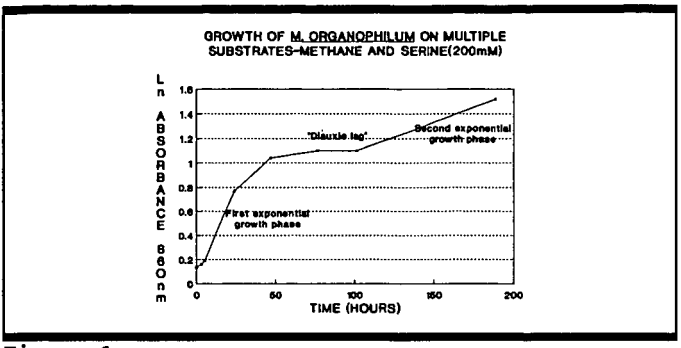

Figure 6

Growth of M. organophilum on methane and serine shows the diauxie phenomenon discovered by Monad(2). The substrates are utilized in two exponential growth cycles. The growth cycles are separated by an intermediate lag phase.

Formic acid could be a product produced by a metabolic block created by the addition of serine since the following part of the pathway precedes serine.

Methane---> Methanol---> Formaldehyde---> Formic Acid

However, formic and acetic acid are also produced by M. organophilum during serine fermentation void of methane (see below).

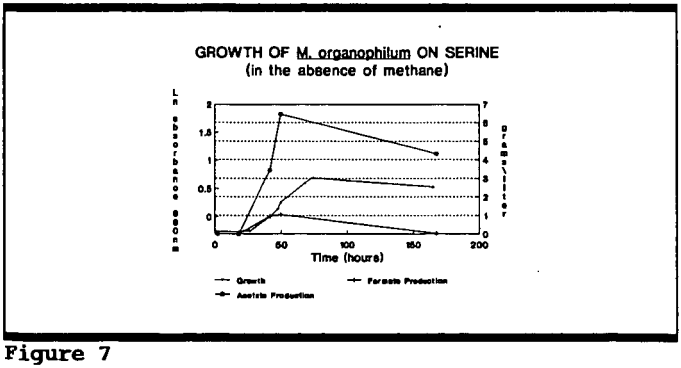

Figure 7

Waber et al (3) have shown the conversion of serine to pyruvate, which is decarboxylated to form acetate by Clostridium acidiurici. Kobota (4) found that serine generated formic acid form a cell-free preparation form Bacillus brevis in the presence of a cofactor, tetrahydrofolic acid. Tetrahydrofolate is present in M. organophilum and is used for 1-carbon group transfer and reduction.

CONCLUSIONS

Methanol accumulated during non-growth periods of methane metabolism by M. organophilum in the presences and absence of inhibitors under the conditions described. The production rate was increased by varying experimental conditions. For example, methanol accumulation increased by a factor of ca. 4 by pregrowing the culture in the presence of an inhibitor. When compared to commercial processes of methanol production, the bioconversion of methanol is ca. 90 times less active. Increasing methanol yields by optimizing culture medium and growth condition is limited by the natural isolate of Methylobacterium organophilum ability to synthesize methanol. Successful exploitation of Methylobacterium organophilum requires the application of genetic techniques for the optimization of methanol production.

Formic acid and acetic acid were growth associated products of serine fermentation by Methylobacterium organophilum.

REFERENCES

1. Patt, T. E., Cole, G. C. and Hanson, R. S., "Methylobacterium, a New Genus of Facultatively Methylotrophic Bacteria," International Journal of Systematic Bacteriology, Apr. 1976, Vol. 26., No. 2, p. 226-229.

2. Monad, J., "Recherches sur la Criossance des Cultures," Bacteriennes Hermannet Cie, Paris, 1942.

3. Waber, Lewis J. and Harland G. Wood, "Mechanism of Acetate Synthesis from CO2 Clostridium acidiurici," Journal of Bacteriology, Nov. 1979, p. 468.

4. Kubota, Kou, "Generation of Formic Acid and Ehtanolamine from Serine in Biosynthesis of Linear Gramicidin by a Cell-Free Preparation of Bacillus brevis (ATCC #8185)," Biochem. and Biophys. Res. Comm., 1982, Vol. 105, No. 2, p. 688,

Biological Production of Methanol from Methane

R. E. Corder, E. R. Johnson, J. L. Vega, E. C. Clausen, and J. L. Gaddy
Department of Chemical Engineering, University of Arkansas
Fayetteville, Arkansas 72701

Cultures of methanotrophs have been isolated that convert methane into methanol. Biocatalytic conversion offers the advantages of good thermal efficiency and low capital cost, since ordinary temperatures and pressures are employed. High product yield in a single-step reaction and simplified purification technology are possible, since methanol is the only product.

These unusual bacteria usually metabolize methane completely to CO_2, with methanol as an intracellular intermediate. Therefore, methanol production requires manipulation of the ordinary enzymatic reactions by regulation of the electron transport and environmental conditions to favor the methane monooxygenase pathway. This paper presents preliminary results of the culture isolation techniques and procedures to manipulate the cultures to produce methanol. These procedures have been successfully demonstrated with two isolates producing up to 1 g/L methanol extracellularly.

INTRODUCTION

Methanol is a major raw material for petrochemical production and is currently under consideration as a liquid fuel. Methanol is produced catalytically by the reaction of hydrogen and carbon monoxide at high pressure (300 psia) and moderate temperature (Strelzoff, 1970). H_2 and CO are obtained from methane by reforming with steam to yield synthesis gas. A second step, involving a water-gas shift reaction, is used to increase the H_2/CO ratio. The reforming step is generally carried out at 800-1000°C and 300 psig, whereas the water gas shift reaction utilizes metal oxide catalysts at 400-500°C and 300 psig (Shah and Stillman, 1970; and Shreve, 1967). These severe conditions result in high capital and operating costs and poor thermal efficiencies. Simpler, more efficient processes are necessary.

Natural gas demand and production declined to less than 17 trillion cu. ft. last year, with reserves dropping below eight years (Oil Gas J., 1986a; Beck, 1987). By 1990, gas imports are expected to be up 300 percent over present levels, despite a continuing decline in demand (Oil Gas J., 1986b). While flaring of natural gas has been substantially reduced in recent years, the U.S. presently wastes about 10×10^{10} cu. ft. annually (Hillard, 1980), or the equivalent of 1.4 billion gallons of methanol (40 percent of our liquid fuel requirement). Also, in many areas, gas wells remain shut-in because potential gas production is too remote or two dilute to justify pipelines and transportation. If simple conversion technology were available to produce liquid fuels on-site, flared and remote gas could be utilized.

Catalytic conversion of coal synthesis gas, using Fischer-Tropsch reactions, has been found to produce methanol and higher alcohols with sustained catalyst activity (Klier *et al.*, 1986; Dombek, 1986). By-products of the Fischer-Tropsch reactions include light hydrocarbon gases, predominantly methane. Methane is also a by-product from some gasification

processes (Mills, 1982). Methane is very stable in the subsequent processing steps to produce liquid fuels. Therefore, a technology or catalyst for converting methane directly into liquid fuels would substantially enhance the efficiency and yields of these processes.

A simple and efficient process for producing methanol from methane would save significant quantities of energy in industrial processes. Also, technology for conversion of small volumes or dilute mixtures of methane would enable production from remote gas and oil wells, saving wasted energy and reducing imports of crude oil. Furthermore, this technology would enhance the application of coal conversion technologies. Methanol production from methane is a mature technology and substantial advances or breakthroughs in catalytic processes are not likely. Therefore, innovative approaches to this problem are necessary.

Biological Conversion of Methane

Of the many biological species and microbiological reactions possible, only the methanotrophs are capable of converting methane. The usual sequence of methane metabolism proceeds to cell biomass and CO_2 with methanol as an intracellular intermediate. The interruption of the enzymatic reactions, by manipulation of the environmental conditions or mutation, could result in a culture that produces an excess of methanol that accumulates extracellularly.

Such a biocatalytic process has substantial economic potential for application to Fischer-Tropsch products, coal synthesis gas and natural gas conversion. Methane, in the gas stream following the Fischer-Tropsch synthesis, would be passed through the biological reactor for conversion to methanol. Similarly, methane in synthesis gas could be converted to methanol prior to or following Fischer-Tropsch synthesis. The conversion would take place in a single step at ordinary temperatures and at atmospheric or elevated pressures, if desirable. No products, other than methanol, are produced by these cultures. Complete methane conversion, with near stoichiometric yields, should be possible. Methanol recovery from the fermentation media could be accomplished by stripping or liquid extraction (extractive fermentation).

Purpose

The purpose of this paper is to present the results from preliminary laboratory experiments aimed at isolating a methanotroph culture that is capable of accumulating methanol as a product. Two isolates have been obtained that are capable of producing up to 1 g/L extracellularly.

MICROBIOLOGY OF METHYLOTROPHS

The biological conversion of methane to methanol by the reaction:

$$CH_4 + 1/2\ O_2 \rightarrow CH_3OH \qquad (1)$$

is carried out by a very specialized group of organisms that are also able to utilize methanol, methylamine or formate (in addition to methane) as sole carbon and energy sources. This class of organisms is called methylotrophs. Organisms that utilize primarily methane are called methanotrophs.

Organisms such as Methylococcus capsulatus and Methylomonas sp. are considered obligate methylotrophs and cannot grow on carbon sources other than methane, methanol, or formate. Energy is derived from the oxidation of these compounds to carbon dioxide, and most of the carbon is obtained from the fixation of formaldehyde by condensation with a pentose phosphate. Microorganisms that cannot utilize methane but can utilize methanol, methylamine and formate (e.g. Hyphomicrobium and a few Pseudomonas species) are generally also considered to be methylotrophs. Two types of methylotrophs have been established on the basis of the type of complex membranous organelles. Type I exhibits a system of paired membranes running throughout the cell or aggregated at its periphery. Type II exhibits a series of bundles composed of disc-shaped membrane vesicles distributed throughout the cell.

Type I methylotrophs utilize the ribulose monophosphate pathway for the assimilation of formaldehyde and have an incomplete tricarboxylic acid cycle. These organisms lack alpha-ketoglutarate dehydrogenase (Patel, 1984). Type II methylotrophs utilize the serine pathway for the assimilation of formaldehyde and have a complete tricarboxylic acid cycle (Large, 1983).

The methane molecule can only be attacked by a substitution mechanism. It was shown in 1970 that growth on methane is accompanied by the incorporation of an oxygen atom from gaseous oxygen into the molecule to give methanol, as was shown in Equation (1). Methane is actually oxidized finally to CO_2, with methanol, formaldehyde, and formate formed as intermediates (Anthony, 1982; and Higgins *et al.*, 1981a):

$$CH_4 + O_2 + 2H^+ \rightarrow H_2O + CH_3OH \rightarrow 2H^+ + HCHO \xrightarrow{1/2O_2} 2H^+ + HCOO^- H^+ \rightarrow CO_2 + 2H^+ \quad (2)$$

This series of reactions occurs intracellularly and no methanol is produced extracellularly. In order for the methanotroph to produce methanol, conditions for the subsequent enzymatic reactions must be made unfavorable. The enzyme, methane monooxygenase, catalyzes the reaction:

$$CH_4 + O_2 + H^+ + NADH \rightarrow NAD^+ + CH_3OH + H_2O \quad (3)$$

The enzyme occurs in both soluble and particulate form. The physical location of the enzyme as a cytoplasmic or extracytoplasmic enzyme has not been determined. Noting that NADH is a substrate, it is generally assumed that the reactions are cytoplasmic. This assumption is also consistent with the fact that they are proton utilizing (Hooper and DiSpirito, 1985). Reducing equivalents from the formaldehyde, formate, and perhaps methanol dehydrogenase reactions are utilized in methane monooxygenase, in the reduction of NAD^+ for biosynthetic reactions, or in electron transport leading to ATP synthesis.

Although the prosthetic group of methanol dehydrogenase is a novel quinone coenzyme (pyrroloquinoline quinone) the enzyme utilizes a soluble cytochrome c as an electron acceptor and is therefore a proton-yielding dehydrogenase (Beardmore-Gray *et al.*, 1983). Localization studies have shown that methanol dehydrogenase (Alefounder and Ferguson, 1981; Burton *et al.*, 1983; and Kasprzak and Steenkamp, 1983; 1984) and the electron acceptors cytochromes C_L, and possibly cytochrome C_H (Beardmore-Gray *et al.*, 1983; Burton *et al.*, 1983;

Jones *et al.*, 1982; and Quilter and Jones, 1984), are in the periplasm (Alefounder and Ferguson, 1981; and Kasprzak and Steenkamp, 1983). Thus, methanol oxidation clearly fits the generalization described in Equation (3) by Hooper and DiSpirito (1985).

Formaldehyde and formate dehydrogenase occur in forms which use either NAD^+ or dyes as electron acceptors (Johnson and Quayle, 1964; and Marison and Wood, 1980). Substrate oxidation is proton yielding and could logically be periplasmic:

$$H_2O + HCHO \rightarrow 2H^+ + 2e^- + HCOOH \quad (4)$$

and

$$HCOOH \rightarrow 2H^+ + 2e^- \; CO_2 \quad (5)$$

Depositing cross-membrane translocation of electrons to the proton-utilizing reduction of NAD^+:

$$H^+ + 2e^- + NAD^+ \rightarrow NADH, \quad (6)$$

the action of a dehydrogenase located in the periplasm would generate a proton gradient in both reactions. This seems not to be the case with the NAD-linked formaldehyde (Kasprzak and Steenkamp, 1983) and formate (Jones *et al.*, 1982) dehydrogenases; since they are soluble and use NAD, they are probably cytoplasmic. The topological location of the dye-linked enzymes is unknown.

In summary, in the methylotrophs, the proton-utilizing methane monooxygenase may be cytoplasmic and the energy-linked proton-yielding oxidation of methanol is periplasmic. Thus, CH_3OH functions as a transmembrane hydrogen transporter. In contrast, NAD-linked oxidations of formaldehyde and formate, which produce reductant for methane monooxygenase, biosynthesis, or electron transport, leading to ATP synthesis and CO_2 for carbon assimilation, are apparently cytoplasmic. Therefore, mechanisms for control of these separate enzyme systems to allow methanol production is feasible and likely. Furthermore, the potential to control electron flow and block specific enzyme sites with inhibitors to increase methanol yields is substantial.

THE PRODUCTION OF CHEMICALS USING METHYLOTROPHS

It is possible to biologically convert methane to methanol using whole cell systems or cell-free enzyme systems. Cell-free systems require an external source of reducing energy supplied by NADH for substrate oxidation. The methylotrophic enzyme which is of greatest interest is methane-monooxygenase which catalyzes the reaction:

$$CH_4 + O_2 + H^+ + NADH \rightarrow NAD^+ + CH_3OH + H_2O \quad (3)$$

This enzyme, although of fundamental importance for bacterial growth on methane, may become industrially important for quite a different reason. Since it is such a non-specific enzyme, it will oxidize a wide number of compounds in addition to methane (Large, 1983), some of which cannot be transformed by traditional industrial chemical methods.

Methane monooxygenase enzyme involved in catalyzing the hydroxylation of methane also catalyzes the oxygenation of various hydrocarbons and cyclic, alicyclic and aromatic compounds (Colby and Dalton, 1976; Colby *et al.*, 1977; Dalton, 1980; Dalton and Colby, 1982; Higgins *et al.*, 1981b; and Patel *et al.*, 1979). Thus, it is possible to convert methane to methanol or other short-chain hydrocarbons to their alcohols using whole cell systems. Patel (1984) reported that in using the soluble enzyme, methane monooxygenase, extracted from Methylobacterium sp. strain CRL-26, he was able to oxidize methane to methanol, ethane to ethanol, propane to 1-propanol and 2-propanol, butane to 1-butanol and 2-butanol and pentane to 1-pentanol and 2-pentanol, etc.

However, unlike simple hydrolases or oxidases, mixed-function oxidases, such as methane monooxygenase, need reduced nicontinamide nucleotides in addition to oxygen in order to function. Cell free systems, such as an immobilized enzyme system, are thus considered costly and impractical to use for the conversion of methane to methanol.

As an alternative to cell free systems, it is also possible to convert methane to methanol using whole cell systems, which supply their own reducing equivalents by substrate oxidation. Methane-utilizing organisms, grown on methane or methanol, have the ability to oxidize and transform a variety of non-growth substrates to commercially useful chemicals. This is due to the broad specificity of enzymes involved in the oxidation of methane to carbon dioxide. The isolation of such organisms, particularly those that might produce methanol from methane, would have broad application.

RESULTS AND DISCUSSION

CULTURE ISOLATION

Experimental studies were carried out in an effort to isolate methanotrophs from anaerobic digester sludge. This source of inoculum was chosen since the sludge contains significant quantities of methane in the liquid phase, and should, therefore, contain methanotrophs capable of using the methane.

Digester sludge was inoculated into a mineral salts medium, shown in Table 1, using a 10 percent by volume inoculum. As noted, the medium was essentially a salts medium, but also contained vitamins found essential for methanogen growth. The gas phase above the liquid media was maintained at 1 atm, and contained 20 volume percent methane and 80 percent air.

A mixed culture developed from this initial seeding was enriched by successive transfer to new media and gas every 72 hours. The enrichment procedure lasted a total of approximately 8 weeks. The enrichment was then

Table 1

Medium for Methylotroph Isolation

	g/L
KNO_3	2.5
Na_2HPO_4	0.21
KH_2PO_4	0.29
$MgSO_4 \cdot 7H_2O$	0.20
$FeSO_4 \cdot 7H_2O$	0.001
Trace elements[a]	1ml/L
Vitamins[b]	10ml/L

---

a The trace elements stock solution, shown below, were diluted 1000 times prior to use.

	mg/L
$CuSO_4$	50
H_3BO_3	10
$MnSO_4 \cdot 4H_2O$	10
$ZnSO_4 \cdot 7H_2O$	70
MoO_3	10

b A methanogen minimal medium, shown below, was diluted 100 times prior to use.

Biotin	2
Folic acid	2
Pyridoxine HCl	10
Thiamine HCl	5
Riboflavin	5
Nicotinic Acid	5
Ca-pantothenate	5
Vitamin B_{12}	0.1
p-amino benzoic acid	5
Thioctic acid	5

streaked onto agar plates utilizing the same media as in Table 1, and incubated under an atmosphere of 20 percent methane, 80 percent air until colonies appeared.

Individual colonies were picked, inoculated into fresh liquid media, and examined for purity. Two of the isolates that were obtained were obligate methanotrophs, and thus were selected for further testing.

CONVERSION OF METHANE TO METHANOL

Utilizing the obligate methanotrophs isolated from digester sludge, experiments were initiated to determine the feasibility of producing methanol from methane. Stoppered 250-ml Erlenmmeyer flasks were used as batch reactors. The liquid media utilized in the experiments was identical to the media of Table 1.

To facilitate mass transfer of methane from the gas phase to the liquid phase for reaction, gentle agitation (approximately 150 rpm) was employed, using a shaker incubator. The organisms were again grown under an atmosphere of 20 percent methane and 80 percent air at one atmosphere total pressure. Two obligate methanotroph isolates were compared in the study, along with the enrichment culture obtained after successive transfer from the digester sludge.

After obtaining growth in the reactors, the gas phase was switched to 100 percent methane in place of the 20:80 methane/air mixture. This substitution was made in order to prevent complete oxidation of methane to CO_2 as was shown in Equation (2). Incubation with gentle agitation occurred for 24 hours.

The results of these preliminary studies is shown in Table 2. Liquid phase analysis for methanol was performed using gas-solid chromatography. As noted, the two pure culture methanotrophs showed an accumulation of methanol, producing 0.5 and 1.0 g/L methanol in 24 hours. These levels of methanol production in 24 hours indicate the potential for good reaction rates in continuous culture. The enrichment, which contained methanotrophs and

Table 2

Biological Conversion of Methane to Methanol
(Preliminary Studies)

	Methanol Produced After 24 hours (g/L)
Isolate #1	0.5
Isolate #2	1.0
Enrichment	0

methanol-utilizing methylotrophs, showed no accumulation of methanol. The differences in the methanol production by the methanotrophs can be contributed to sensitivity to the presence of methanol, activity of the culture, and the ability of the cultures to utilize methanol as a substrate.

The results of these preliminary experiments are quite encouraging and demonstrate that the organisms are capable of producing methanol extracellularly at fast rates. Low cell densities and gentle agitation were used and, consequently, low methanol concentrations were obtained in the short reaction time. A measurement of the cell density in the flask showed a very low cell concentration of 0.3 g/L on a dry weight basis. A higher cell mass concentration (analogous to a higher catalyst concentration) would increase reaction rate to yield more product in the 24 hour period.

The experimental conditions can undoubtedly be improved to maximize methanol yields. Also reaction rates would be increased by providing better mass transfer of methane and oxygen from the bulk gas phase to the organisms in the liquid phase. The total pressure in the experiments was only 1 atmosphere. Higher pressures would be expected to significantly enhance reaction rate. Significantly higher methanol concentrations should be possible under improved conditions of cell density, reaction conditions and system design.

REFERENCES

Alefounder, P. R. and S. J. Ferguson. 1981. A periplasmic location for methanol dehydrogenase from Paracoccus denitrificans, implications for proton pumping by cytochrome aa_3. Biochem. Biohys. Res. Commun. 98: 778-784.

Anthony, C. 1982. The Biochemistry of Methylotrophs. Academic Press, Inc., New York.

Beardmore-Gray, M., D. T. O'Keefe, and C. Anthony. 1983. The methanol: cytochrome C. oxidoreductase activity of methylotrophs. J. Gen. Microbiol. 129: 923-933.

Beck, R. J., Oil and Gas J., 42 (Jan 26, 1987).

Burton, S. M., D. Byrom, M. Carrer, G.D.D. Jones and C. W. Jones. 1983. The oxidation of methylated amines by the methylotrophic bacterium Methylophilus methylotrophus. FEMS Microbiol. Lett. 17: 185-190

Colby, J. and H. Dalton. 1976. Some properties of a soluble methane monooxygenase from Methylococcus capsulatus strain Bath. Biochem. J. 157: 495-497.

Colby, J., D. I. Stirling and H. Dalton. 1977. The soluble methane monooxygenas of Methylococcus capsulatus (Bath.). Its ability to oxygenate n-alkanes, n-alkenes, ethers and alicyclic, aromatic and heterocyclic compounds. Biochem. J. 165: 395-402.

Dalton, H. 1980. Oxidation of hydrocarbons by methane monooxygenase from a variety of microbes. Adv. Appl. Microbiol. 26:71.87.

Dalton, H., and J. Colby. 1982. Methane monooxygenase: an iron-sulfur flavoprotein comples. p. 763-767. In V. Massey and C. H. Williams (ed.) Flavins and Flavoprotein. Elsevier/North-Holland Pub. Co., N.Y.

Dombek, D. B. 1986. Optimum Fuel Alcohol Mixtures from Syngas Oxygenate Synthesis, Proceedings Indirect Liquefaction Review, PETC.

Higgins, I. J., D. Best, R. C. Hammond, and D. Scott. 1981a. Methane-oxidizing microorganisms. Microbiol. Rev. 45:556-590.

Higgins, I. J., D. Best and D. Scott. 1981b. Hydrocarbon oxidation by Methylosinas trichosparium: Metabolic implication of the lack of substrate specificity of methane monooxygenase. p. 11-20. In H. Dalton (ed.) Microbial Growth on C_1 Compounds. Hayden Publishing Co., London.

Hillard, J. H., Natural Gas, Kirk-Othmer Encyl. of Chem. Tech., 11, 630, Wiley (1980).

Hooper, A. B. and A. A. DiSpirito. 1985. In bacteria which grow on simple reductants, generation of a proton gradient involves extracytoplasmic oxidation of substrate. Microbiol. Rev. 49: 140-157.

Johnson, P. A., and J. R. Quayle. 1964. Microbial growth on C_1 compounds. Oxidation of methanol, formaldehyde and formate by methane-grown Pseudomonas AMI. Biochem. J. 93: 281-290.

Jones, C. W., S. A. Kingsbury, and M. J. Dawson. 1982. The partial resolution and dye mediated reconstitution of methanol oxidase activity in Methylophilus methylotrophus. FEMS Microbiol Lett. 13: 195-200

Kasprzak, A. A. and D. J. Steenkamp. 1983. Localization of the major dehydrogenases in two methylotrophs by radiochemical labeling. J. Bacteriol. 156:348-353.

Klier, K., K. J. Smith and J. G. Nunan. 1986. Direct Synthesis of Methanol ls, Oxygenate Synthesis - F-T Products, Proceedings Indirect Liquefaction Review, PETC.

Large, P. J. 1983. Methylotrophy and methanogenesis. American Society for Microbiology, Washington, D.C.

Marison, I. W., and A. H. Wood. 1980. Partial purification and characrization of a dye-linked formaldehyde dehydrogenase from Hyphomicrobium X. J. Gen. Microbiol. 117:305-313.

Mills, G. A. Synfuels from Coal Progress in USA. 1982. Energy Progress, (57).

Patel, R. N. 1984. Methane Monooxygenase from Methylobacterium sp. ain CRl-26, in Microbial Growth on C_1 Compounds. (R. L. Crawford and R. S. Hanson eds.) pp 83-90.

Patel, R. N., C. T. Hou, A. I. Laskin, A. Felix, and P. Derelanko. 1979. Microbial oxidation of gaseous hydrocarbons: hydroxylation of n-alkanes and epoxidation of n-alkenes by cell-free particulate fractions of methane utilizing bacteria. J. Bacteriol. 139:675-679

Quilter, J. A. and C. W. Jones. 1984. The organization of methanol dehydrogenase and C-type cytochromes on the respiratory membrane of Methylophilus methylotrophus. FEBS Lett. 174:167-172.

Shah, M. and J. Stillman. 1970. Ind. Engr. Chem. Proc. Des. and Dev. 62 (12) p. 59.

Shreve, R. N. 1967. Chemical Process Industries, McGraw-Hill, New York.

Strelzoff, S., Chem. Engr. Symp. Ser., 66, 98 (1970).

_____, Oil & Gas J., 29 (Oct. 6, 1986a).

_____, Oil & Gas J., 36 (Sept. 29, 1986b).

COMPUTER-AIDED MOLECULAR DESIGN OF ALKANE-ACTIVATION CATALYSTS

John A. Shelnutt, Frances V. Stohl, Barry Granoff

Sandia National Laboratories, Albuquerque, NM 87185

Introduction

Methane can provide an abundant source of liquid fuels if an efficient method of conversion can be found. Direct conversion, without an initial steam reforming step to carbon monoxide and hydrogen, offers several significant advantages. These include improved efficiency, reduced capital costs, and more effective resource utilization. The key to success lies in the development of a catalyst that will activate the relatively inert carbon-hydrogen bond in methane. Several approaches are under active investigation, including oxidative coupling, partial oxidation by molecular oxygen at high temperature, photochemical conversion, and biomimetic processes.[1-3] Our work focuses on a novel biomimetic approach to the development of catalysts for activation of methane, using computer-aided molecular design (CAMD) techniques.

The biomimetic CAMD methodology consists of several elements: (1) Design activities are guided by the structural and chemical information about naturally occurring biological catalysts that carry out alkane oxidation to alcohols. The macromolecular biological catalysts are investigated to determine the features that need to be designed into a synthetic catalyst in order to mimic the alkane-oxidation function. (2) Molecular mechanics calculations are used to evaluate possible designs for catalysts based on synthetic metalloporphyrins. The metalloporphyrins have been chosen because they occur at the active site of many monooxygenases and other enzymes that catalyze C_1 chemistry. Also, the porphyrin macrocycle provides a platform upon which additional molecular architecture is erected to provide the structural features required to mimic the enzymes. Recent Russian work[4] has demonstrated methane-to-methanol conversion using an iron-porphyrin catalyst; thus, methane-activation catalysts based on the metalloporphyrins are feasible. (3) The computer designed catalysts are then synthesized. (4) The synthetic catalysts are characterized by various spectroscopic techniques including Raman-difference, transient Raman, FTIR, NMR, and UV-visible absorption spectroscopies. We are also using these spectroscopic probes to further structurally characterize some of the enzymes of interest (methylreductase[5-7] and heme proteins[8]). (5) The designed catalysts are tested in alkane-oxidation reactions. The activity test results and results of the structural studies are evaluated to obtain structure-activity relationships that form a basis for making further improvements in the catalyst. This feedback procedure gives an iterative method for optimizing catalytic properties.

The reaction catalyzed by the monooxygenase cytochrome P_{450} uses molecular oxygen to oxidize alkanes at ambient temperatures. The reaction may be amenable to molecular engineering techniques that will result in a synthetic methane-oxidation catalyst. The active site of cytochrome P_{450} contains an iron-porphyrin (heme) prosthetic group. Cytochrome P_{450} uses two equivalents of reduced nicotinamide adenine dinucleotide (NADH) to activate molecular oxygen; the resulting high oxidation-state Fe-oxo intermediate then attacks a C-H bond of the alkane by inserting an oxygen atom.

The protein matrix surrounding the iron porphyrin serves to protect and control access to the catalytic site. Because the X-ray crystal structure of cytochrome P_{450} is known, we can use the structure of the active site of the enzyme to guide the design of a synthetic analog specifically engineered for methane activation rather than oxidation of biological substrate molecules. The

X-ray crystal structure of cytochrome P_{450} of *Pseudomonas putida*[9] shows several features of the active site that might be engineered into a synthetic porphyrin. First, the enzyme has a hydrophobic pocket of the same size and shape as the substrate (camphor). The pocket promotes selective binding of the substrate molecule without axial coordination to the metal. The pocket also orients the camphor molecule so that only a specific carbon atom of camphor is (regioselectively) hydroxylated. Second, the pocket is rigid, thus maintaining its size and shape in the absence of substrate. The pocket's rigidity prevents the enzyme from self oxidation and probably self destruction. Finally, the asymmetric environment of the iron porphyrin in the protein provides a mercapto-sulfur ligand opposite the substrate binding pocket. The electron donating thiolate ligand is thought to facilitate cleavage of the O-O bond, thus, promoting formation of the active oxo intermediate.

To design a homogeneous metalloporphyrin-based catalyst for methane activation, two major problems must be addressed. First, a catalytic center capable of hydroxylating methane with high catalyst-turnover rates is required. This property is determined by the choice of metal, axial ligands, and electronic properties of the porphyrin macrocycle. We are addressing this problem by examining a variety of metalloporphyrin catalysts with a range of alkanes of decreasing molecular weights. The idea is to identify the porphyrins with high activity for the harder-to-oxidize gaseous hydrocarbons, methane in particular. The second major problem is to control which species have access to the active site. Because alkanes bind only via weak van der Waals interactions, detection of alkane binding itself presents a formidable obstacle to experimental studies aimed at determining what species can enter the cavity. One approach is to use comparative studies of the hydroxylation of various alkanes to determine which alkanes can enter the pocket. These studies also provide information about such properties as the size and shape of the pocket and the ability to select the carbon atom at which hydroxylation occurs (regioselectivity).

Here, we report on recent efforts to design, synthesize and test a regioselective alkane-to-alcohol catalyst based on the carboranyl porphyrins. The bulky carboranyl units attached to porphyrins like the one shown in Figure 1 provide a means of controlling the chemistry at the site of O_2 activation and C-H bond addition. By varying the structure of the porphyrin macrocycle and the nature of the connectors between the carborane units and the phenyl rings, a cavity was designed that controls access of various substrates, oxidants, products, and solvents to the reactive metal center. In this way, these porphyrins are being engineered to mimic the active site of cytochrome P_{450}.

Experimental Procedures

Materials. The catalysts used in this work include manganese(III) tetra(pentafluorophenyl) porphyrin (MnTpFPPX), where X represents an axial ligand, manganese(III) tetra(2'-carboranylphenyl-anilide) porphyrin chloride (MnTCBPPCl), and the manganese(III)-chloride derivative (MnTDNPPCl) of tetra(2',6'-dinitrophenyl) porphyrin free base (H_2TDNPP). H_2TpFPPCl was obtained from Porphyrin Products and converted to the Mn(III) derivative. The icosahedral carboranyl porphyrin, which was synthesized at the University of California at San Francisco by Stephen Kahl[10] using the Rothemund condensation, was converted anerobically to the Mn(III)Cl derivative by dissolving it in methanol containing $MnCl_2$ at room temperature. Isomerization of the carboranylphenyl substituents is not expected under these conditions. H_2TDNPP was synthesized[11] using a modification of the method recently reported by Lindsey.[12] Methylene chloride (99+%) was used as the solvent in the activity tests. Methylene bromide or methylene chloride were used in imidazole titration experiments. The oxidant was either O_2 or iodosylbenzene (IOB) prepared from the reaction of iodosobenzene

diacetate with NaOH.[13] The alkanes used for various tests were cyclohexane (99+%), and n-hexane (99%). Sodium borohydride ($NaBH_4$) was used as a reductant (analogous to NADH in the cyctochrome P_{450} reaction) when O_2 was used as the oxidant. $NaBH_4$ was obtained commercially and used without further purification. Imidazole (Im) was obtained commercially and purified by distillation.

Reaction Conditions. Reactions with cyclohexane and hexane were performed in the solution phase in an argon atmosphere glove box. Methylene chloride was the solvent. The ratio of reactant:oxidant:catalyst was 1100:20:1 on a mole basis. These reactions were carried out at ambient temperatures (about 30° C) and at atmospheric pressure. Reactants were stirred at 1000 rpm. Reaction times were 2 h. For the run with MnTDNPP, a solution of 3.98 μmoles of the porphyrin and 17.57 mg of iodosylbenzene in 1.1 ml of methylene chloride and 0.5 ml of cyclohexane was stirred in a glove box for two hours. Product yields were 2 and 9 μmoles of cyclohexanone and cyclohexanol, respectively.

Product Analysis. Oxidation products were identified using gas chromatography/mass spectrometry techniques and quantified using capillary column gas chromatographic techniques with commercially available compounds as standards. Product yields are reported as the number of catalyst turn-overs during the 2 h run. Typically, however, the reaction stops after only 30 min, because the supply of oxidant is exausted.

Molecular Modeling. CAMD was carried out on an Evans&Sutherland PS390 graphics work station using a MicroVAX II host computer. Three dimensional graphical display and molecular energy-optimization and dynamics calculations were performed using BIOGRAF software (BioDesign).

Results and Discussion

A Mn(III)-carboranyl porphyrin that has some of the structural features of cytochrome P_{450} is shown in Figure 1. The porphyrin (α^4-MnTCBPP) has all four ortho substituents on the phenyl rings oriented toward the same side of the porphyrin plane (α^4 isomer). For the α^4 isomer, the bulky carborane groups at the ends of the 3-atom chain, which links them to the phenyl rings, form a pocket adjacent to the Mn atom in the macrocycle. A possible cavity can be seen in the graphical display of the carboranyl porphyrin (Figure 1). The energy-minimized structure with van der Waals surfaces displayed (not shown) best shows that the pocket exists and is large enough to contain methane and molecular oxygen. Further, the cavity is small enough to prevent other test-system components (e. g. solvent, promoters) from reaching the reactive center. Thus, the carboranyl porphyrin shows potential for providing the size-recognition features required for selective substrate binding. Moreover, molecular dynamics calculations in the presence of model organic solvents (e. g. pentane) show that it is energetically favorable for methane to bind in the pocket of the oxo intermediate. Two features that we would like to tailor into the porphyrin are not yet incorporated. First, the dynamics calculation shows that the carboranyl-porphyrin pocket is not as rigid as we think is required based on the enzyme's X-ray crystal structures.[9] And, second, P_{450}'s thiolate ligand has not been provided, although we have been able to mimic the thiolate ligand with a nitrogenous base (imidazole). Although these two features are not incorporated in an optimum way into the catalyst, nevertheless, experimental studies of the catalyst provide information on how well the cavity controls reactions occurring at the protected site, and, the experimental results obtained using the carboranyl porphyrin can be compared to predictions of the molecular modeling.

One prediction of the molecular modeling studies is that a nitrogenous ligand such as imidazole is too large to coordinate to the metal on the hindered

side of the porphyrin because it sterically cannot fit into the methane binding pocket. Imidazole can still coordinate at the open face of the α^4 isomer, however. In contrast, for porphyrins that are not sterically hindered, such as Mn(III) tetraphenyl porphyrin (MnTPP) and MnTpFPP, both faces of the macrocycle are available for axial ligation of imidazole. Indeed, changes in the uv-visible absorption spectrum of MnTPP and MnTpFPP, obtained as a function of imidazole concentration, show that two imidazole molecules successively coordinate (equilibrium association constants for MnTpFPP with Im in methylene bromide, $\log K_1 = 2.0$; $\log K_2 = 3.1$). On the other hand, the spectral changes for the Mn(III) α^4-carboranyl porphyrin indicate that only one imidazole molecule binds and that this one-to-one complex is completely formed at 0.1 M imidazole (in methylene chloride, $\log K = 2.5$). For the unhindered porphyrins very little (~20%) of the 1:1 complex is formed before subsequent formation of the 2:1 complex.

One consequence of the lack of coordination of imidazole on the hindered face of the carboranyl porphyrin is that we have successfully mimicked the single axial ligand of the iron in cytochrome P_{450}. In the protein, only one thiolate ligand binds because only one ligand is available from the heme's asymmetric protein environment; in the carboranyl porphyrin case only one ligand can bind because of imidazole's lack of access to the small cavity formed by the carborane units. The mimicry of the thiolate ligand of cytochrome P_{450} by an imidazole is good since a single imidazole ligand is known from our work and that of others[14,15] to promote the catalytic activity of manganese porphyrins.

We can also exploit the formation of the 1:1 imidazole complex with the carboranyl porphyrin to block alkane-activation reactions at the open face of the porphyrin and force the reaction to occur in the cavity. We wish to block the open face because the reaction at this site is not expected to show significant regioselectivity for primary carbons. The bars in Figure 2 illustrate the relative yields of alcohols under various reaction conditions. The first bar on the left shows the yield of hexanols for an unhindered porphyrin, in this case MnTpFPP. The MnTpFPP result is shown for comparison with the α^4-MnTCBPP tests. (In this case, we have circumvented the use of molecular oxygen as the oxidant by using a single oxygen donor (iodosylbenzene) to generate the active intermediate directly without the use of reductants. The iodosylbenzene oxidant system is more stable and chemically less harsh than the reductant-O_2 system.) When imidazole is absent (second bar in Figure 2), the open face of α^4-MnTCBPP is available to cyclohexane, which is hydroxylated with a yield comparable to the unhindered porphyrin. The molecular modeling work indicates that the reaction primarily occurs on the open face because neither cyclohexane nor iodosylbenzene have access to the metal site on the sterically blocked face of the carboranyl porphyrin.

The third bar in Figure 2 illustrates that when imidazole is added (0.1 M) the yield is greatly reduced demonstrating that the coordination of imidazole effectively blocks the alkane-oxidation reaction. This result is consistent with our studies of the yield as a function of imidazole concentration for unhindered porphyrins. Such studies show that the complex with imidazole blocking both axial ligand sites is inactive. In the case of the carboranyl porphyrin, one axial position is sterically blocked and the other has imidazole bound; therefore, little activity is observed. A small amount of substrate oxidation might still occur at the open face because of rapid equilibrium of imidazole association and dissociation at the manganese.

The fourth bar illustrates that when hexane rather than cyclohexane is used as the substrate only a trace amount of hexanol is produced. Less hexane is oxidized than cyclohexane (third bar, Figure 2) partly because hexane has two

primary carbons, which are harder to oxidize than the carbons of cyclohexane. However, it is not clear why so little hexanol is produced relative to cyclohexanol. One might have expected some hexane oxidation since CAMD techniques show that the end of the hexane molecule could reach the protected metal site. However, molecular modeling also suggests that the oxo intermediate cannot be formed in the pocket because iodosylbenzene cannot readily reach the manganese atom.

Finally, if molecular oxygen, which can enter the pocket, is used as the oxidant, then we might expect some hydroxylation of hexane with regioselectivity for the primary alcohol. The fifth bar in Figure 2 shows the yield of hexanols obtained when O_2 is used as the oxidant. In this test sodium borohydride is used to reduce the catalyst, which then binds O_2. This species is subsequently reduced again yielding the active manganese-oxo intermediate. The total yield of hexanols is minute primarily because the $NaBH_4$-O_2 system rapidly destroys the catalyst,[16] as shown by the rapid bleaching of the porphyrin absorbance during the reaction. Another reason for the low yield is that it is statistically unlikely for the end of the hexane molecule to work its way into the cavity. Nevertheless, some activity is observed. Preliminary results (not shown) indicate that the yield of primary alcohol (1-ol) increases relative to the secondary alcohols (2-ol and 3-ol) when compared to an unhindered porphyrin (first bar). A less harsh O_2 activation reaction than the $NaBH_4$ system is necessary to increase the yield. Preliminary estimates of the primary regioselectivity for the MnTCBPP-imidazole-$NaBH_4$-O_2 system appears to compare favorably with hydroxylation of hexane by the bis-pocket porphyrin, Mn(III) tetra(triphenylphenyl) porphyrin,[17] also a size selective catalyst. The primary regioselectivity of the latter porphyrin is better than for some cyctochromes P_{450},[18-20] showing that a synthetic catalyst can be as regioselective as the enzyme itself.

One way to solve the problem of protecting the open face of the carboranyl porphyrins is to synthesize a porphyrin having no open faces. One possibility is the *di*-ortho-phenyl analog of the carboranyl porphyrin, which is shown in Figure 3. Recently, we have succeeded in synthesizing the precursor of this class of bis-deep-pocket porphyrins, namely H_2TDNPP and its diamino derivative.[11] Efforts are underway to synthesize several bis-deep-pocket porphyrins based on H_2TDNPP.

The manganese(III) derivative of H_2TDNPPCl is interesting in its own right as a potential methane-activation catalyst because (1) it provides shallow cavities at the metal on both faces of the macrocycle and (2) the iron derivative of the related mono-nitro-phenyl-porphyrin has recently been reported to activate methane.[4] We have not yet tried to oxidize methane with MnTDNPP, but we have demonstrated that MnTDNPPCl has catalytic activity for converting alkanes to alcohols as demonstrated by the oxidation of cyclohexane. Turnover numbers for the 2-h run were 0.5 for cyclohexanone and 2.2 for cyclohexanol. Uv-visible absorption spectra at the end of the run showed the presence of a Mn(IV) or Mn(V) porphyrin intermediate species, thus, indicating that the reaction had probably not run to completion.

Conclusions

We have shown that the chemistry occurring at the open face of the deep-pocket porphyrin can be controlled by axial ligation, which forces the reaction to take place in the cavity. Preliminary tests indicate regioselectivity of alkane oxidation by a manganese(III) deep-pocket porphyrin in a reaction using O_2 as the oxidant.

MnTDNPP, a precursor in the synthesis of deep-pocket porphyrins with the pockets on both faces of the porphyrin, has been synthesized and its manganese derivative was shown to be active in alkane oxidation. MnTDNPP may also be interesting from the point of view of methane and ethane activation.

Acknowledgements

We thank Stephen Kahl for kindly providing the carboranyl porphyrin, Dan Trudell and Carlos Quintana for technical assistance. This work performed at Sandia National Laboratories and supported by the U. S. Department of Energy Contract DE-AC04-76DP00789.

References

1. Gesser, H. D.; Hunter, N., Chem. Rev. **1985**, 85, 235.
2. Jones, A. C.; Leonard, J. J.; Sofranko, J. A., J. Catal. **1987**, 103, 311.
3. Groves, J. T. in *Metal Ion Activation of Dioxygen*, Ed. Spiro, T. G. (Wiley: New York), Chpt. 3, 1980.
4. Belova, V. S.; Khenkin, A. M.; Shilov, A. E., Kinet. Katal. **1987**, 28, 1016.
5. Shelnutt, J. A.; Shiemke, A. K.; Scott, R. A., Div. Fuel Chem. Preprints, Vol. 32, Eds. Ratcliffe, C. T.; Suuberg, E. M. American Chemical Society: Washington) 1987, pg. 272.
6. Shiemke, A. K.; Scott, R. A.; Shelnutt, J. A., J. Am. Chem. Soc. **1988**, 110, 1645.
7. Shelnutt, J. A., J. Am. Chem. Soc. **1987**, 109, 4169.
8. Muhoberac, B. B.; Shelnutt, J. A.; Ondrias, M. R., FEBS Lett. **1988**, in press.
9. Poulos, T. L.; Finzel, B. C.; Gunsalus, I. C.; Wagner, G. C.; Kraut, J., J. Biol. Chem. **1985**, 260, 16122.
10. Kahl, S. B., in *Neutron Capture Therapy*, Ed. Hatanaka, H. (Mishimura Co.) 1986.
11. Quintana, C. A.; Assink, R. A.; Shelnutt, J. A., J. Am. Chem. Soc. submitted.
12. Lindsey, J. S.; Schreiman, I. C.; Hsu, H. C.; Kearney, P. C.; Marguerettaz, A. M., J. Org. Chem. **1987**, 52, 827.
13. Saltzman, H.; Sharefkin, J. G., Organ. Synth. **1963**, 43, 60.
14. Battioni, P.; Renaud, J.-P.; Bartoli, J. F.; Mansuy, D., J. Chem. Commun. **1986**, 341.
15. Meunier, B.; de Carvalho, M.-E.; Bortolini, O.; Momenteau, M., Inorg. Chem. **1988**, 27, 161.
16. Tabushi, I.; Koga, N., J. Am. Chem. Soc. **1979**, 101, 6456.
17. Cook, B. R.; Reinhert, T. J.; Suslick, K. S., J. Am. Chem. Soc. **1986**, 108, 7281.
18. Frommer, U.; Ullrich, V.; Staudinder, H.; Orrenius, S., Biochem. Biophys. Acta **1972**, 280, 487.
19. Ellin, A.; Orrenius, S., Molec. Cell Biochem. **1975**, 8, 69.
20. Morohashi, K.; Sanano, H.; Okada, Y., Omura, T., J. Biochem. **1983**, 93, 413.

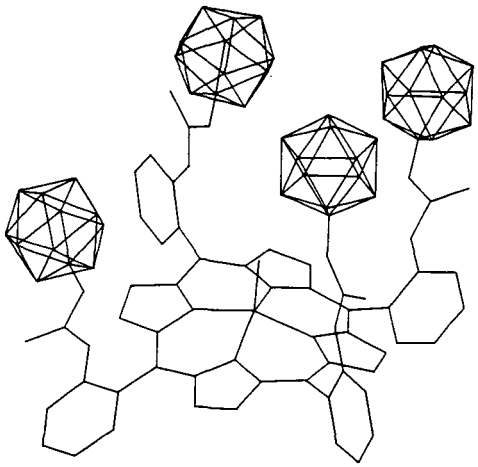

Figure 1. Oxo-metallo-α^4-tetra(2'-carboranylphenyl-anilide) porphyrin. Energy minimized BIOGRAF structure (not global minimum).

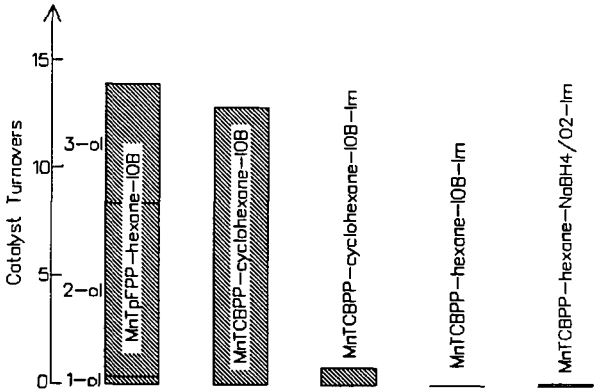

Figure 2. Alkane hydroxylation by designed Mn(III)-α^4-tetra(2'-carboranyl-phenyl-anilide) porphyrin catalyst.

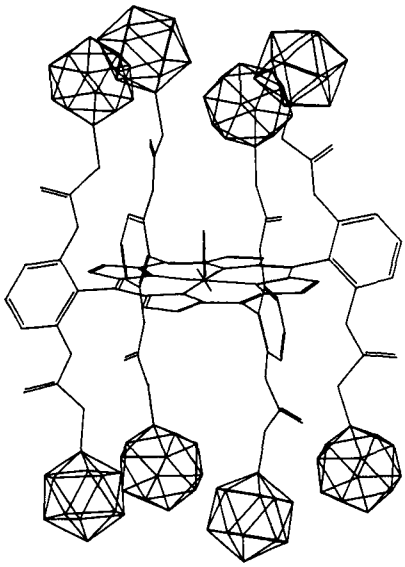

Figure 3. Example of a bis-deep-pocket carboranyl porphyrin that can be synthesized from tetra(2',6'-dinitrophenyl) porphyrin. BIOGRAF structure not fully energy minimized.